Identification, Characterisation and Quantification of Degradation Adducts of CyMe$_4$-BTBP

Doctor of Philosophy

School of Chemistry, Food and Pharmacy – Department of Chemistry

Jasraj Singh Babra

October 2021

Declaration

I, Jasraj Singh Babra, hereby declare, that this thesis has been solely composed by myself and that the work carried out by my own person. I also declare that it has not been submitted, in full or partially, previously for another degree, except where it has been specified, acknowledged, and referenced.

Signed

Jasraj Singh Babra

October 2021

Acknowledgements

First and foremost, I would like to offer my sincerest gratitude to Professor Laurence Harwood for allowing me to be one of his last PhD students and the giving me the chance to work within your excellent research group and to explore the world through the many conferences, even if we only ever see the airport, conference room and the hotel. I am particularly grateful for all your support, and advice during my PhD, as well as all your jokes that always seem to get worse as the night goes on. I wish you the very best in retirement, few academics manage to fully break free of the hold of research.

I would also like to give thanks to Dr Chris Smith for your stellar lab supervision and helping me put out fires, sometimes quite literally. Your scientific insight has often sparked new ideas or pointed out the flaws in my endless book of bad ideas. I also want to thank the academic staff at the Department of Chemistry who have helped me both academically and personally, specifically: Dr Andy Russell, Dr John McKendrick, Dr Fred Davis, Prof. Wayne Hayes, and Dr Phillipa Cranwell. My thanks also go to those who keep the lights on and the department moving, Phil Mason, Gez Griffin, Ray Lau, Ben Heaton, Chris Harris, and George Lacey.

I would like to thank the Harwood research group, who understand the "great delight" that our chemistry is. It was a pleasure to work alongside all of you in particular Dr Ashfaq Afsar, Dr James Westwood, Dr Iain Hopkins and specifically Ms. Zoe Selfe who stood next to me the entire PhD and helped me move during the Great Transition to the newly refurbished Lab 269 where we marvelled at our new water feature.

I would also like to offer my sincerest gratitude to all my friends from the office: Adam O'Donnell, Alex Gavriel, Charlotte Edwards-Gayle, Hannah Bowden, Iain Hopkins, Jack Cheeseman, James Westwood, Jessi Godleman, Jessica Hutchinson, Lewis Hart, Max Johnson,

Oli Balmford, Sam Burholt, Sara Salimi, Tahkur Singh Babra and Zoe Selfe. You have all given me laughs over the years, and exceptional lunch time conversations.

Finally, and most importantly, I would like to thank those closest to me, my Dad, Jagjeet Singh, my Mum, Pavinder Kaur and my brother Tahkur Singh. To my Mum and Dad, thank you for your never-ending support, you have provided me with everything I could ever ask for and more, I could not have done this without you. To Tahkur, thank you for inspiring me all these years and pushing me further that I thought possible, your provision of joyous laughter throughout my life has been nothing short of amazing. Thank you.

Abstract

CyMe$_4$-BTBP and CyMe$_4$-BTPhen are ligands planned for use in the selective actinide process (SANEX). The process was devised to extract the minor actinides from the lanthanides found in post-DIAMEX 4M HNO$_3$ raffinate into the organic diluent cyclohexanone or 1-octanol. However, the raffinate is radiotoxic emitting α- and γ-radiation, which in turn propagates the radiolysis of these ligands resulting in degradation products. This thesis outlines the progress towards identifying and characterising the degradation adducts of CyMe$_4$-BTBP in both cyclohexanone and 1-octanol by endeavouring to synthesize the degradation adducts.

Abbreviations and Acronyms

An	Actinide
Bipy	2,2'-Bipyridine
BTBP	*Bis*-triazinylbipyridine
BTP	*Bis*-triazinylpyridine
BTPhen	*Bis*-triazinylphenanthroline
D	Distribution ratio
DIAMEX	Diamide extraction
DMDOHEMA	*N,N'*-dimethyl-*N,N'*-dioctyl[(hexyloxy)ethyl]malonamide
DMF	N,N-dimethylformamide
DMSO	Dimethyl sulfoxide
D_w	Distribution weight ratio
GANEX	Group actinide extraction
GenIV	Generation IV reactor
GW	Gigawatt
HLLW	High level liquid waste
HLW	High level waste
i-SANEX	Innovative-Selective actinide extraction
kBq	Kilobecquerel
kGy	KiloGray
LiDMAE	Lithium dimethylaminoethanol
LLW	Low level waste
Ln	Lanthanide
m-CPBA	*meta*-Chloroperbenzoic acid
Mins	Minutes
MOX	Mixed oxide fuel
Phen	1,10-Phenanthroline
PUREX	Plutonium uranium extraction
SANEX	Selective actinide extraction
SF	Separation factor
TALSPEAK	Trivalent Actinide Lanthanide Separation with Phosphorus reagent Extraction from Aqueous Komplexes
TBP	Tributyl phosphate
TERPY	2,2:6',2"-terpyridine
THF	Tetrahydrofuran
TODGA	*N,N,N',N'*-tetraoctyldiglycolamide
TRUEX	Transuranic extraction process

Contents

Chapter 1 – A Brief History of the Reprocessing of Spent Nuclear Fuel
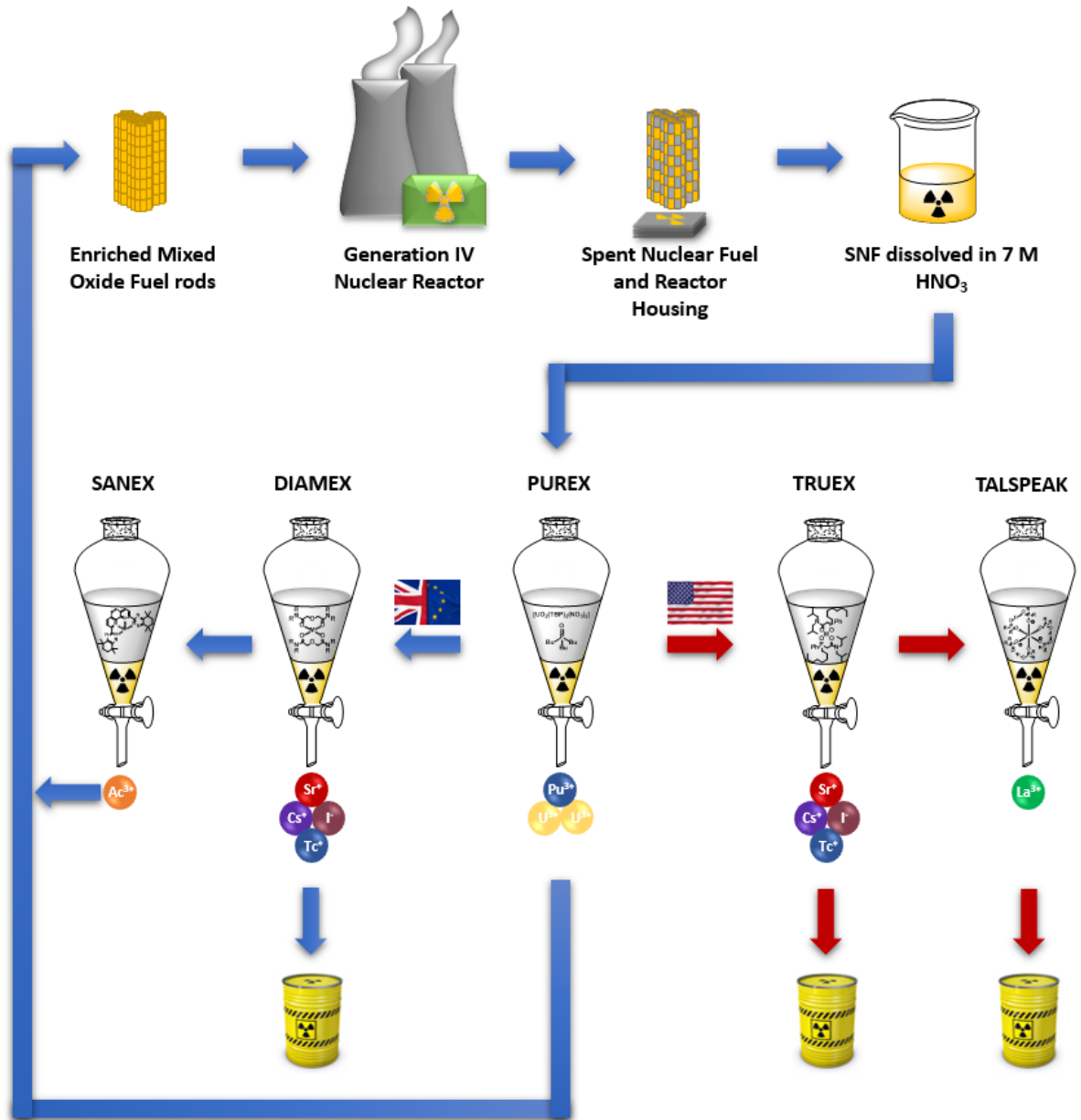
1.1 Introduction

Fossil fuel reserves are rapidly being exhausted and, at the same time, the energy requirement to satisfy the growing population and infrastructure is exponentially increasing. To supply the world with a stable source of electricity is a problem that must be solved soon and burning through our dwindling supply of fossil fuels is no longer the solution.[1,2]

The burning of fossil fuels has led to the increased concentration of greenhouse gases that are polluting the atmosphere, with methane, carbon dioxide, sulfur dioxide and many other volatile organic compounds (VOC's).[3] In recent decades, many nations have resorted to renewable energy, building vast solar and wind turbine farms followed with research into nuclear fusion.[4] However, while these systems are a step in the right direction and are certainly cleaner than the fossil fuels, they each have downfalls; solar panels are only efficient and cost effective in direct sunlight, wind turbines not only need certain wind speeds for efficient power production but also require rare earth minerals that are toxic to extract and nuclear fusion is yet to be demonstrated outside the laboratory.[5] The logical option in the medium term is to expand the use of nuclear fission to generate electricity for the growing populations of the world.

1.1.2 Nuclear Fission

The story of how nuclear power generation came to be is one of interest and has earned both the chemists and physicists involved a place in the history books. In the year 1789, German chemist, Martin Heinrich Klaproth discovered a new element, uranium, unaware of its future potential. Over 100 years later, in 1896, Pierre and Marie Curie uncovered a new phenomenon, radioactivity,[6,7] linking work, from the previous year, by Wilhelm Rontgen,[8] Henri Becquerel[9] and Paul Ulrich Villard who discovered X-rays, alpha- and beta-, and gamma-

radiation, respectively. Ernest Rutherford made the next discovery in 1902 showing radioactivity as a spontaneous event emitting an α- or β-particle from the nucleus of an atom.[10] Isotopes were the next discovery in 1911 by Fredrick Soddy.[11] In the next 20-25 years, James Chadwick discovered the neutron,[12,13] and Cockcroft and Walton produced the first nuclear transformation by using accelerated protons and colliding them with atoms.[14] Later, Enrico Fermi showed that using neutrons instead of protons produced much heavier elements.[6] Niels Bohr made the final major discovery, of nuclear fission in 1938.[15,16]

If we skip forward to the present era, nuclear power is most often generated using enriched uranium (U^{235}) or mixed oxide fuel (MOX). From a chemical stand point, the process of nuclear fission occurs when a thermal neutron is fired into the U^{235} atom, which releases energy and splits into two, often unstable, smaller elements or nuclides and produces more neutrons, starting a chain reaction (Figure 1.1).[17] The number of neutrons and the composition of the nuclides released are controlled by statistical probability; therefore an accurate chemical formula cannot be written. However, the law of conservation of mass must always be held true, and so the number of protons, neutrons and electrons on either side of the reaction must be equal.[17] If the number of neutrons is not controlled, the rate of the fission reaction will increase exponentially, eventually breaching the thermal limits of the cooling systems surrounding the reactor and causing an explosion.
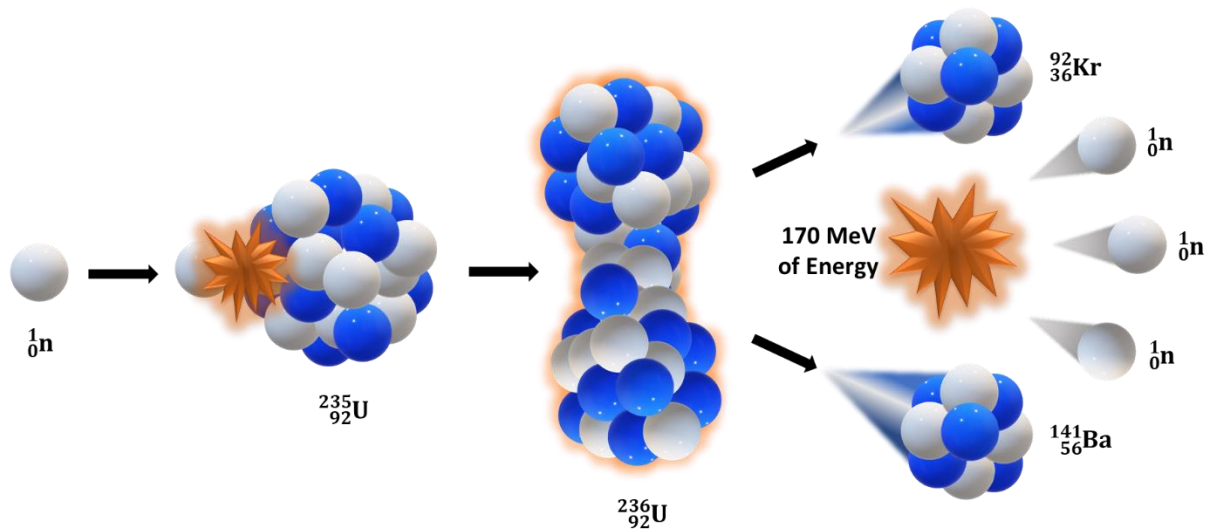
Figure 1.1: Example diagram of the fission of U^{235}.[17]

Mixed oxide fuels are a mixture of U^{235} and Pu^{239}, with the Pu content varying from 1.5% to 30%, dependent on the type of reactor used.[17–20] MOX fuel has the added benefit of using weapons-grade plutonium, so that countries cannot produce and stockpile plutonium for nuclear weapons.

1.1.3 Current Nuclear Reactor Types

According to the International Atomic Energy Agency (IAEA) there are 443 nuclear reactors operating in the world, generating 392 GW of electrical power, with a further 56 in construction and 99 planned as of 2020.[21] Amongst the 443, there are several types of nuclear reactor deployed, 300 of which are Pressurised Water Reactors (PWR), for power generation and smaller modules utilised by the nuclear navies.[21–23] The second most common reactor type are boiling water reactors (BWR) with 65 currently operational. Thereafter, the next 14 are Gas Cooled Reactors (GCR/AGR) employing CO_2 for cooling and are exclusively used in the United Kingdom (UK) (**Figure 1.2**). Lastly in Russia, twelve Light Water Graphite Reactors (LWGR) and two Fast Neutron Reactors are currently generating electricity.[21–23]
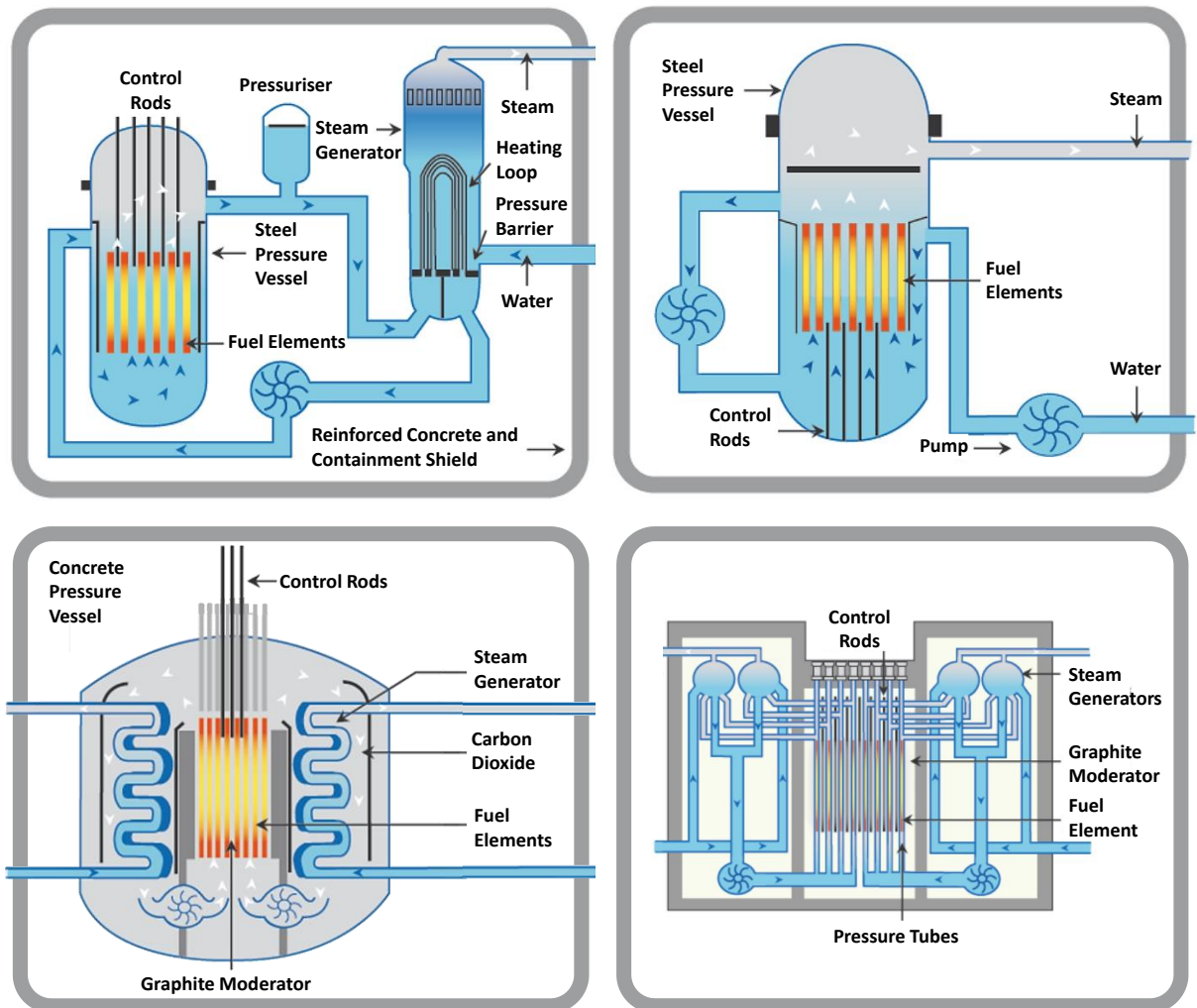
Figure 1.2: General assemblies of Pressurised Water Reactor (Top Left), Boiling Water Reactor (Top Right), Gas Cooled Reactor (Bottom Left) and Light Water Graphite Reactors (Bottom Right).[6]

1.1.4 Generation IV Reactors

Generation IV reactors are the next generation of nuclear reactors, with increased efficiency and use of different fuel sources compared to the previous generation III reactors.[24] There are currently six main variations of Generation IV reactors that are planned to be used, where variations differ between the use of fast or thermal neutrons, coolant technology, and fuel.[25] Most Generation IV reactors also include a closed fuel loop where very little waste is generated in the process of running.[24]

The first type of Generation IV reactors is that of Gas-Cooled Fast Reactors (GFR), employing helium to cool the reactors over the CO_2 currently used in AGR's in the UK. Additionally, these

GFR's use fast neutrons and a tertiary steam unit to increase electricity generation. The second type of reactor is the Lead-Cooled Fast Reactor (LFR), using either depleted uranium or thorium fuel matrices as fuel sources and liquid lead or Pb-Bi alloy for cooling at atmospheric pressure. The third reactor type is the Molten Salt Reactor (MSR), where the fissile material is suspended/dissolved in the coolant rather than using conventional rods (Figure 1.3). The fissile material here is proposed to be uranium fluoride. This type of reactor can be utilised with both thermal or fast neutrons.[24–26]
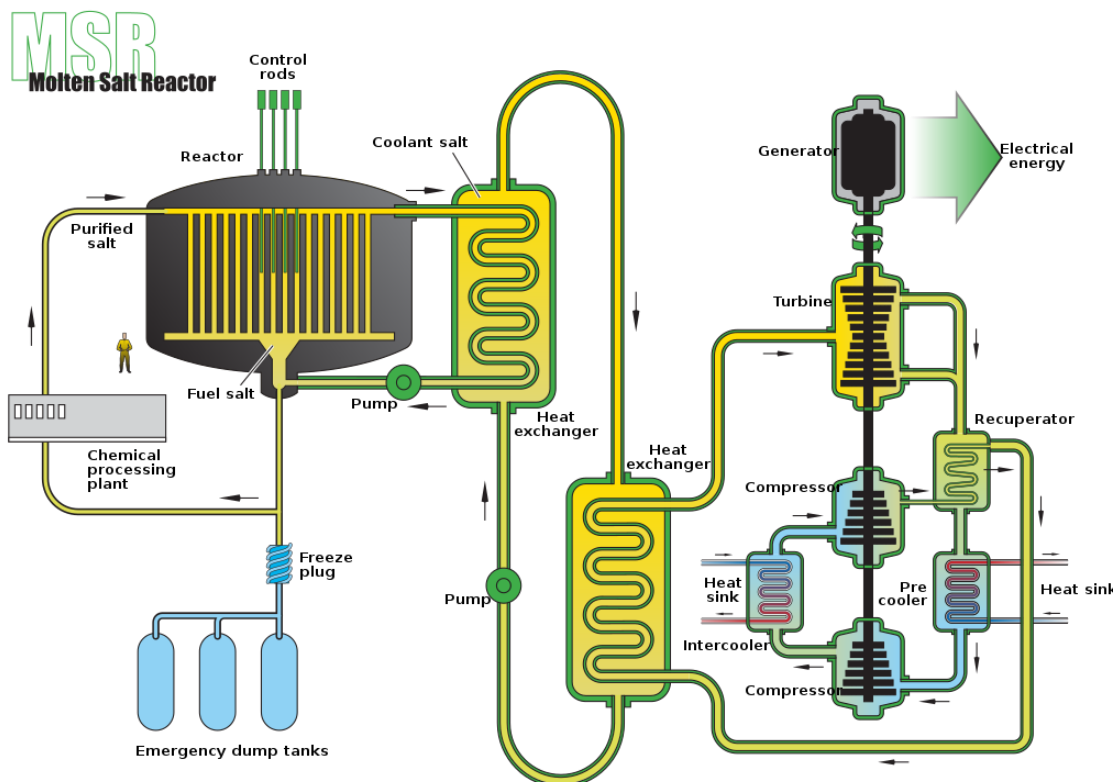
Figure 1.3: Example diagram of molten salt reactor system.[27]

The fourth reactor, known as the Sodium-Cooled Fast Reactor (SFR), will utilise depleted uranium as fuel and liquid sodium as coolant at a temperature of 500-550 °C, similar to that of the LFR. The fifth reactor type is the Supercritical Water-Cooled Reactor, which operates at very high pressures of 22 MPa at 374 °C. In contrary to many of the other systems, the

supercritical water drives the turbines to generate the electricity. The disadvantage to this system is that it has an open loop fuel cycle which is not efficient for waste management, nor for environmental reasons. The last Gen IV reactor type is the Very-High Temperature Gas Reactor, which is a graphite-moderated helium-cooled reactor similar to GFR's. However, these reactors are set to operate at 1250 °C using UO_2 as a fuel source and use an open fuel cycle, which again leaves the issue of dealing with the spent nuclear fuel produced by these new reactors.

1.2 Spent Nuclear Fuel

Nuclear power is not a renewable means of generating electricity and still uses the Earth's resources, as well as, producing spent nuclear fuel (SNF) which is extremely radioactive and will require over 300,000 years to degrade to background radiation levels if simply stored.[28] This nuclear legacy is one of the biggest challenges to the nuclear industry worldwide.

Currently, SNF from reactors is stored above ground in depositories around the world.[29] The most radioactive materials, the used fuel rods, are submerged in cooling ponds for up to 3 years; allowing the most unstable and radiotoxic elements to decay, due to their short half-lives. Fuel cladding, which can also be extremely radiotoxic, is also submitted to this treatment. To be reprocessed, the rods and reactor cladding are removed from the pools, broken down, crushed and dissolved in 7 M nitric acid, to generate an aqueous waste stream.[30,31]

The major constituents of SNF are: uranium (U^{238}), plutonium (U^{239}), fission products such as strontium (Sr^{90}), caesium (Cs^{137}), iodine, (I^{129}) and technetium (Tc^{99}), and the minor actinides neptunium (Np^{237}), americium (Am^{241}), and curium (Cm^{244}) (Figure 1.4).[28] The uranium in SNF

has an enrichment level close to natural occurring uranium ore. Therefore, if separated, the

uranium together with the extracted plutonium can be reused in nuclear reactors.

Uranium		**Fission Products**	
U-238 – 93%		Sr-90 – 0.1%	
U-235 – 0.7%		Cs-137 – 0.2%	
		I-129 – 0.03%	
		Tc-99 – 0.1%	

Plutonium
Pu-238 – 0.04%
Pu-239 – 0.7%
Pu-240 – 0.3%
Pu-241 – 0.2%
Pu-242 – 0.1%

Minor Actinides
Np-237 – 0.07%
Am-241 – 0.03%
Cm-244 – 0.01%
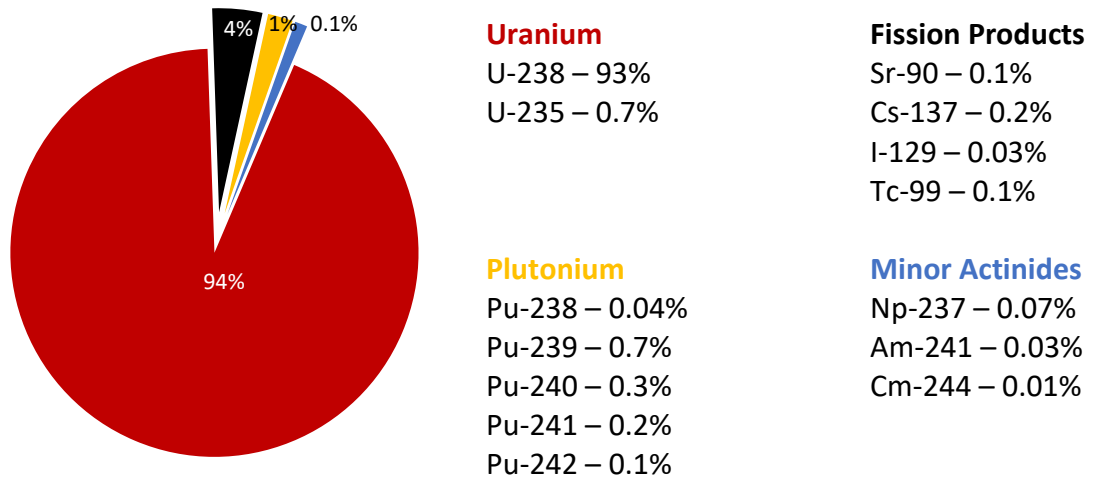
Figure 1.4: Approximate composition of spent nuclear fuel.[28]

Reprocessing the uranium and plutonium from reactors will reduce the amount of waste that

is deposited in storage. It also reduces the radiotoxicity and heat output of the SNF, and

reduces the time for the radioactivity of the SNF to return to that of the pitchblende ore from

which is was derived, from 300,000 years to 9000 years (Figure 1.5).[28]
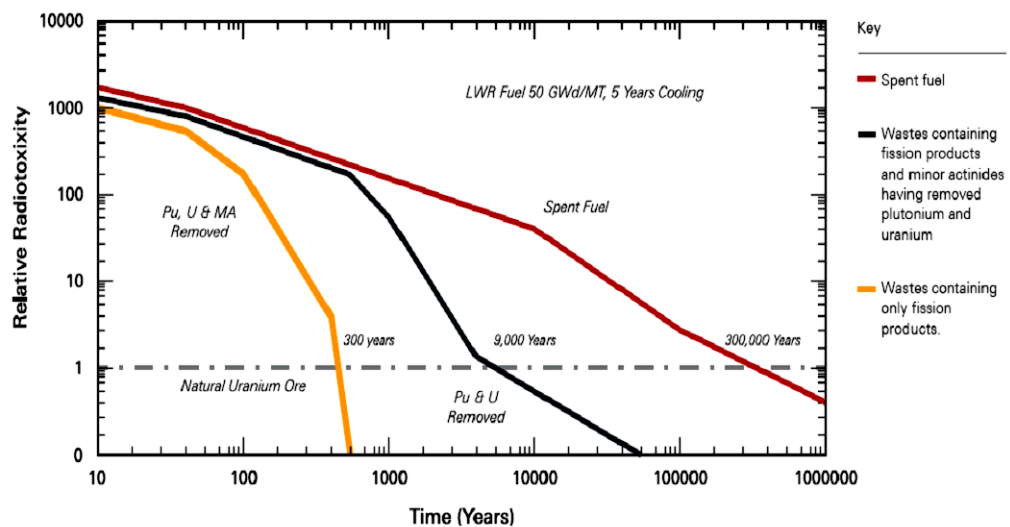
Figure 1.5: Degradation of spent nuclear fuel (red), if Pu and U are removed (grey), and if minor actinides are removed (yellow).[28]

Table 1.1: Approximate composition and half-lives of U, Pu, Np, Am, Cm radioisotopes found in spent nuclear fuel.[32]

Radionuclide	Half Life (years)	Approx. Mass in SNF (Kg)
^{234}U	2.47×10^5	3
^{235}U	7.10×10^8	215
^{236}U	2.39×10^7	114
^{238}U	4.51×10^9	25,700
Total		26,032
^{238}Pu	86	6
^{239}Pu	2.44×10^4	144
^{240}Pu	6.58×10^3	59
^{241}Pu	13	28
^{242}Pu	3.79×10^5	10
Total		247
^{237}Np	2.14×10^6	20
Total		20
^{242}Am	141	0.01
^{243}Am	7950	2.48
Total		3.81
^{242}Cm	163 (days)	0.133
^{243}Cm	32	0.002
^{244}Cm	18	0.911
^{245}Cm	9300	0.055
^{246}Cm	5500	0.006
Total		1.11
Overall		26,303.92

The amounts of uranium and plutonium radioisotopes dwarf the amounts of minor actinides in SNF (Table 1.1). However, the minor actinides cannot be disregarded as they are extremely radiotoxic and are the major thermal contributors to the SNF.[30,33]

The remaining elements present in SNF are the fission and corrosion products, where fission products result from decay chains of fissile material and the corrosion products are a result of the degradation of the fuel cladding and of the steel containment. The various fission and corrosion products are in a higher abundance in the SNF than the actinides, which makes the selective partitioning of the minor actinides into the organic phase during liquid-liquid extraction much more difficult and thus fission and corrosion products must be removed before any minor actinide partitioning can take place.[17,34]

If the minor actinides, along with the uranium and plutonium, could be removed from SNF then the radiotoxicity of the waste would decrease to 300 years to reach a safe level. This poses the problem of how to remove minor actinides in the presence of far higher quantities of the chemically very similar lanthanides. One approach, developed several decades ago, was to use organic ligands that can be dissolved in an organic solvent (odourless kerosene) and mixed with the SNF to extract metal ions selectively from the SNF.[35] An industrial process has been designed to extract uranium, plutonium, minor actinides and lanthanides selectively from an aqueous stream (Scheme 1.1). The Plutonium and Uranium EXtraction (PUREX) process has already been applied in Russia, France and the United Kingdom.[36] The full portioning process is detailed in Scheme 1.1.
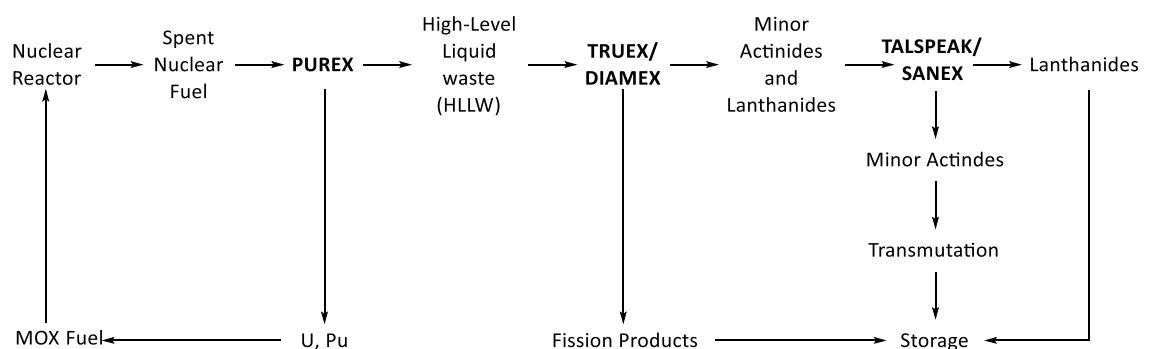
Scheme 1.1: Proposed plan to reprocess SNF.

1.3 Reprocessing Spent Nuclear Fuel

1.3.1 Extraction Methodology

In the investigations discussed below, various techniques to quantify the effectiveness of a ligand during a selective extraction process are outlined. The radioisotopes Eu^{152} and Am^{241} are generally used to represent the lanthanide and actinide series respectively and Cm^{244} is also used to determine actinide-actinide separations.[37,38] In liquid-liquid extraction, where both an aqueous phase containing the metal ions and the organic phase containing the extractant are mixed thoroughly, the **Distribution Ratio, D_M** is the amount of extracted metal present in the organic phase with respect to the metal remaining in the aqueous phase and has no units.

$$D_M = \frac{[M]_{Org}}{[M]_{Aq}}$$

Equation 1.1: Calculation of Distribution Ratios.

Often in liquid-liquid extraction, more than one metal species is present in solution. Therefore, it is possible to measure the relative extraction of one metal compared to another; most commonly Am(III) and Eu(III). The **Separation Factor, SF_{M_1/M_2}** is the ratio of each metal species' distribution ratios (D_M) values and relays the measure of selectivity of the extractant for one metal species over the other, with the larger the separation factor, the more selective the extracting ligand.

$$SF_{M_1/M_2} = \frac{D_{M_1}}{D_{M_2}}$$

Equation 1.2: Calculation of Separation Factors.

Weight distribution ratios, D_w, of solid phase studies are calculated slightly differently to those used in liquid-liquid extractions (**Equation 1.3**). Where A_0 is the activity of the uncontacted aqueous phase before extraction, A_s is the activity of the aqueous phase after extraction, w is the weight of the solid phase extractant and V is the volume of aqueous phase used in the extraction.[39] The D_w represents the ratio of radioactivity of α- and γ- emissions of each radioisotope in the standard solution and the supernatant, and separation factors are calculated as before, $SF_{Am/Eu} = D_{wAm} / D_{wEu}$ or $SF_{Am/Cm} = D_{wAm} / D_{wCm}$.

$$D_w = \frac{(A_0 - A_s)}{A_s} \times \frac{V}{w}$$

Equation 1.3: Calculations for weight distribution ratios.

1.3.2 PUREX Process

Developed in the USA, as a result of the Manhattan project during World War II, the PUREX process removes plutonium and uranium separately from SNF.[36] During the war, obtaining plutonium was the main reason for the separation. Presently however, the uranium is an equally valuable component. For safety reasons, to remove any potential for proliferation, the separated plutonium is mixed with the uranium and converted into enriched mixed metal oxide fuel (MOX).[40]

The process, which is still used in Russia, France, and the UK, employs liquid-liquid extraction chemistries. Here, a solution of tributyl phosphate **1** solution (20-30%) (TBP) in odourless kerosene is used to extract from an acidic 7 M HNO_3 aqueous solution containing $UO_2(NO_3)_2$ and $Pu(NO_3)_4$.[41] TBP **1**, is synthesised using phosphorus oxychloride **2** and *n*-butanol **3** in the presence of pyridine to neutralise the HCl formed (Scheme 1.2). The reaction yields approximately 70% on a 200 g scale and is produced industrially on the tonne scale.[42]
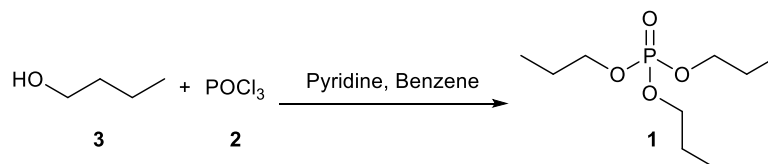
Scheme 1.2: Synthesis of TBP.

TBP **1** extracts uranium and plutonium complexes present in solution in the +6 and +4 states respectively from 3-6 M nitric acid feed in the form of $[M(NO_3)_x(TBP)_2]$ (M = UO_2 or Pu where x = 2 or 4 respectively) (Scheme 1.3).[43] The other metal ions in SNF are only weakly bound to TBP therefore, they are not extracted into the organic phase.

TBP **1** extracts uranium efficiently ($SF_{U/Fission\ Products} \approx 250$) and plutonium ($SF_{Pu/Fission\ Products} \approx 60$) at 28% saturation of **1** with optimal $[HNO_3]$ at 2-3 M to maximise separation from fission products.[44] The only downside to the PUREX process is that small quantities of neptunium and technetium are extracted with the uranium and plutonium. The impurities must be separated, before the uranium and plutonium can be used as fuel.[45]
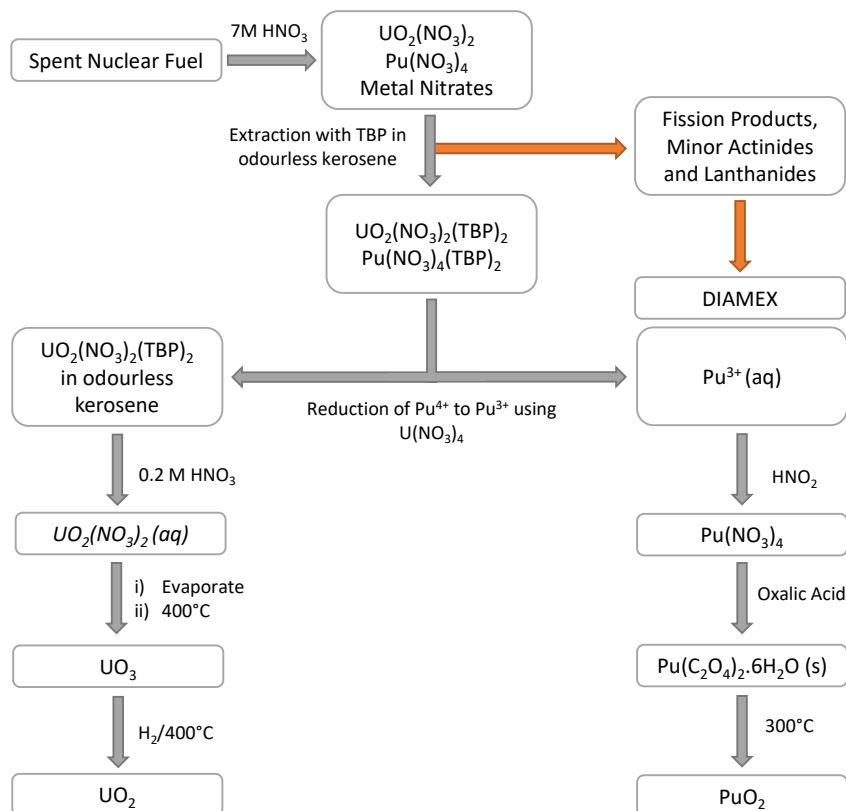
Scheme 1.3: PUREX extraction diagram.[46]

13

1.3.3 DIAMEX and TRUEX Processes

Europe and America have different methods regarding the treatment of post-PUREX raffinate. Europe's approach utilises a diamide extraction process (DIAMEX). Developed by the French Commissariat d'Énergie Atomique (CEA), the process uses nonselective bidentate malondiamides to extract all lanthanides and the minor actinides from unwanted fission products.

Presently, the ligands used in the DIAMEX process are *N,N'*-dimethyl-*N,N'*-dioctyl[(hexyloxy)ethyl]-malonamide (DMDOHEMA) **4** and *N,N,N'N'*-tetraoctyldiglycolamide (TODGA) **5** as shown in Scheme 1.4.[47] Structural modification of TODGA **5** resulting in dimethyl-TODGA **6** has shown performance increases in hot tests on actual PUREX high level liquid waste. The methyl groups on TODGA **6** appear to slow degradation due to the highly acidic environment which is proposed to be due to a reduced propensity towards enolization. If this is indeed the case, potentially tetramethyl-TODGA **7** would further slow the degradation.[17]
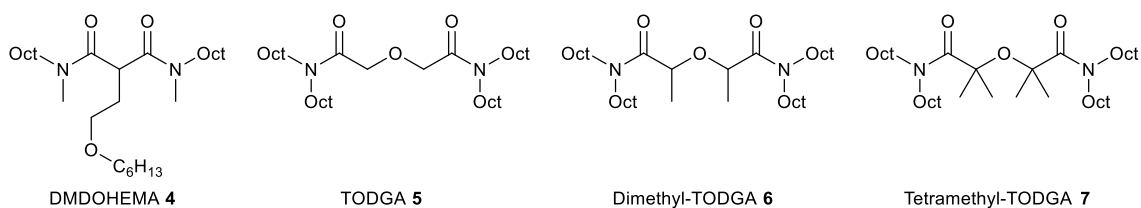
Scheme 1.4: Ligands used in DIAMEX Processes.

DMDOHEMA **4** can be synthesised using a convergent synthetic route, where diethyl malonate **8** is converted to compound **10** by heating to reflux in the presence of *N*-methyloctan-1-amine **9** (Scheme 1.5). Separately, 1-bromohexane **11** undergoes etherification with ethylene glycol, where the alcohol product **12** is tosylated to afford **13** (Scheme 1.5). Reacting both **10** and **13**

together with sodium hydride as base, yields DMDOHEMA **4** in 26% overall yield over the longest route.[48]
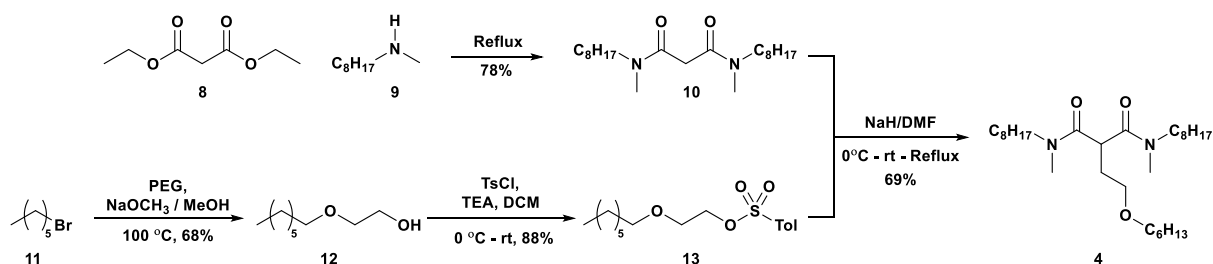
Scheme 1.5: Synthesis of DMDOHEMA from commercial materials.

Extraction results on simulated PUREX raffinate showed good selectivity towards the f-block metals in the presence of metals from periods V and VI. Non-f-block metals showed distribution ratios between 0.001 (Rb) and 1.74 (Y); whereas the distribution ratios for f-block metals proved higher between 3.6 (Gd) and 8.8 (^{241}Am). Leading to minimum separation factors of $SF_{Ga/Y}$ = 2.07 and maximum separation factors $SF_{Am/Rb}$ = 8800.[49]

The TRUEX, transuranic extraction process, was developed by the Argonne National Laboratories, USA, wherein carbamoylmethylphosphine oxide (CMPO) **14** is used to extract trivalent actinides and lanthanides from the PUREX stream (Figure 1.6).[36]
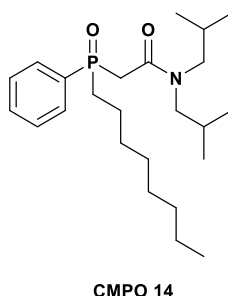
CMPO 14

Figure 1.6: TRUEX Ligand, Carbamoylmethylphosphine (CMPO) 14.

Trivalent actinides are extracted using a 0.2 M concentration of CMPO **14** with 1.2 M *n*-dodecane and TBP **1** to inhibit the formation of a third phase and reduce degradation of CMPO

14. Increasing [HNO_3] reduces the separation factor between the f-block metals and the fission products. Distribution ratios of the f-block elements occur between 12 (Am) − 5.3 (La); whereas, the maximum distribution ratio from the fission products belonged to yttrium (D = 3.1). [36,36]

The key difference between the TRUEX and DIAMEX processes is that the latter process obeys the "CHON rule"; whereby ligands should only contain the elements of carbon, hydrogen, oxygen, and nitrogen. This prevents the production of corrosive acidic products upon the incineration of the ligands when their lifetime has reached its limit.[50]

The final step in the clean-up would be to separate the minor actinides from the lanthanides so that the minor actinides can be used as fuel in the new Generation IV reactors and transmuted to non-fissile or short half-life species. The lanthanides have a higher neutron cross-capture radii; resulting in increased shielding of the actinides from the neutrons in the transmutation process acting as 'neutron poisons'.[51,52]

1.3.4 TALSPEAK Process

The Trivalent Actinide Lanthanide Separation with Phosphorus reagent Extraction from Aqueous Komplexes or TALSPEAK process was developed in the 1960s by Boyd Weaver at the Oak Ridge National Laboratory.[53] The process involved separating the lanthanides from the actinides in post-PUREX raffinate. The TALSPEAK process incorporates the use of di-(2-ethylhexyl)phosphoric acid (DEHPA) **15** in 1,4-diisopropylbenzene **16** as extractant and diluent respectively, but also requires a buffer, diethylenetriamine-*N,N,N,N',N'',N''*-pentaacetic acid (DTPA) **17**, which acts as a selective-actinide holdback reagent.

<div align="center">

Di-(2-ethylhexyl)-phosphoric acid
(DEHPA)
15

diethylenetriamine-*N,N,N',N'',N''*-pentaacetic acid
(DTPA)
17

1,4-diisopropylbenzene
16

</div>
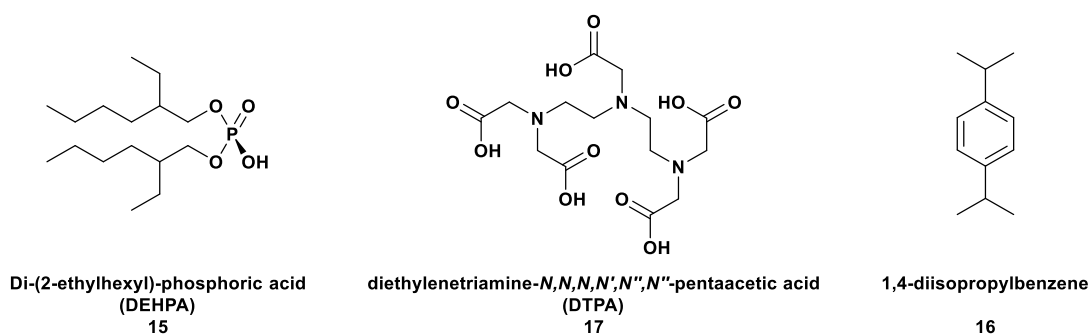
Figure 1.7: Structures of molecules used in the TALSPEAK process.

Synthesis of the phosphoric acid **15** is facilitated by hydrolysis of trisubstituted phosphate esters **18**, using 2 M sodium hydroxide. Unfortunately, both mono- **19** and di-substituted phosphate esters **15** are formed but can be separated by virtue of their relative solubilities (Scheme 1.6). DTPA **17** and 1,4-diisopropylbenzene **16** are both available commercially.[54]
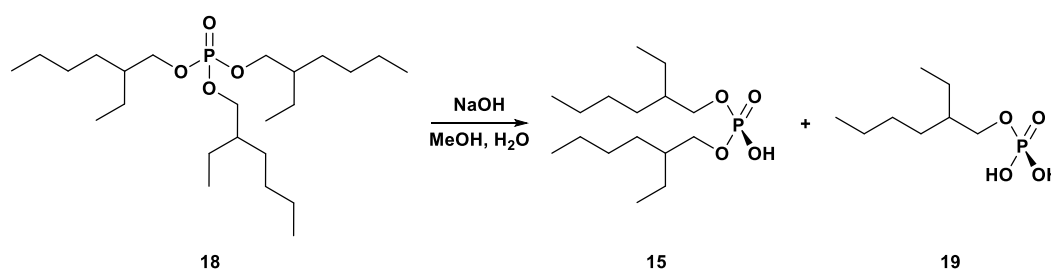
Scheme 1.6: Synthesis of DEHPA by hydrolysis.

Extraction studies show efficient separation of Am^{3+} from Nd^{3+} (limiting pair) with approximate separation factors of 100, with all lanthanides separated from Am^{3+}. However, the process has not been scaled up to an industrial level because rigid control of pH is necessary and phase-transfer kinetics are not ideal. Therefore, high concentrations of buffer (0.5-2 M H/buffer) are required.[55] Whilst TALSPEAK is preferred in the USA, in Europe an arguable more robust process has been developed, the SANEX process.

1.3.5 SANEX Process

The selective actinide extraction process (SANEX) has been adopted in Europe to separate the minor actinides from the lanthanide species in feed from the DIAMEX process. This process is currently in development and is the focus of attention of many European agencies and universities.

For a ligand to qualify for the SANEX process, a set of stringent criteria must be satisfied. Both the ligand, and ligand-metal complexes must be soluble in odourless kerosene.[56] The selectivity of the ligand must be so that the actinide : lanthanide separation factor must be greater than 5 : 1. However, for the process to be useful, stripping of the metal from the ligand must be easily achieved, preferably without destroying the ligand in the process. The ligand must also be able to withstand strong acidic (*circa.* 4M HNO_3) conditions of the post-PUREX process raffinate and the intense radiolytic flux of the post DIAMEX feed. Furthermore, the ligand must be readily synthesized from commercially available materials in a process that is scalable. Lastly, the ligand should abide by the CHON principle, so safe disposal can be facilitated by incineration, without producing acidic by-products that could damage equipment. Ligands with nitrogen or sulfur electron donors have been seen to be more selective due to the covalent nature of the bonds formed between the metal and the ligand, and their inclusion has been central in design of ligands.[57,58]

1.3.6 *i*-SANEX and GANEX

Alongside the development of the SANEX process, several other processes have been proposed, with *i*-SANEX and GANEX gaining the most traction out of many.[59] *i*-SANEX or innovative-SANEX was developed at the Karlsruhe Institute of technology by Geist *et al*; where ligands used in the DIAMEX process are used to extract all actinide(III) and lanthanide(III) ions

followed by selectively stripping the elements with another hydrophilic ligand. The hydrophilic ligands chosen was a sulfonated bistriazine bipyridine ligand (BTBP's) that will be discussed later in section 1.4.[60,61]

Group actinide extraction or GANEX revolves around the co-extraction of the trans-uranic elements (Np, Pu, Am, Cm) directly from the spent nuclear fuel already dissolved in 7M HNO_3. The GANEX process is postulated to run on uranium-free SNF, i.e. post-PUREX raffinate. The main advantage of GANEX is the removal of many processing steps, such as DIAMEX and SANEX saving the economical strain of building these processing plants. The ligands intended for use, are TODGA and DMDOHEMA or a BTPhen system with a variety of additives.[62,63]

1.4 Ligands for SANEX

1.4.1 *S*-Donor Ligands

Although the remit for SANEX was to eliminate the use of any ligand/material that contained elements other than carbon, hydrogen, oxygen and nitrogen, earlier examples of actinide selective ligands were *S*-donor ligands.[64] Dithiophosphinic acids **22-25** (Figure 1.8) are commercially available acids that were tested for their extraction properties against Am(III) and Eu(III) and demonstrated high separation factors of up to $SF_{Am/Eu}$ >4000.[65] However, when **23** was combined with basic *N*-donor ligands such as 2,2'-bipyridine and 1,10-phenanthroline the selectivity increased ($SF_{Am/Eu}$ >30,000 at pH 3.7).[64] Unfortunately these ligands showed rapid degradation under γ-radiation and were not stable at high [HNO_3].[66]

R= **20** n-octyl,
21 1-methylheptyl,
22 2-ethhylhexyl,
23 2,4,4-trimethylpentyl
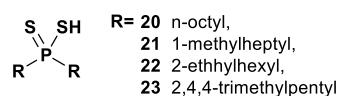
Figure 1.8: Dithiophosphinic acids

1.4.2 *N*-Donor Ligands

One of the earlier heterocyclic *N*-donor ligands developed used the 2,2':6',2'-terpyridine **24** (TERPY) backbone. The ligand **24** was able to extract actinide metals from weakly acidic systems in the presence of 2-bromodecanoic acid.[67–69] However, increasing the acidity of the system showed decreased distribution ratios of actinides and poor solubility in many of the proposed organic solvents. Modifications were made to alleviate the solubility issues by adding bulky t-butyl groups **25** or, long carbon chains **26** but the increase in basicity led to protonation of the heterocycles and the precipitation of the protonated ligand.[30,70]

TERPY
24

Tri-*t*-Butyl-TERPY
25

Dioctyl-TERPY
26
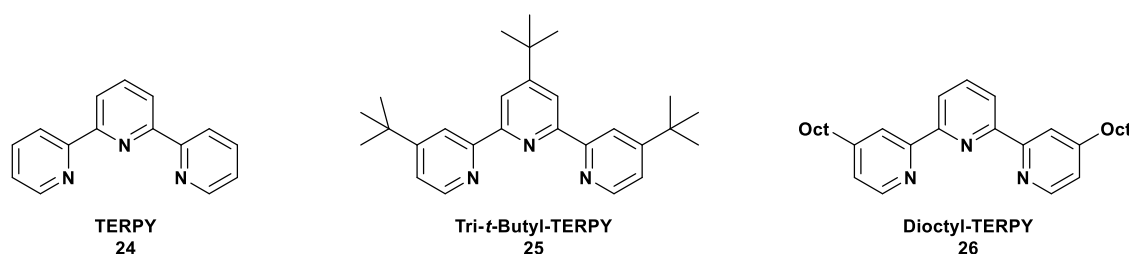
Figure 1.9: Structures of common TERPY ligands.

Following on directly from the TERPY ligands **24-26** were the 2,4,6-tri-2-pyridyl-1,3,5-triazine **27** (TPTZ) ligands (Figure 1.10) with the aim to lower the basicity of the overall ligand.[50,57] When tested for liquid-liquid extraction studies TPTZ **27** showed greater distribution ratios than TERPY **24** and was one of the first *N*-donor ligands to have a separation factor of SF$_{Am/Eu}$ > 10, although still at low [HNO$_3$]. The persistent issue that had plagued the TERPY **24** ligand, of being protonated in high concentrations of acid was still prevalent in the TPTZ ligands.[35,57,58]

TPTZ
27

Trimethyl-TPTZ
28

Tri-*t*-butyl-TPTZ
29
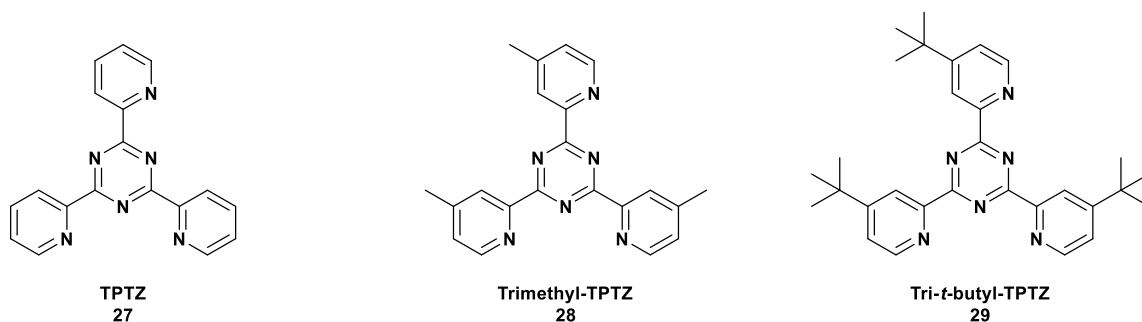
Figure 1.10: TPTZ ligands 27-29.

1.4.3 BTP Ligands

At this time, the primary issue with the *N*-donor ligands was the basicity of the ligands, and it was thought that, by using the 1,2,4-triazine moiety, a lower basicity could be achieved due to a phenomenon known as the α-effect; wherein an lone pair bearing atom would show increased nucleophilicity if α- to it was another atom with a lone pair, without increasing the basicity of the original atom.[71] The principle behind this phenomenon is due to the unshared lone pair raising the HOMO of the adjacent atom, leading to an increased affinity for soft cations and decreased affinity for protons. The increased overlap of orbitals between the non-binding lone pair and the binding lone pair increases the covalent nature of the bond.[72]

Thus, the ligand backbone of the 2,6-bis(1,2,4-triazin-3yl)pyridine (BTP) ligands was developed. The original synthesis of the BTP ligands was reported in 1971 by Case, where he took pyridine-2,6-dicarbonitrile and treated it with hydrazine hydrate to lead to the corresponding bis-aminohydrazide, subsequently reacting with *vicinal* diketones to allow a variety of BTP ligands to be synthesized (Scheme 1.7).[73]

The reduced level of protonation led to the BTP ligands **32** showing high $SF_{Am/Cm} > 100$ at high [HNO_3] (1-4M) without the need for additives. The synthesis of these ligands allowed for a multitude of different substrates to be attached to the southern triazine moiety that led to increases in the solubility of the ligand **32-37**.[74] In the solvent extraction studies, as the concentration of the ligand was increased, the rate of extraction increased proportionately. However, above 1M HNO_3 the extraction decreased as a result of the protonation of the ligand. Unfortunately, the ligand showed major degradation when submitted to a hot test using PUREX raffinate.[75]

21
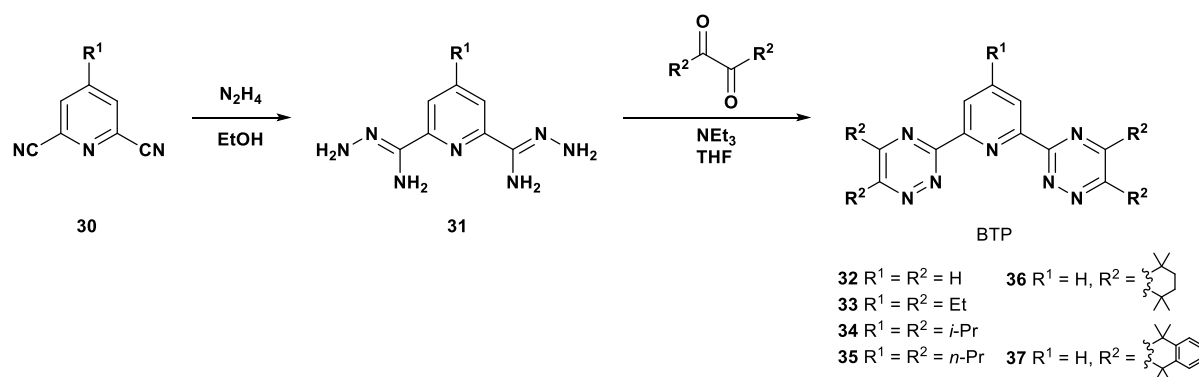
Scheme 1.7: Synthesis of BTP ligands.

The Harwood group hypothesized that the presence of benzylic hydrogen atoms on the side chains of the triazine rings were likely to be susceptible to homolytic cleavage by hydroxy radicals formed in the raffinate as a result of radiolysis.[50,67] Therefore, it was decided to eliminate all benzylic positions on the ligand and future ligands to minimise the degradation. The first attempt at limiting degradation was to use t-butyl groups in the alkyl positions on the triazine rings. However, attempts at condensation resulted in no conversion to the desired product (Scheme 1.8). This was rationalized that the energy of rotation barrier by the 1,2-diketone **39** was too high and it remained in the *trans-* conformation and not the *cis-* conformation needed for the reaction to occur.[76]
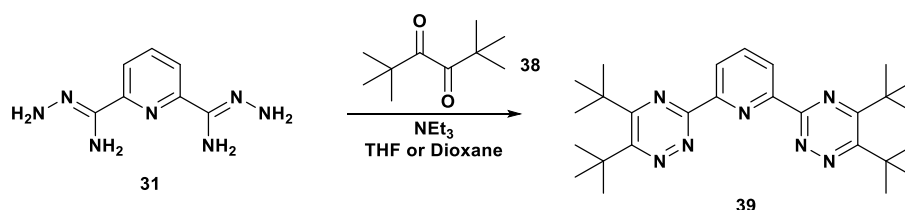
Scheme 1.8: Attempted condensation reaction of di-*tert*-butyldiketone 39 with BTP Bisaminohydrazide 31.

It was suggested that, to alleviate the high energy rotation barrier, the di-*tert*-butyl moieties should be locked into their *cis*-conformer by tying them into a ring, this led to the formation of the CyMe$_4$ moiety. The ligand showed excellent stability towards nitric acid withstanding

22

boiling 3M HNO_3 and a benzylated variant of the $CyMe_4$-BTP **36** showed good stability to γ-degradation with a dose of 100 kGy.[33]

The cyclic *vicinal* diketone **43** can be synthesised from ethyl isobutyrate **40** by forming the enolate using LDA and reacting with the ditosylate of ethylene glycol. Using molten sodium in the presence of trimethylsilyl chloride, an acyloin ring closure is performed cyclohexene bis-trimethylsilyl enol ether **42**, which is subjected to an oxidative cleavage to form the desired diketone **43**.
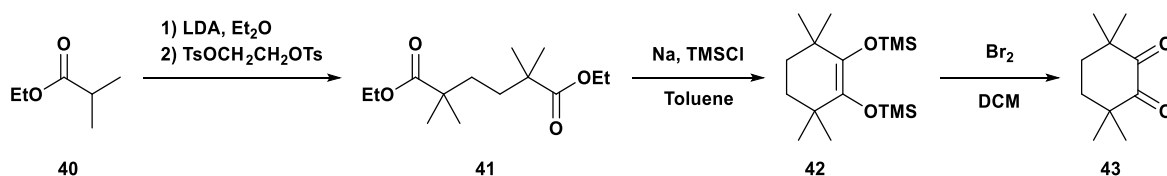
Scheme 1.9: Synthesis of CyMe$_4$-Diketone

Liquid-liquid extraction studies of $CyMe_4$-BTP **36** showed acceptable extraction kinetics with high distribution ratios (*ca.* 500) and high separation factors ($SF_{Am/Eu} > 5000$). However, the ligand exhibited a high binding efficiency and therefore, back extracting/stripping the ligand of the metal was inefficient. The cause of this was discovered when metal complexes with the ligand were found to be 3:1 ligand : Ln(III) (Figure 1.11). As a result the 9-coordinate metal had no vacant sites for interaction the glycolic acid stripping agent.[52,77]

23
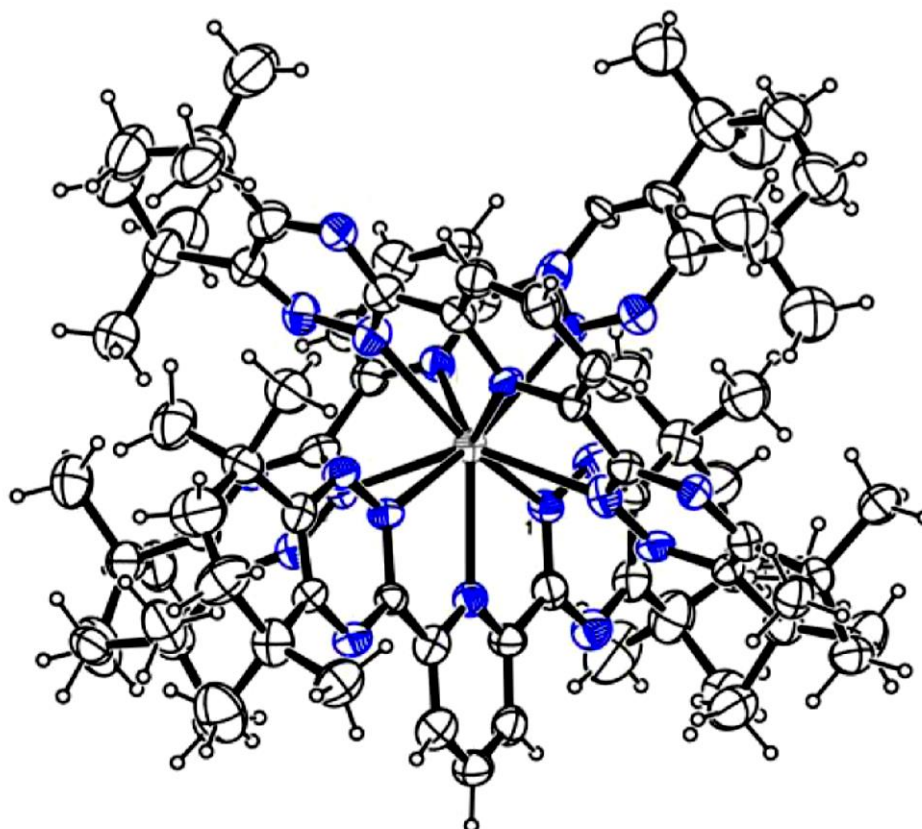
Figure 1.11: X-Ray crystallographic structure of [Y(CyMe$_4$-BTP]$_3$.[Y(NO$_3$)$_5$].NO$_3$, counterions and solvent have been omitted for clarity. Blue = nitrogen. See ref. for crystallographic details.[78]

1.4.4 BTBP Ligand

To alleviate the crowding around the metal centre a larger ligand was needed so that the stripping agents could bind to the metal in the complex for back extraction. Hence, swapping the pyridine core of the BTP to the bipyridine was considered to be the path forward. The now tetradentate ligands allowed a weaker ligand field resulting in 1:1 and 1:2 complexes and therefore leaving room for back-stripping with glycolic acid.[67,79]

CyMe$_4$-BTBP **53** was initially synthesised using a four-step process starting from 2,2'-bipyridine **44** (Scheme 1.10). Bis-N-oxidation of 2,2-bipyridine **44** using hydrogen peroxide and acetic acid leads to bis-2,2'-pyridine N-oxide **45**. A Reissert-Henze cyanation reaction with trimethylsilyl cyanide and benzoyl chloride produces the dinitrile **46**. Following this, the

dinitrile is reacted with hydrazine in ethanol to form the bis-aminohydrazide **47**. Reacting with

the CyMe$_4$-diketone **43** in the presence of triethylamine in tetrahydrofuran yields CyMe$_4$-BTBP

53.[80]
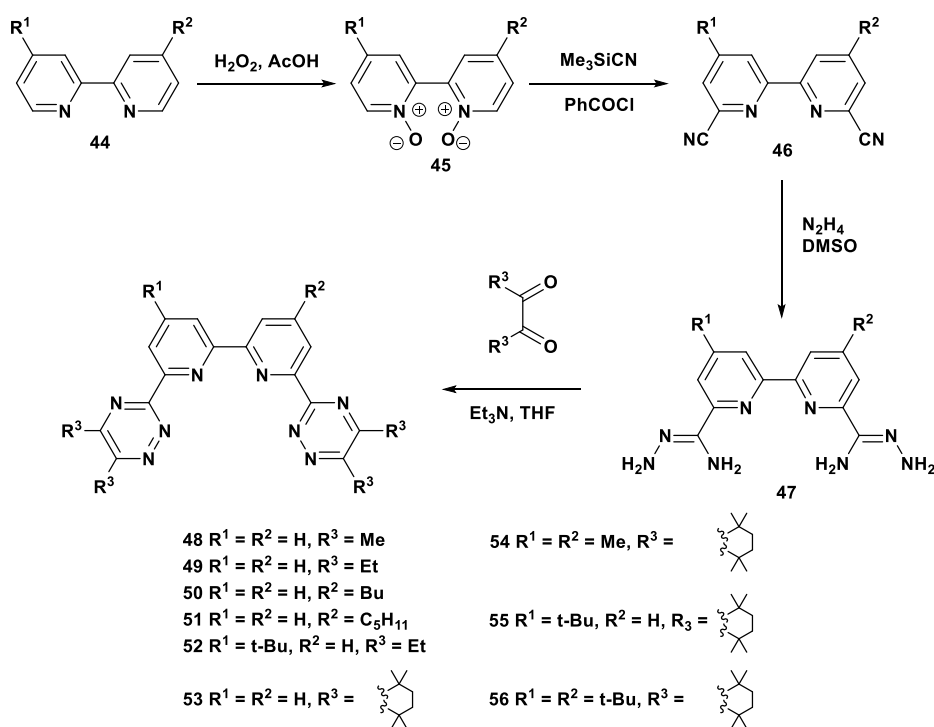
Scheme 1.10: Synthesis of CyMe$_4$-BTBP 1.

Studies showed that CyMe$_4$-BTBP **53** would preferentially extract Am(III) to Eu(III) in 3 M nitric

acid with high distribution ratios of Am(III) (*ca.* 650) and high selectivity for actinides over

lanthanides with separation factors *ca.* 150 from 1M HNO$_3$ solutions.[52,77,80–83] CyMe$_4$-BTBP **53**

also showed considerable resistance to degradation, enduring exposure to 1 M nitric acid for

2 months.[82]

However, the rate of ligation was slow, and needed to be improved. Therefore, DMDOHEMA

4 was added to the organic phase to improve kinetics, despite any such additives being

undesirable. The poor kinetics of extraction were clarified by computational mechanics

studies that supported the proposal by the Harwood group that the lowest energy conformer

state was where the carbon-carbon bond between the pyridines was rotated 180° from the binding conformation depicted in Scheme 1.11.[79]
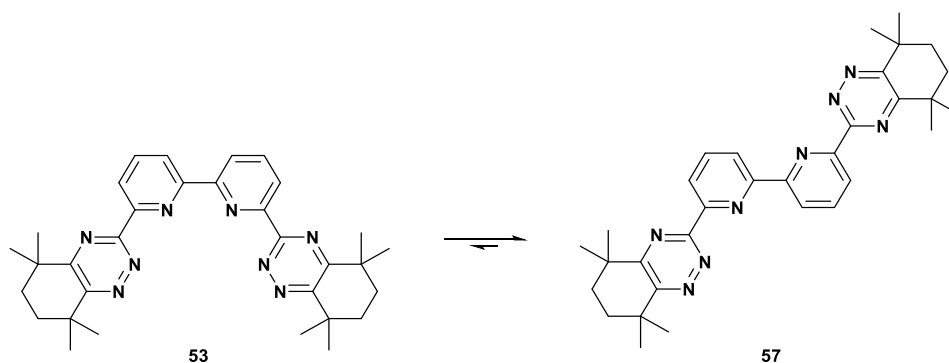
Scheme 1.11: Structure of CyMe$_4$-BTBP 53.

CyMe$_4$-BTBP **53** in the presence of TBP **3** has been shown to extract Am, Pu, Np and U into cyclohexanone from 4 M nitric acid. This leads to the possibility of a GANEX (group actinide extraction) process that could be applied to post PUREX feed, which could then bypass the DIAMEX process entirely.[83]

Structures of the BTBP ligand **53** complexed with lanthanides have been analysed by single crystal X-ray crystallography (Figure 1.12). The analysis performed by Harwood *et al.* showed two near perpendicular CyMe$_4$-BTBP **53** ligands ligating to the lanthanide complex each in a tetradentate fashion. A single bi-dentate nitrate ion was also seen coordinating with the metal in the inner sphere of the lanthanide. Rather than the 9-coordinate complex for BTP **36** shown earlier (Figure 1.11) the BTBP ligand was a 10-coordinate complex as well as a 2:1 rather than 3:1 complex.
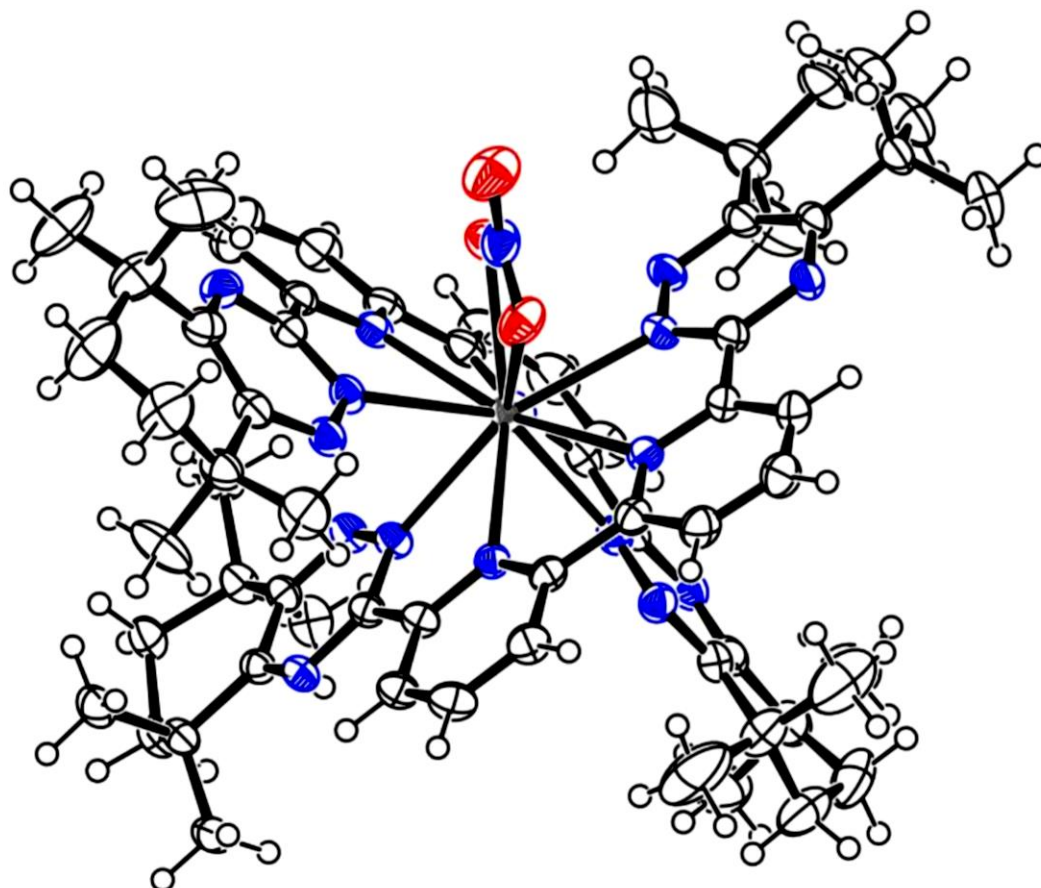
Figure 1.12: X-ray crystallographic structure of [Eu(CyMe₄-BTBP)₂(NO₃)].[Eu(NO₃)₅]. Counter ions and solvent molecules have been omitted for clarity. Blue = Nitrogen and Red = Oxygen.

CyMe₄-BTBP **53** was also studied against post-DIAMEX raffinate in a laboratory scale extraction test. Centrifugal separators (9 for extraction, 4 for stripping and 3 for scrubbing) were used at the Institute for Trans-Uranic Elements (ITU) in Karlsruhe in Germany and the study showed encouraging results, CyMe₄-BTBP **53** paired with DMDOHEMA **4** in 1-octanol recovered 99.9% of both Am(III) and Cm(III) from the DIAMEX raffinate. When **53** was paired with TBP in PUREX conditions with the dissolved SNF, Am (III), Pu (III), Np (III), and U (III) were selectively extracted, which would later spawn the idea of a GANEX process (see section 1.3.6). As a result of these tests, CyMe₄-BTBP **53** is widely recognized as the European benchmark for all SANEX ligands.[52,82]

1.4.5 BTPhen Ligands

The slow rate of extraction of CyMe$_4$-BTBP **53** was considered to be due to the need for rotation around the carbon-carbon single bond between the pyridine rings of the free ligand resulting in a higher energy binding conformation (Scheme 1.11). Therefore, to restrict the ligand in its binding conformation, Lewis, while working in the Harwood group, suggested introducing a third aromatic ring to block any rotation, leading to the study of phenanthroline-based ligands.[83]

CyMe$_4$-BTPhen **72** can be synthesised from neocuproine **58** in six steps. Treating neocuproine with benzoyl peroxide in the presence of recrystalised *N*-chlorosuccinimide in chloroform led to the formation of the bis-1,10-trichloro **59** compound. Treating **59** with sulfuric acid followed by methanol yielded the bis-methyl ester **60** and reacting that product with ammonium hydroxide and ammonium chloride furnished the diamide **61**. Dehydration of the diamide by treatment with oxalyl chloride in DMF led to the dinitrile **62**. Subsequent steps followed the synthetic route used to synthesise CyMe$_4$-BTBP **53** wherein addition of hydrazine hydrate to the dinitrile produced the bis-hydrazine hydrate **63**, which then was condensed with the CyMe$_4$-diketone to give the target ligand CyMe$_4$-BTPhen **72**.[84]

Extraction studies showed that CyMe$_4$-BTPhen **72** in octanol separated Am(III) and Eu(III) extremely efficiently, with high distribution ratios for americium ($D_{Am} > 1000$) and low values for europium ($D_{Eu} < 10$). The high distribution ratios showed that the new CyMe$_4$-BTPhen ligand **72** was more two orders of magnitude more efficient that the previous CyMe$_4$-BTBP ligand **53** whilst still maintaining the high separation factors (SF$_{Am/Eu}$ = 200 − 400) from acidic solutions (1 − 4M HNO$_3$. Furthermore, the extraction kinetics were faster than CyMe$_4$-BTBP

53, approximately 15 mins compared to >60 mins for **53** with no phase transfer additive required, unlike with the BTBP ligand **53**.[83]
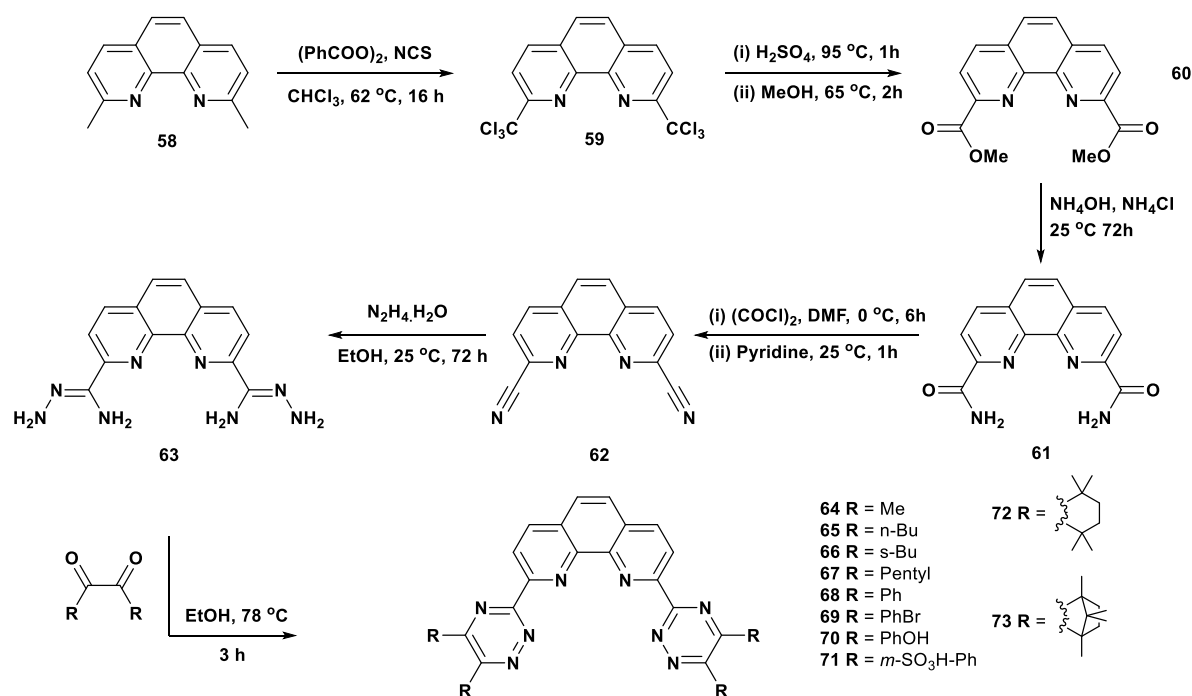
Scheme 1.12: Synthesis of CyMe$_4$-BTPhen.

Likewise with the previous BTBP metal complexes, single crystal X-ray studies of CyMe$_4$-BTPhen **72** with lanthanides showed them to exist as 2:1 complexes, and the metal centre to be 10-coordinate, ligating with two tetra-dentate ligands and one bidentate nitrate ion in the inner sphere. The studies also showed that there is sufficient space for stripping ions to coordinate to displace the metal from the ligand.[85]

Harwood *et al.* subsequently reported the X-ray structure of a CyMe$_4$-BTPhen complex with a 1:1 ratio of metal to ligand, although the metal used was yttrium. Whilst yttrium is a transition metal, the element behaves similarly to the lanthanides and is considered a rare-earth element surrogate by many.[86,87] The BTPhen **72** 1:1 complex was found to contain three bidentate nitrate ions in the inner sphere of the complex.[83] This was later supported by collaborative work by Harwood with Whitehead *et al.* in 2017 on complexing CyMe$_4$-BTPhen **72** with europium.[88]
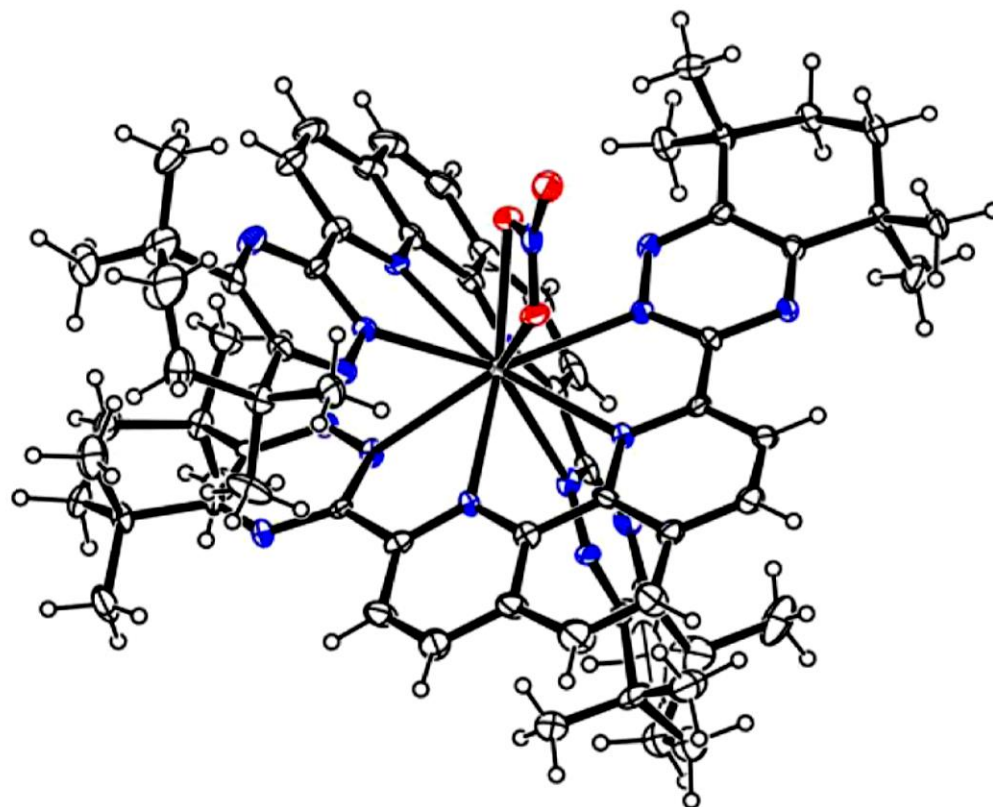
Figure 1.13: X-Ray crystal structure of [Eu(CyMe₄-BTPhen)₂(NO₃)].[Eu(NO₃)₅]. Counter-ions and solvent molecules have been omitted for clarity. Blue = nitrogen and red = oxygen.[85]
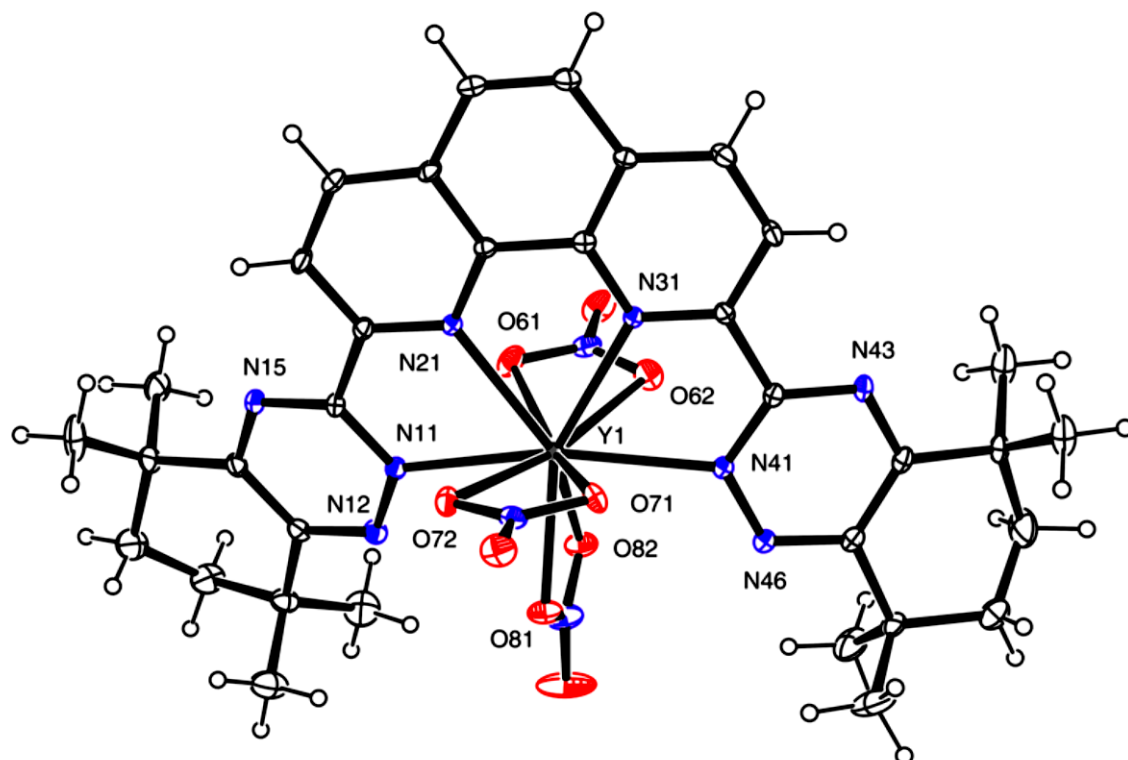
Figure 1.14: X-Ray crystal structure of [Y(CyMe₄-BTPhen)₂(NO₃)].[Eu(NO₃)₅]. Counter-ions and solvent molecules have been omitted for clarity. Blue = nitrogen and red = oxygen.[85]

1.5 Radiolytic Degradation of the SANEX Ligands

The ligands suggested for use in the SANEX process, and indeed all the ligands used in the reprocessing of spent nuclear fuel, undergo radiolytic degradation in aqueous nitric acid of some nature. Each ligand that is to be employed at any stage of the process, must have the degradation pathways mapped and analysed for any potential negative effects so that they can be understood before any partitioning can occur on the industrial scale.

There are three methods of degradation of ligands in each system. The first being by acid hydrolysis from the 1-7M HNO_3 present in the system in which the SNF is dissolved. This type of degradation is easiest to ascertain by exposing the ligand to nitric acid of known concentration at the proposed temperature of the process and monitoring by NMR spectroscopy and mass spectrometry. CyMe$_4$-BTP **36** and CyMe$_4$-BTBP **53** both passed the acid stability tests with no degradation seen. Indeed the BTBP ligand **53** survived prolonged boiling in 3M nitric acid.[89]

The other two types of degradation are stem from the radiation from the metal ions present in the solutions. Direct radiolysis (sometimes referred to as primary radiolysis) results from interactions due to direct energy transfer from the radiation/radiation source to a molecule; whereas indirect radiolysis is caused by the reactions between a molecule and either species formed from direct radiolysis, in aqueous systems commonly the hydroxyl radical.[78,90] As a result, indirect radiolysis will continue after the radiation source has been removed from the solution, until all chain reactions are terminated.

In general, laboratory scale testing has been carried out at 5-10 mM solutions of the ligand in the diluents therefore, it is most likely that the degradation that is experienced is indirect and the diluent in used in the test absorbs most of the radiation undergoing primary radiation.[91,92]

Therefore, it is crucial to choose a solvent that has good radiostability to ensure the lifespan of the both the ligand in use.

In a SANEX type process, the estimated dose of radiation to the organic phase is between 29 and 14300 Gy/h,[93] depending on the fuel being processed and the rate at which it was used when generating power. Therefore, on an annual basis the dose can be from 250 kGy and 125,000 kGy (See footnote [i])[92] and any ligand proposed for a continuous SANEX process, must show as little degradation as possible.

1.5.1 Irradiation of CyMe$_4$-BTBP

CyMe$_4$-BTBP **53** has been subjected to a variety of irradiation studies, each investigating the effects of irradiation on the ligand.[93–99] Schmidt *et al.* irradiated samples of **53** in 1-octanol with and without the presence of an 1M HNO$_3$ phase and, at prescribed intervals, measured D_{Am} and D_{Eu} values. It was found that, when in contact with the aqueous phase, the distribution ratios stayed mostly constant across the $0 - 300$ kGy test. However, when the aqueous phase was not present, both D_{Am} and D_{Eu} decreased toward zero, although, the D_{Eu} decreased quicker than the D_{Am} (Figure 1.15).
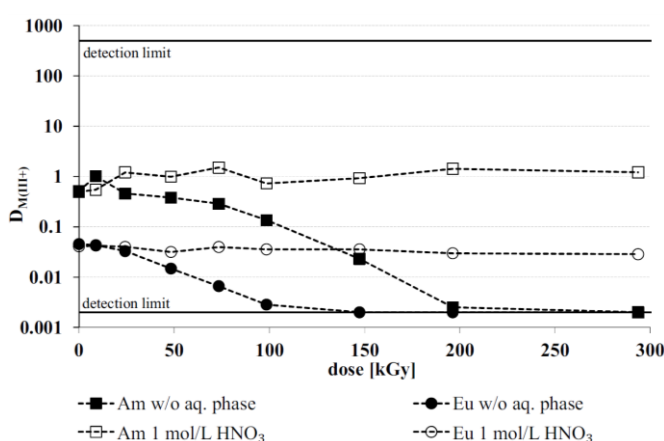
Figure 1.15: Distribution ratios against increasing amounts of irradiation of CyMe$_4$-BTBP 53 in 1-octanol.

---

i) The Gray (Gy) is a unit of ionizing radiation, where 1 Gy is defined as when 1 Joule of radiation energy is absorbed by 1 kg of matter.

The sample irradiated with 100 kGy, as analysed by Schmidt *et al*. (Figure 1.16), showed that **53** was degrading but also indicated that a pathway of indirect degradation where the irradiated solvent was reacting with the ligand was taking place and not the direct radiolysis. The diluent, 1-octanol, was shown to add to the ligand increasing the molecular weight by 130 Da, corresponding to the molecular weight of 1-octanol. It was also shown that the presence of *bis*-solvated ligands were present and very small quantities of *tris*-solvated species. Interestingly, degradation in the presence of an aqueous phase was vastly reduced, showing fewer adducts. Horne *et al.* proposed this phenomenon to be due to the formation of NO_3 radicals, which are approximately 2 orders of magnitude slower at degrading BTP **36** and BTBP **53** ligands.[99]
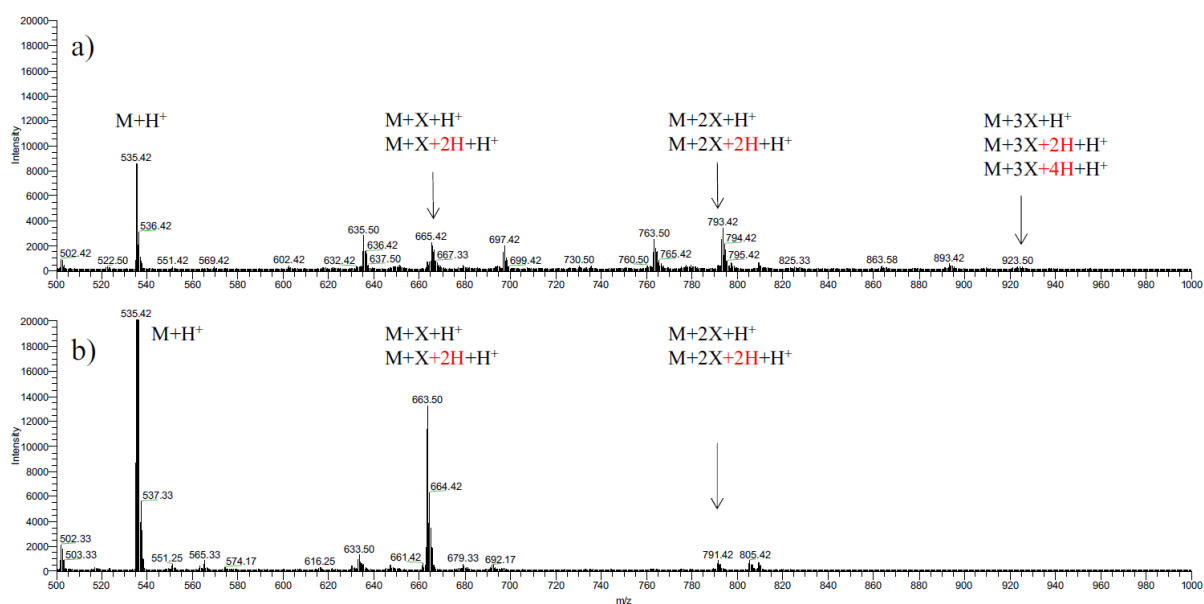
Figure 1.16: Mass spectra of irradiated CyMe$_4$-BTBP 53, a) Irradiation without contact with 1M HNO$_3$ phase, b) Irradiation of CyMe$_4$-BTBP 53 when in contact with 1M HNO$_3$.

1.5.2 Irradiation of CyMe$_4$-BTPhen

There have been fewer irradiation studies of CyMe$_4$-BTPhen than BTBP. However, the same study by Schmidt *et. al.* showed interesting results (Figure 1.17). When irradiated, the vast

majority of ligands become less efficient with the extraction of actinides; whereas CyMe$_4$-BTPhen showed improved extraction capabilities for Am(III) against Eu(III) when the aqueous phase was present, reaching the detection limit of the equipment used. The reasoning presented was attributed to the radiolytic build-up of the extracting species although Harwood has proposed that it could be attributed to the increase in solubility of the degraded ligands, increasing the extraction capabilities. It should also be noted that this effect did not occur when the aqueous phase was not present, but a slower decline in extraction was seen between 0 – 25 kGy.
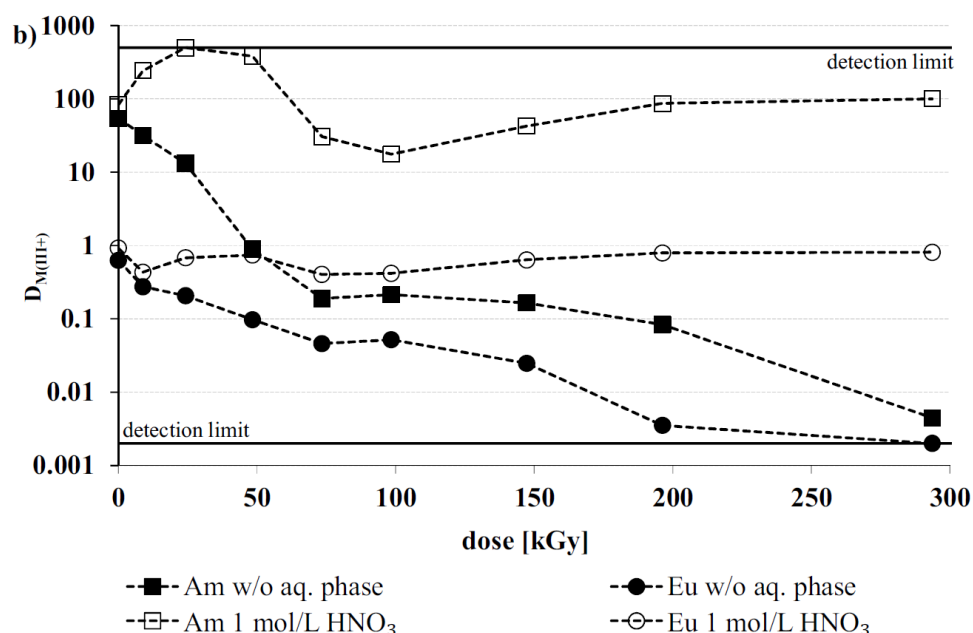
Figure 1.17: Distribution ratios of CyMe$_4$-BTPhen 72 with increasing irradiation with and without an aqueous phase.

When submitted for mass spectrometric analysis, the ligand shared very similar characteristics with the degraded CyMe$_4$-BTBP **53** ligand, where indirect radiolysis was indicated, with the ligand reacting with irradiated solvents forming BTPhen-solvent adducts. Again, there were fewer degraded adducts when the 1M HNO$_3$ was present, probably due to the reasons stated above in section 1.5.1.
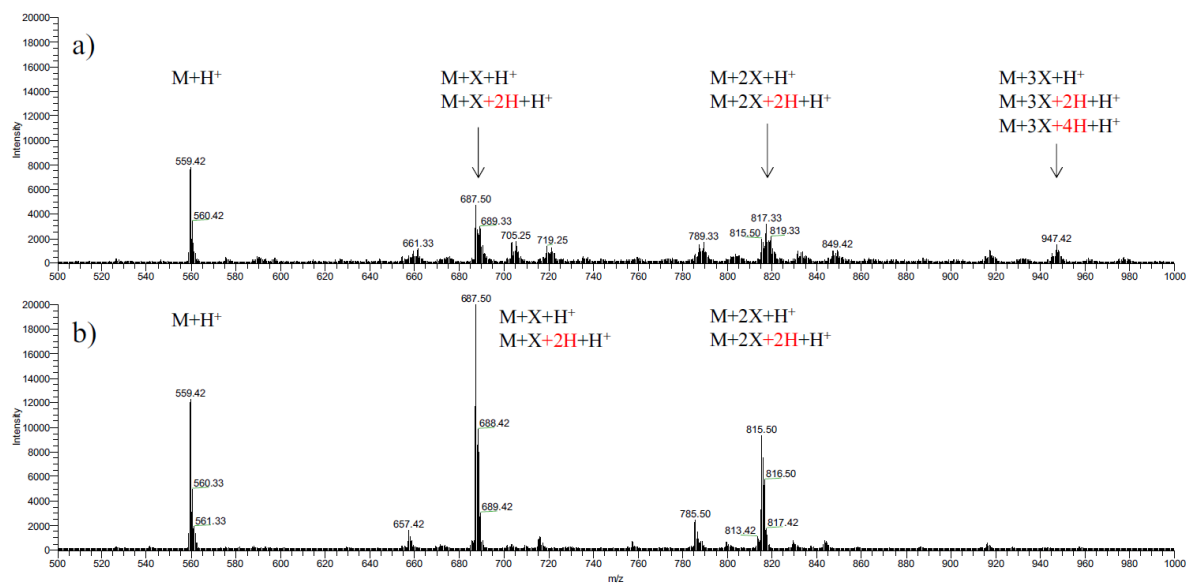
Figure 1.18: Mass spectra of BTPhen radiolysis, a) with and b) without 1M HNO$_3$.

Chapter 2 – Results and Discussion
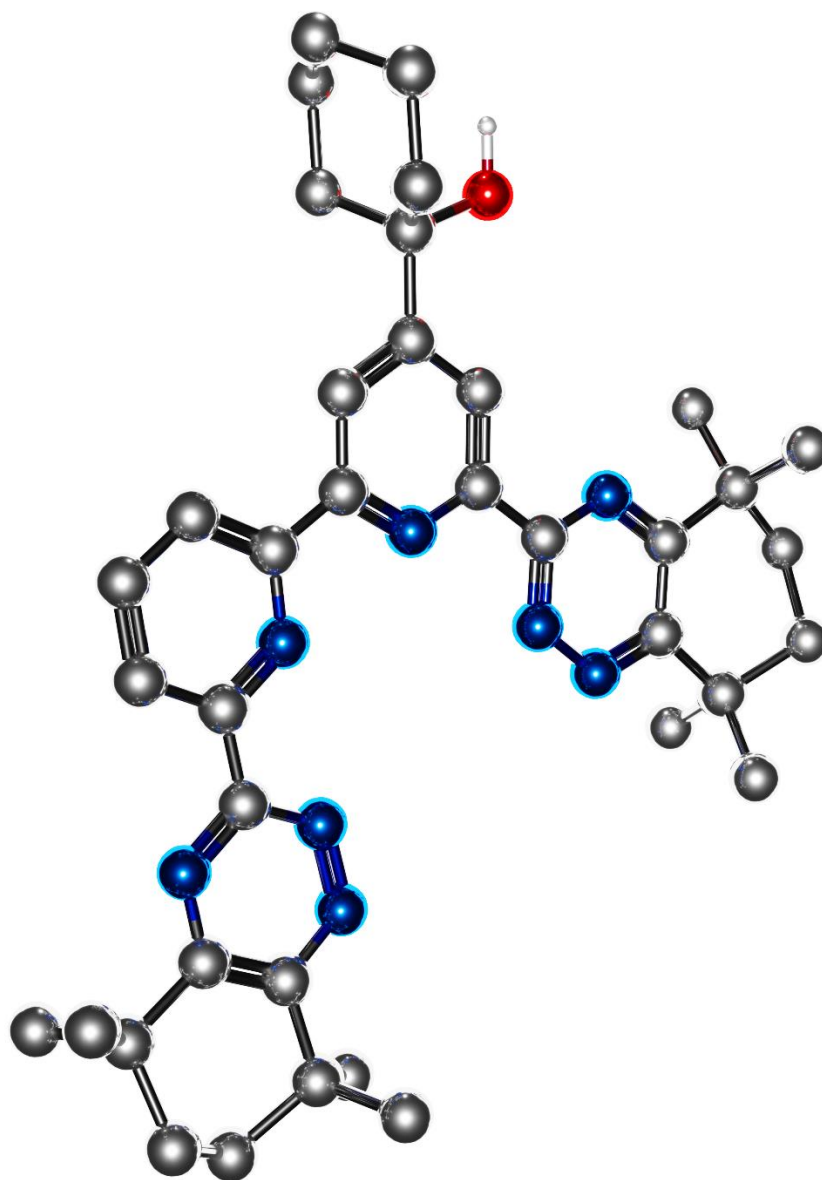
2.1 Project Objectives

With CyMe₄-BTBP **53** selected as the European benchmark for the SANEX process at laboratory scale, if destined to be used in industry, it is necessary to understand the degradation pathways of CyMe₄-BTBP **53** that exist when reprocessing spent nuclear fuel. However, mass spectrometry alone, is not a quantitative technique. Definitive characterisation of the degradation products and their absolute quantities have yet to be determined. To achieve this, we proposed to synthesize approximately 100 mg quantities of the proposed degradation products in order to determine specific response factors and to use quantitative HPLC analysis to determine the amounts of each component in the mixtures. Simultaneously, it will also be useful to study products resulting from repeat irradiation experiments under more defined conditions, with a variety of dosages of radiation.

2.2 Degradation Products of CyMe₄-BTBP

Prior to the start of this work, CyMe₄-BTBP **53** was synthesized by the Harwood group and irradiated by Jaroslav Svhela, then at the Institute of Inorganic Chemistry Academy of Science in the Czech Republic. Irradiated samples were submitted to mass spectrometry ionized using Electrospray Ionization (ESI) and sent back to the Harwood group for analysis. The samples were irradiated at 100 kGy and 400 kGy in both cyclohexanone and 1-octanol.

2.2.1 Degradation at 100 kGy of Ionising Radiation in Cyclohexanone
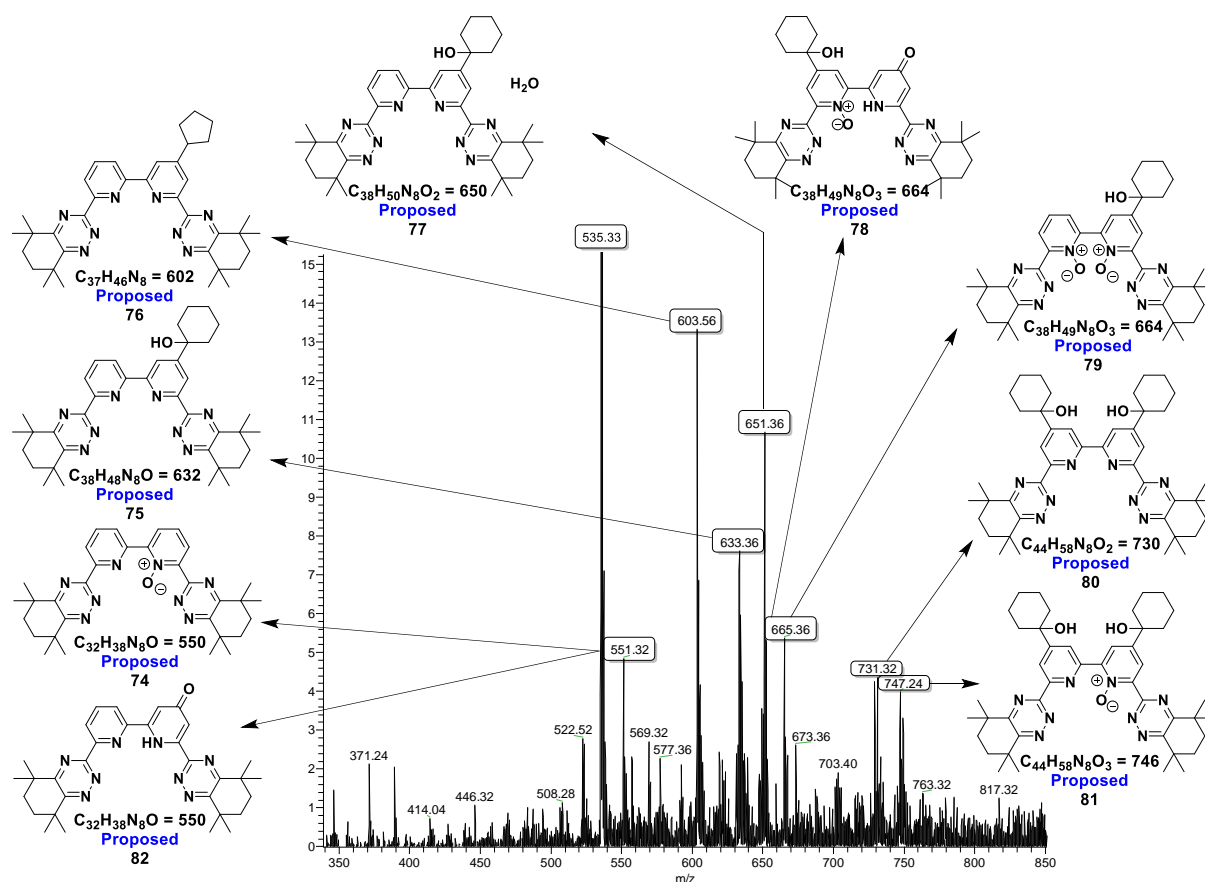
Figure 2.1: Mass spectrum and proposed characterisation of signals from the degradation of the CyMe₄-BTBP 53 in cyclohexanone after 100 kGy of ionising radiation.

The above data show the formation of adducts with little fragmentation of the CyMe₄-Ligand **53**, with the major ion peaks at: $[M+H]^+$ = 535, 551, 603, 633, 651, 665, 731 and 747 Da to the nearest Dalton. CyMe₄-BTBP **53** has a molecular weight of $[M+H]^+$ = 535 and therefore Harwood proposed the 551 signal, with a difference of 16 Da, corresponding to the ligand plus an oxygen atom, most likely from the formation of an *N*-oxide **74**. However, attack from a hydroxy radical could result in a pyridone species **82**. The signal at 633 has been proposed, by Harwood to correspond to the solvent-substituted ligand **75**, with the peak at 603 suggesting a loss of formaldehyde from the solvent adduct within the spectrometer (Scheme 2.1). The ion at 651 suggests the addition of water to the solvent adduct **77**. The peak at 665 could correspond to two different molecules, *N*-oxidation of the solvent adduct **79** shown in Figure

2.1, or attack by a hydroxyl radical species could facilitate the formation of a pyridone ring followed by *N*-oxidation at the other pyridine ring **78**, which facilitates the addition of a solvent molecule (Scheme 2.2). Ions at 731 and 747 suggest the formation of a ligand with two solvent molecules attached and then mono-*N*-oxidation of the disubstituted molecule respectively.[100]

Scheme 2.1: Mechanism of formation of ion peaks 632 and 603.

Scheme 2.2: Mechanism of formation of degradation product corresponding to 665.
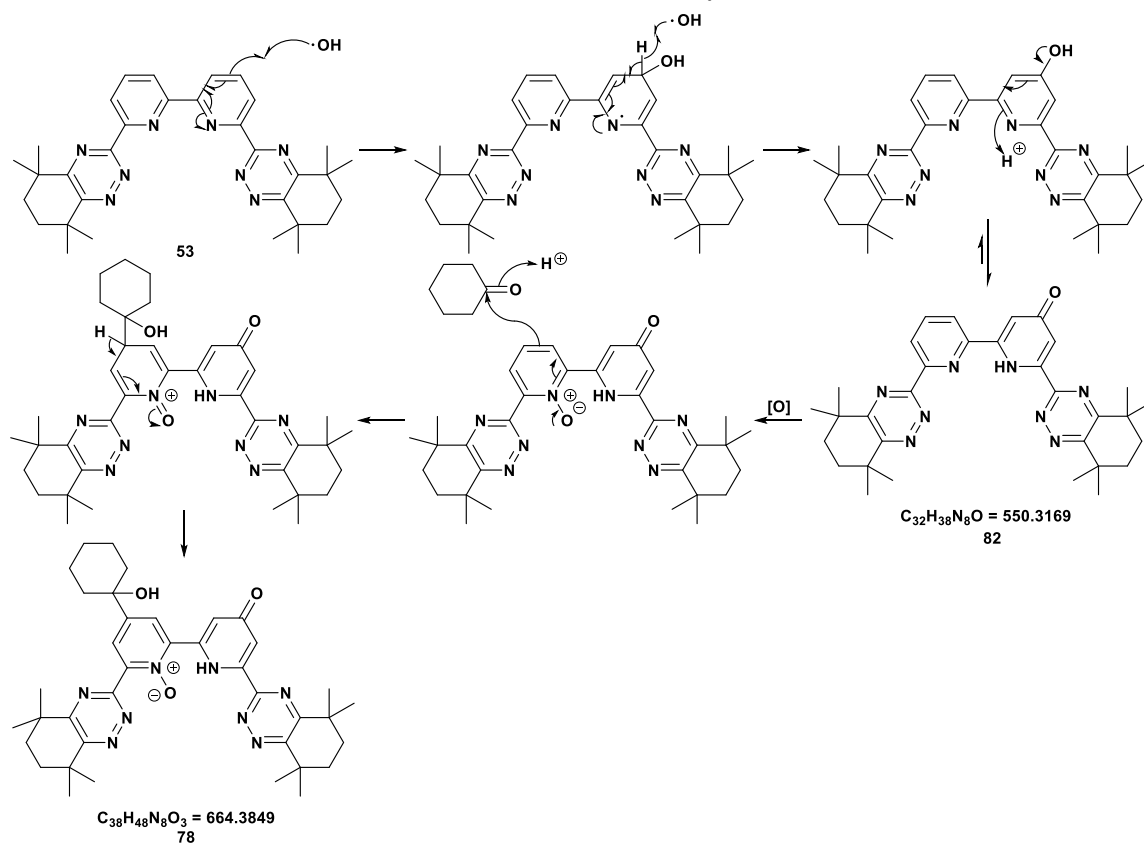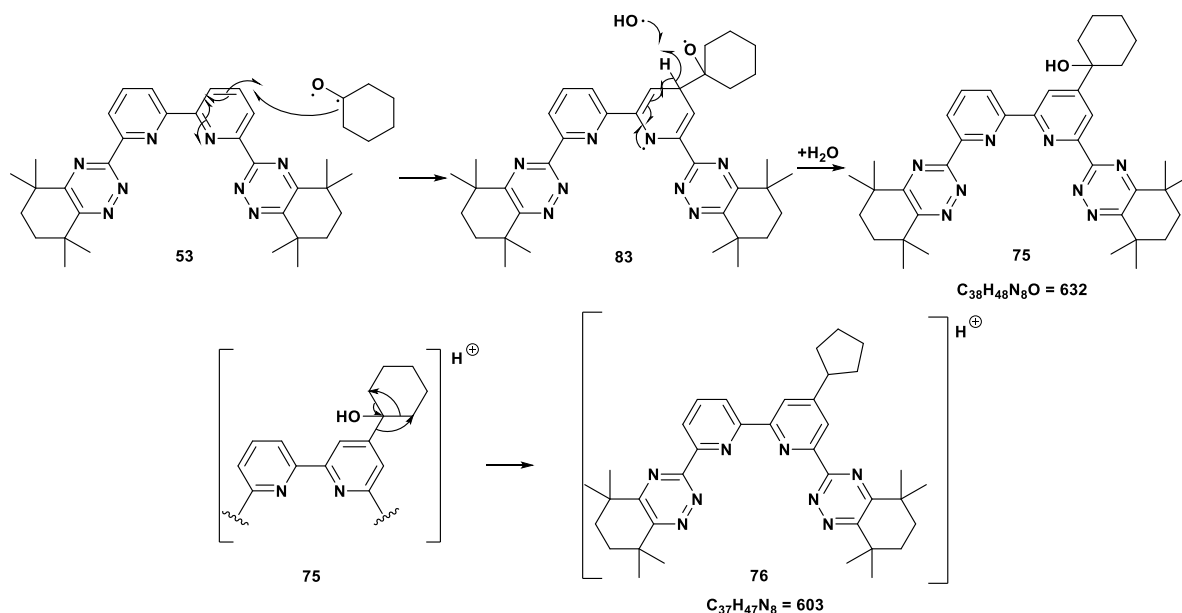
2.2.2 Degradation at 400 kGy of Ionizing Radiation

Svhela also subjected a sample of CyMe₄-BTBP **53** to 400 kGy to study the effects at this ionizing radiation level. As above, the irradiated sample was analysed by mass spectrometry (Figure 2.2).
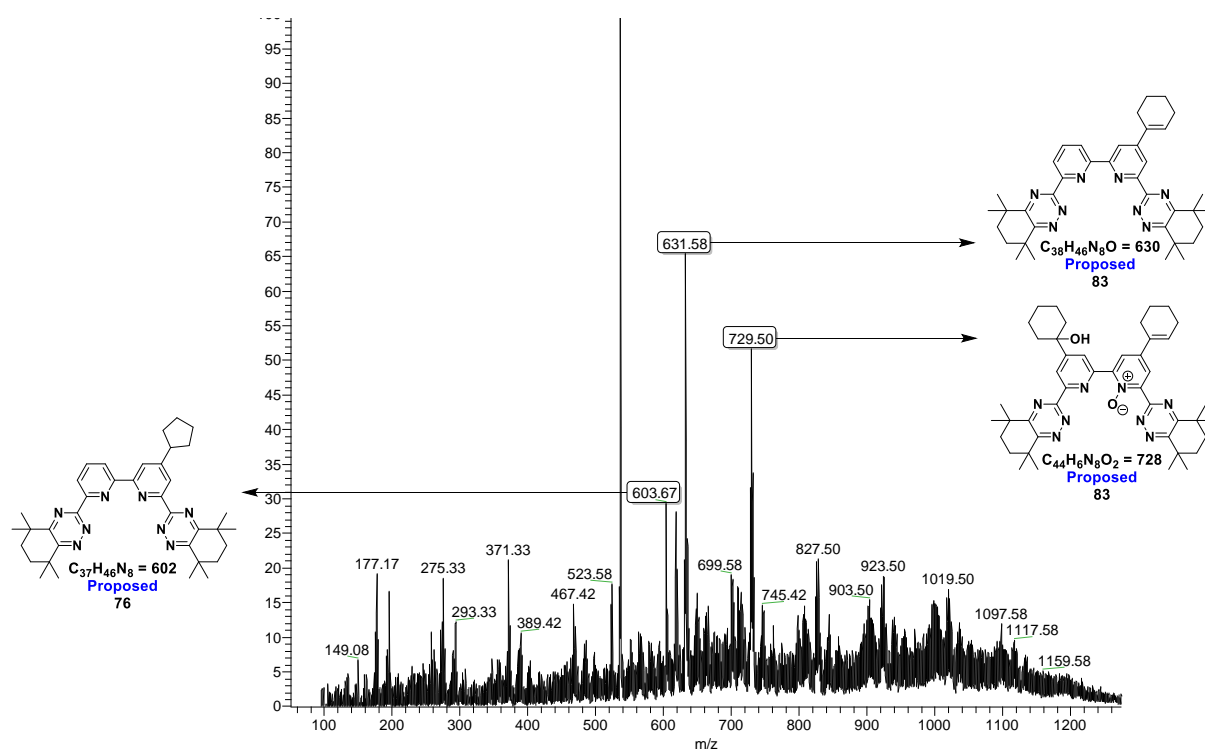
Figure 2.2: Mass Spectrum of degradation products subjected to 400 kGy.

Three major ion peaks were observed in the mass spectrum, $[M+H]^+$ = 603, 631, and 729. The peak at 603 suggested the loss of formaldehyde from the solvent adduct in the spectrometer, as above. The signal at 634 indicated elimination of the hydroxyl group on the mono-solvated adduct and that at 729 suggested a mono-oxidation of the pyridine ring, followed by elimination of the tertiary alcohol on the same ring, as well as the solvation of the other pyridine ring at the 4-position.

It is worth noting that relative abundances of the ions in the higher irradiation experiment are larger than the lower irradiation study. This is possibly due to the relative concentrations of

the sample submitted to the mass spectrometer and this will need to be tested again to confirm.

2.2.3 Degradation Products of CyMe$_4$-BTBP in 1-Octanol

The alternative solvent to be used in the SANEX process is 1-octanol, and therefore degradation products must be deduced in this medium. Holger Schmidt at Jülich subjected 10 mmolL^{-1} samples of CyMe$_4$-BTBP **53** in octanol to 100 kGy of ionizing gamma irradiation, in the presence of a nitric acid phase and without. As before, the samples were analysed by mass spectrometry (Figure 2.3).

Inspection of the mass spectrum of the sample irradiated in the absence of a nitric acid phase showed similar results to the cyclohexanone degradation studies mentioned above (Figure 2.3a). Mass ion peaks were seen at 535, 635, 665, 697, 763 and 793. CyMe$_4$-BTBP **53** has a [M+H]$^+$ of 535, and 1-octanol [M+H]$^+$ of 131. Therefore, peak 665 would appear to correspond to a mono-solvated ligand where aromaticity of the ring is broken **85**, and 793 to bis-solvated ligand where the aromaticity of one pyridine ring is broken but the other is not **87**. Ion 635 shows loss of 30 mass units, signifying the loss of formaldehyde; which coincidently ion 763 also exhibits. Peak 697 could represent two different molecules in which the shift of 32 mass units from 665 suggests either the bis-*N*-oxidation of the bipyridine core **89**; or the formation of a pyridone **90** structure similar to the mechanism in Scheme 2.2.

Figure 2.3a indicates the oxidation of one of the C=C double bonds in the pyridine ring. This was deduced from the shift in mass by 130 Da, rather than 128 Da, which indicates that an additional two hydrogen atoms are present in the degraded ligand (Scheme 2.3). Disrupting the aromaticity of the pyridine rings is extremely unfavourable and would suggest that these degradation products would not be stable under the extraction conditions. Comparison with

the cyclohexanone solvent degradation shows there is no break of aromaticity leading to more stable products. These irradiation studies would need to be retested to authenticate these results' reliability and accuracy.
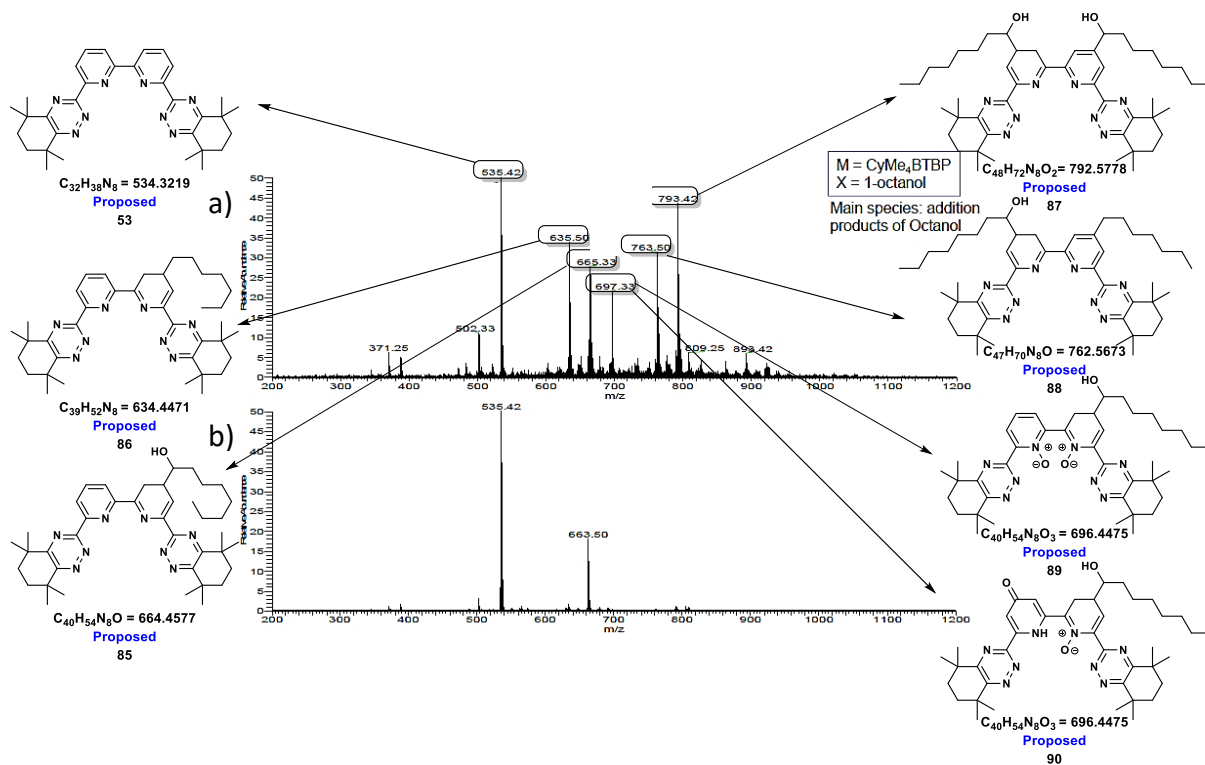
Figure 2.3: Mass spectra for the degradation of CyMe4-BTBP in 1-octanol, a) organic phase, b) organic phase with 4 M nitric acid phase.[101]
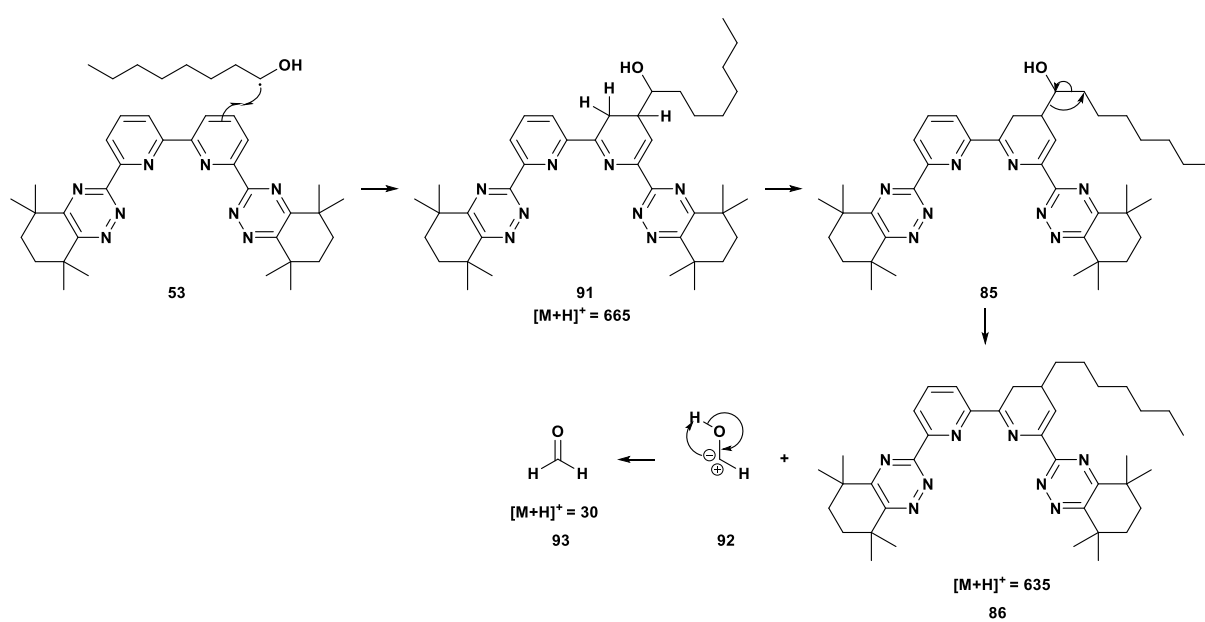
Scheme 2.3: Mechanism of formation of 1-octanol CyMe₄-BTBP degradation products.

Analysis of the spectrum from the sample of ligand irradiated in the presence of the nitric acid phase indicated less degradation had occurred compared to the spectrum in Figure 2.3a. The two peaks present were undegraded CyMe₄-BTBP **53** (535) and mono-solvated **85** (663) ions. Smaller, almost negligible peaks are indicated approximately at the 793 region, signifying formation of bis-solvated ligands **87**. Indeed, this would suggest that minimal degradation occurs when in contact with SNF. This is in keeping with other results indicating that nitric acid acts to protect organic molecules against indirect radiolysis.[79,93,101]

2.3 Degradation Products of CyMe₄-BTPhen in 1-Octanol

In the same study by Schmidt, a 10 mmolL⁻¹ sample of CyMe₄-BTPhen **72** was also subjected to 100 kGy of irradiation. As before, the test samples were irradiated with and without the presence of a nitric acid aqueous phase and each sample was submitted for mass spectrometric studies (Figure 2.4, Figure 2.5).
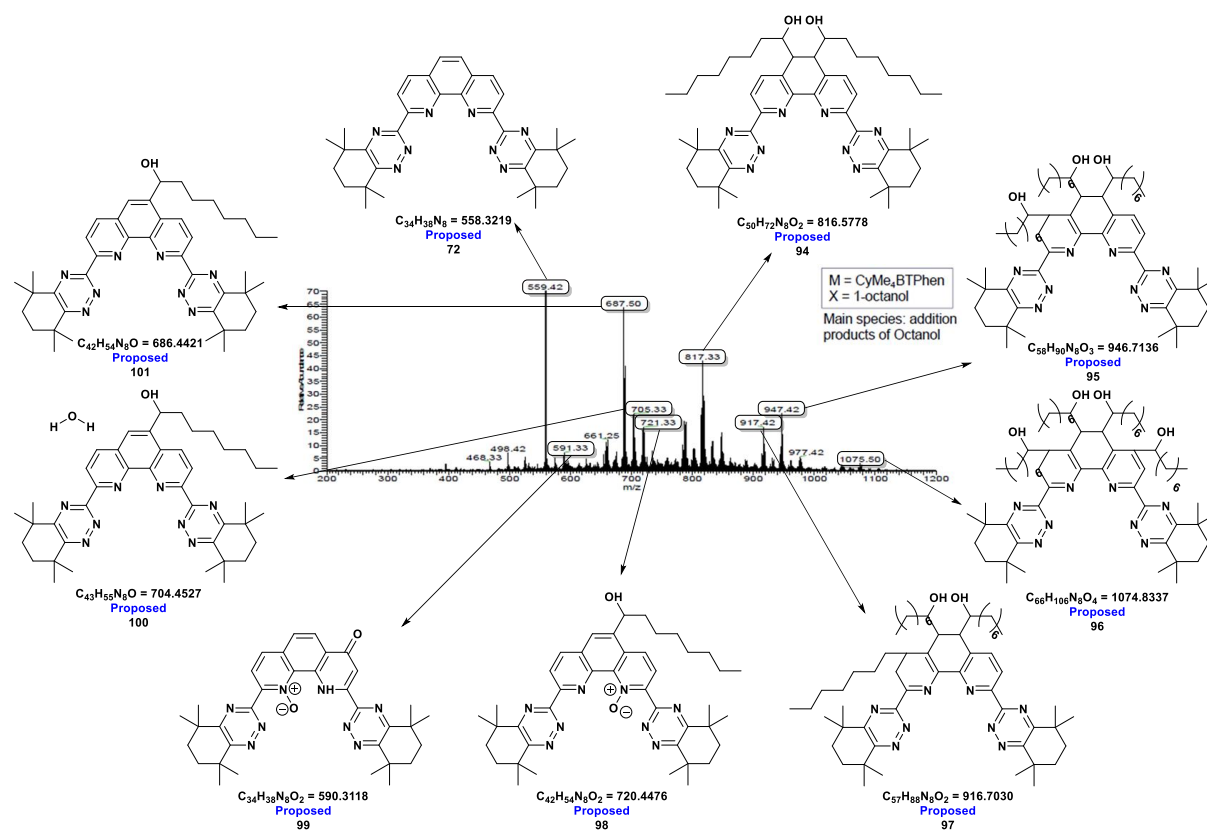
Figure 2.4: Characterised mass spectrum of irradiated CyMe₄-BTPhen 72 without nitric acid phase.

43

The mass spectrum shows mass ion peaks at $[M+H]^+$ = 559, 591, 687, 705, 721, 817, 917, 947 and 1075. The peak at 559 corresponds to undegraded BTPhen **72** and 591 could indicate the formation of the bis-*N*-oxide. However, this is very unlikely due to the steric strain on the 1,10-phenanthroline ring, and this product has never been obtained experimentally. Therefore, it is probable that the pyridone **99** forms as before with the BTBP ligand. Peak 687 indicates the formation of a mono-solvated adduct **101**, the precise location being unknown. The peak at 705 would suggest the addition of water to the mono-solvated adduct, but again, where this reacts in also unknown. The peak at 721 could correspond to the *N*-oxidation of this molecule. A possible bis-solvated adduct **94** was observed at 817 and the peak at 947 suggests a tris-solvated molecule **95** with two hydrogenated bonds. The peak at 917 indicates once again the loss of formaldehyde from **95** in the spectrometer. Lastly, peak 1075 suggests the formation of tetrakis-solvated adduct **96**.

Irradiation in presence of nitric acid layer yielded similar results, although again with fewer degradation products. The mass ion peaks observed were $[M+H]^+$ = 559, 657, 687, 785 and 815. As before, the peak at 559 corresponds to CyMe₄-BTPhen **72**. The peak at 687 corresponds to mono-solvated adduct **101**; whereas that at 657 indicates again a loss of formaldehyde within the spectrometer. Similarly, the peak at 815 indicates the formation of a bis-solvated adduct **102** and that at 785 implies the *in-situ* loss of formaldehyde from **102**.

Whilst these results were a good foundation to start the synthetic work, more data were required. Irradiated samples were needed to perform quantitative HPLC-MS to compare against synthesized versions of these degradation products as well as results for CyMe₄-BTPhen **72** in cyclohexanone therefore, more samples need to be synthesized for irradiation.

C34H38N8 = 558.3219
Proposed
72

C42H54N8O = 686.4421
Proposed
101

C50H70N8O2 = 814.5622
Proposed
102

C41H52N8 = 656.4315
Proposed
104

C49H68N8O = 784.5516
Proposed
103
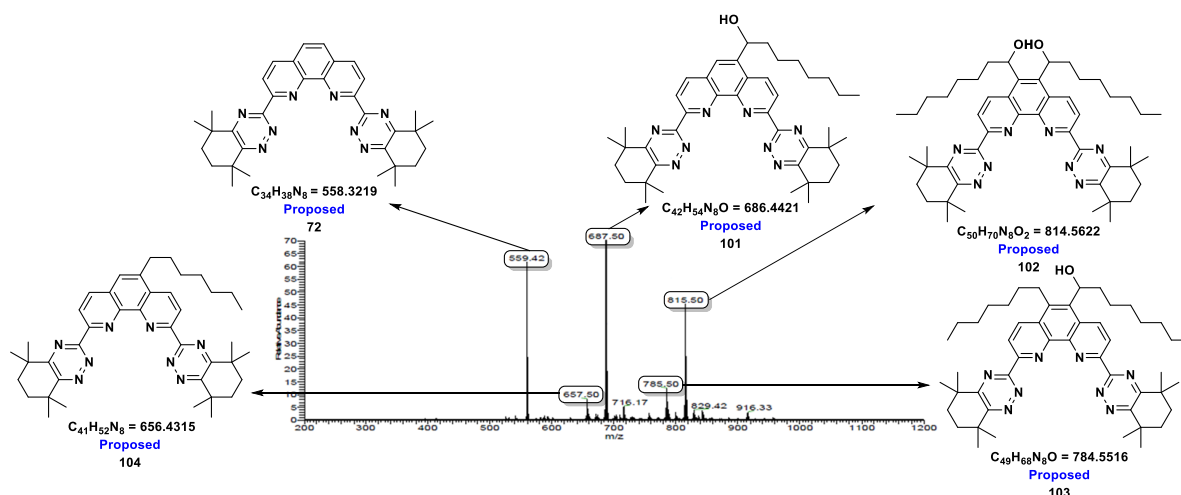
Figure 2.5: Characterised mass spectrum of irradiated CyMe4-BTPhen in presence of nitric acid.

2.4 Synthesis of CyMe4-BTBP and CyMe4-BTPhen

CyMe4-BTBP **53** was synthesized as outlined in section 1.4.4, where 2,2'-bipyridine **44** was *bis*-oxidized using acetic acid and hydrogen peroxide in 93% yield followed by a modified Reissert-Henze reaction with trimethylsilyl cyanide and benzoyl chloride that afforded the *bis*-nitrile **46**. Treating with excess hydrazine hydrate in DMSO overnight at ambient temperature allowed the *bis*(aminohydrazide) **47** and the following condensation with the CyMe4-diketone **43** in THF afforded **53** in 45% overall yield over 4 steps (Scheme 2.4).
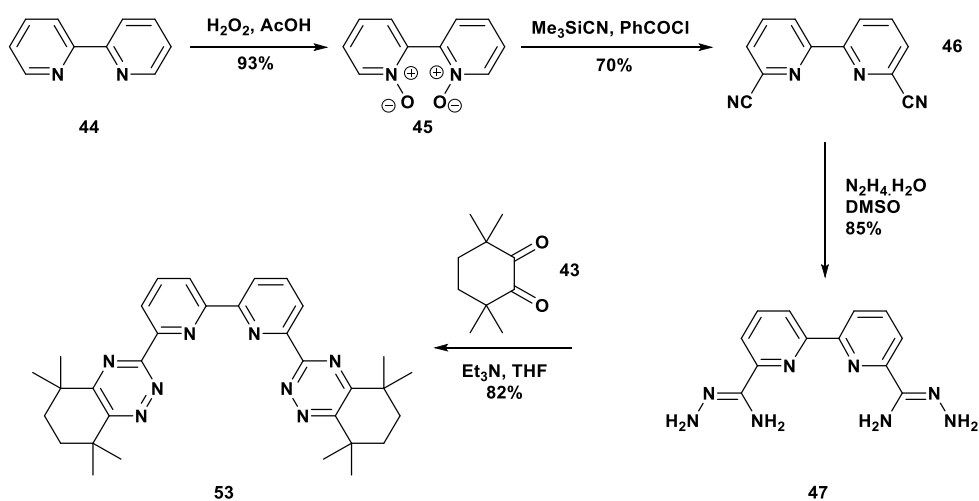
Scheme 2.4: Synthesis of CyMe4-BTBP.

45

Likewise, CyMe$_4$-BTPhen **72** was synthesized as described in section 1.4.5. Neocuproine **58** was reacted with recrystallised NCS and 0.2 molar equivalents of *m*-CPBA to furnish the hexachloro compound **59** that was hydrolysed by treating with excess concentrated sulfuric acid and the mixture slowly quenched with methanol. The *bis*-ester **60** was amidated using ammonium hydroxide with ammonium chloride to lead to the *bis*-amide **61** in 94% yield. The amide was dehydrated with phosphorus oxychloride to the dicarbonitrile **62** in 88% yield, which was treated with hydrazine hydrate in DMSO to yield the *bis*-(aminohyrazide) **63**. Finally, **72** was synthesized by condensation with the CyMe$_4$-diketone **43** under the same conditions as with the BTBP ligand with an overall yield of 16% over 6 steps (Scheme 2.5).
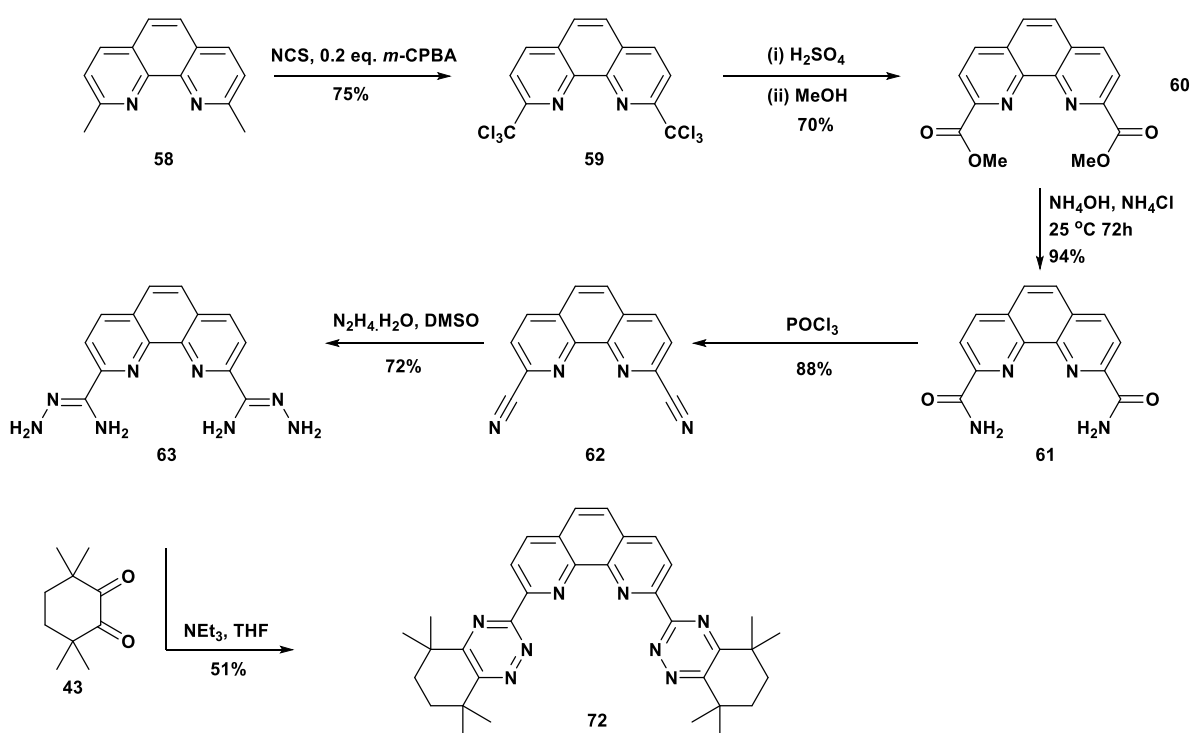
Scheme 2.5: Synthesis of CyMe$_4$-BTPhen.

Unfortunately, these ligands could not be processed on site and therefore had to be shipped to other research groups at the Czech Technical University in Prague and to California State University Long Beach. However, probably due to the COVID-19 pandemic, the samples were

never received, and the analysis was not able to be completed. Therefore, synthetic routes to the degradation adducts suggested by the results provided by Schmidt were designed.

2.5 Synthesis of *mono*-solvated CyMe₄-BTBP Degradation Adducts

With CyMe₄-BTBP **53** being the selected ligand for the laboratory-scale EU SANEX process, it was decided to focus on the degradation adducts in both cyclohexanone and octanol. The target molecules could be synthesized from a common precursor, 4-bromo-CyMe₄-BTBP **105** for *mono*-solvated adducts or 4,4'-dibromo-CyMe₄-BTBP **106** *bis*-solvated adducts (Scheme 2.6).
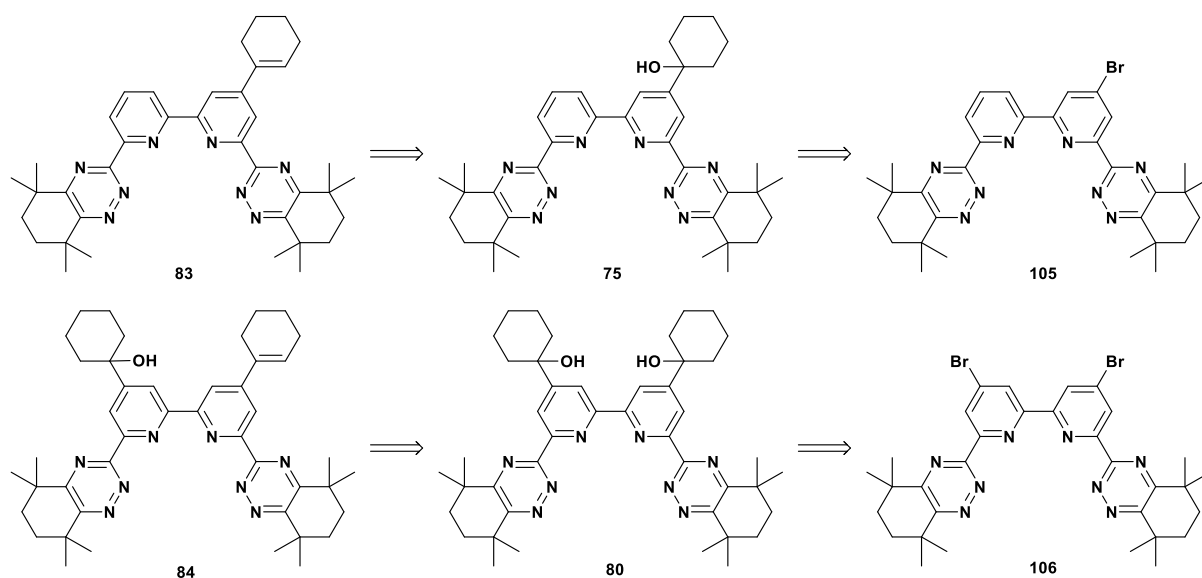
Scheme 2.6: Retrosynthesis of Cyclohexanone Degradation Adducts.

Earlier work within the Harwood group[80] has shown that the mono-bromo compound **105** can be synthesized from 2,2-bipyridine **44** (Scheme 2.7). The synthesis involves the oxidation of 2,2-bipyridine **44** to its mono-*N*-oxide form **107** using *m*-chloroperbenzoic acid (*m*-CPBA) then undergoing nitration, at the 4-position, facilitated by potassium nitrate and sulfuric acid. The following substitution reaction produces 4-bromo-2,2'-bipyridine *N*-oxide **109** using acetyl bromide and acetic acid. As before, the second nitrogen on the bipyridyl core is oxidized.

47

Following this, trimethylsilyl cyanide and benzoyl bromide introduces nitrile groups at in the *2* and *11* positions. As previously, treating dinitrile **111** with hydrazine forms the *bis*-(aminohydrazide) **112**, which condenses with the diketone **43** to produce the desired bromo-compound **105**.[100] This synthetic route has several flaws and results in an overall yield of 0.4% over seven steps, with major weaknesses being that the first, second, fourth, and fifth steps are all low yielding, (highlighted in red in Scheme 2.7). This synthetic route applied by Harwood *et al.*[80] was thought to be the most readily applicable route to desired bromo compound due to synthetic experience within the group. However, further reading showed alternative reactions for different applications, and we proposed new routes to synthesizing compound **105**, as discussed below.
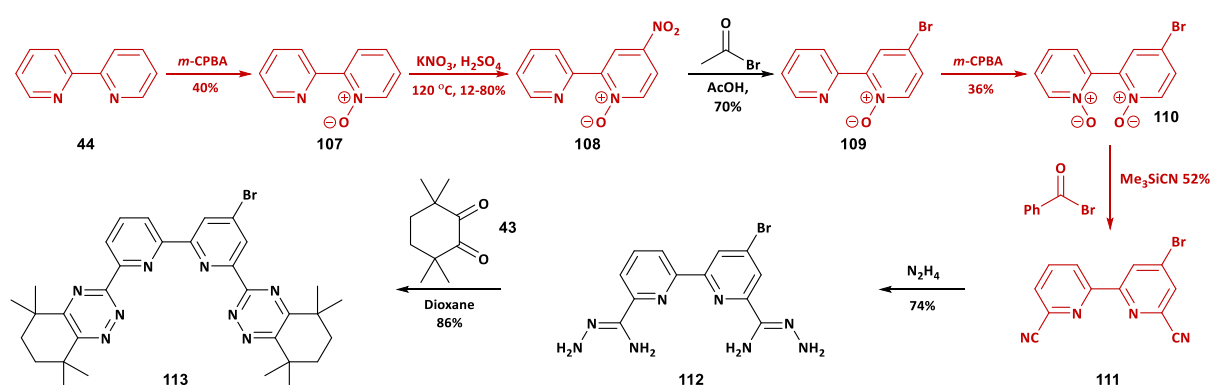
Scheme 2.7: Synthesis of 4-Bromo-CyMe₄-BTBP.

2.5.1 Synthesis of 2,2'-Bipyridine *N*-oxide

The original synthesis started with the *N*-oxidation of commercially available 2,2-bipyridine **44** using *m*-CPBA; yielding an impure product that required extensive base washing to remove *m*-chlorobenzoic acid.
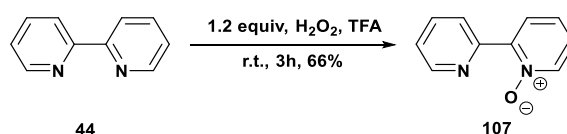
Scheme 2.8: *N*-Oxidation of 2,2-Bipyridine with H₂O₂ and TFA.

An alternative to this method reported by Zalas *et al.*[102] used 30% hydrogen peroxide in trifluoroacetic acid **114**, which react together to form trifluoroperacetic acid **117**, acting as the active oxidising agent. Computational studies by Rubio *et al.* indicate that the mechanism for the formation of the active agent involves nucleophilic attack by the peroxide to the activated carboxylic acid, followed by elimination of water (Scheme 2.9).[103]
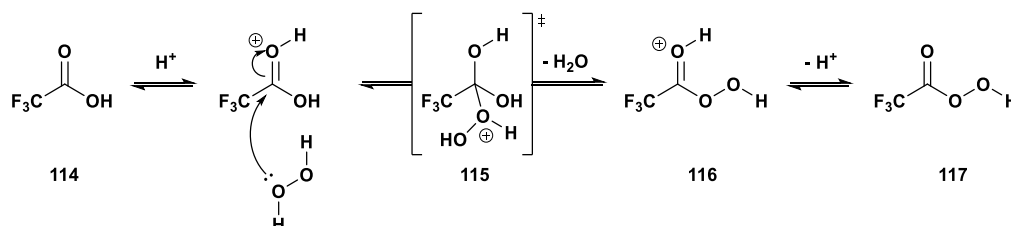
Scheme 2.9: Mechanism of formation of trifluoroperacetic acid.

When carried out in the laboratory, the reaction yielded the desired *N*-oxide in 66% yield, as evidenced in the ¹H NMR spectrum of the crude product (Figure 2.6), containing very few impurities. However, whilst this reaction showed promise, other methods were also investigated to synthesize **107**.
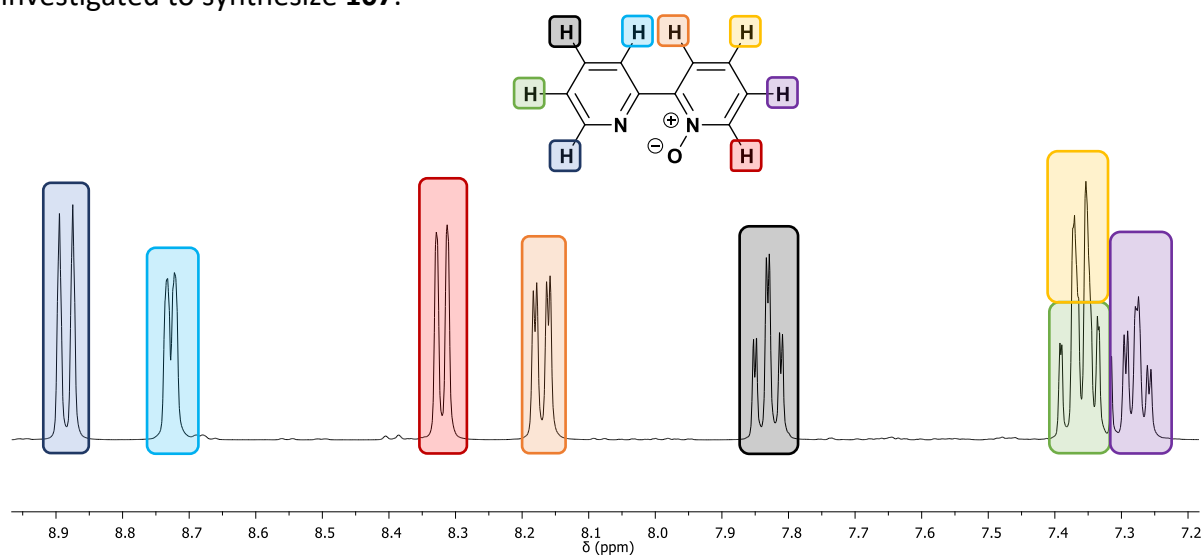
Figure 2.6: ¹H NMR of 2,2'-bipyridine *N*-oxide.

Two alternative procedures were investigated, both of which used the urea adduct of hydrogen peroxide and either phthalic anhydride[104] or formic acid (Scheme 2.10).[105] Both pathways promised a quick and efficient work-up procedure and high yields.
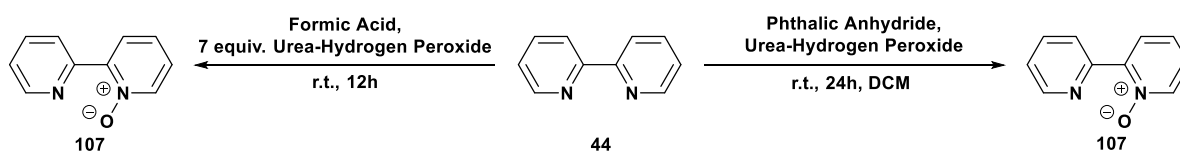
Scheme 2.10: Two methods of synthesising 2,2'-Bipyridine *N*-oxide.

However, it was observed that *N*-oxidation of bipyridine **44** using phthalic anhydride only progressed to 50% completion after 30h. Contrary to the phthalic anhydride pathway, the formic acid reaction went to completion on a 1 g scale within 16 hours giving a 94% yield of a pure colourless solid.

Despite the apparent advantage of this approach, whilst the small-scale reaction produced no noticeable exothermic reaction, upon scale up the reaction detonated on warming to room temperature. Further investigation, provided evidence that at 80-85 °C performic acid spontaneously explodes, particularly when in contact with metal.[106] Therefore, the procedure was deemed unsuitable due to the unsafe and unscalable nature of the reaction.

Having assessed different methods to synthesize the *N*-oxide **107**, it was decided to concentrate on the hydrogen peroxide and TFA **114** reaction. The first step was to increase the concentration of peroxide from 1.2 equivalents to 5 equivalents and to reduce the temperature to 0 °C when basifying, to avoid sudden temperature changes from the exothermic basification (Scheme 2.11). These changes increased the yield from 66% to 96% on a 10 g scale with the purity of the product **107** not compromised (Figure 2.7).
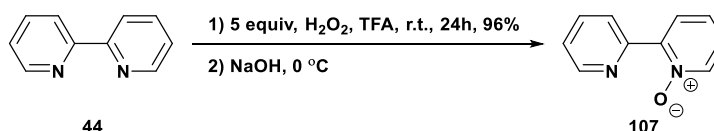
Scheme 2.11: Improved synthesis of Bipyridine *N*-oxide using TFA and hydrogen peroxide.
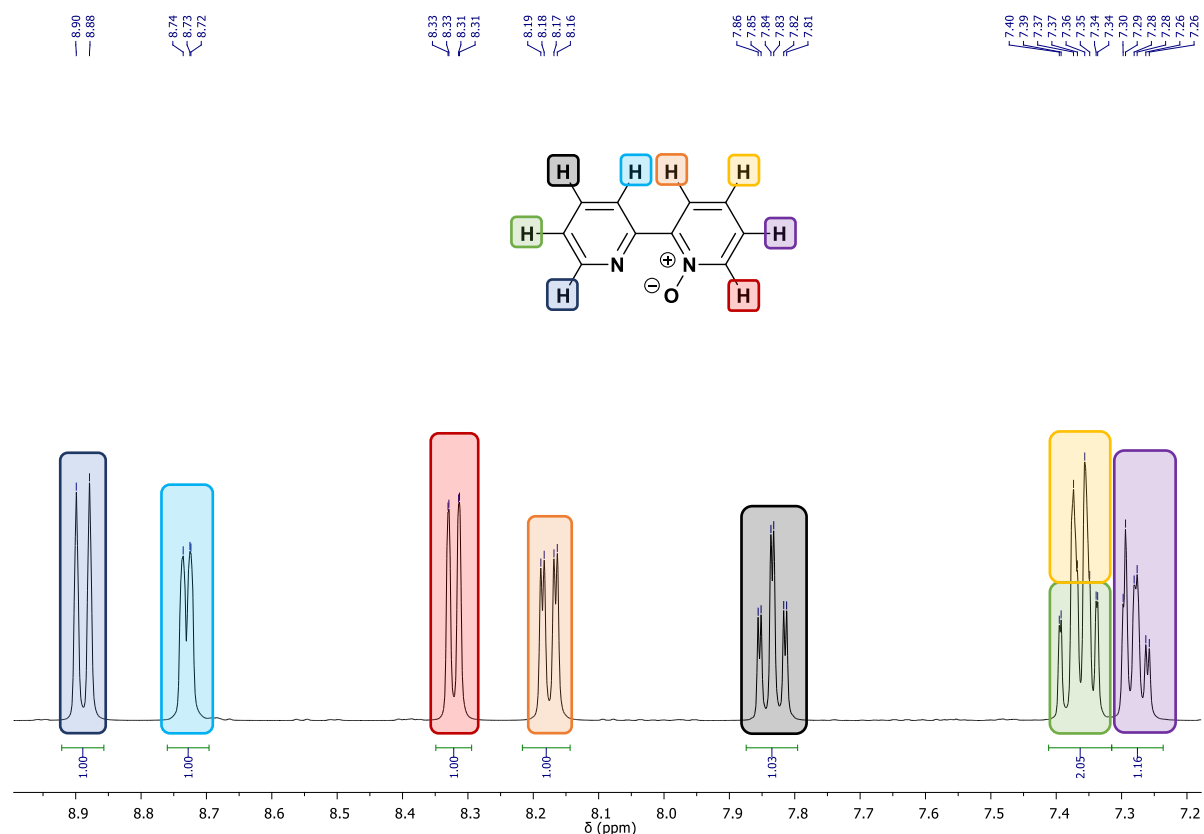
Figure 2.7: ¹H NMR of Bipyridine *N*-oxide with improved method using TFA and hydrogen peroxide.

This reaction exhibits surprising selectivity, with only the mono-*N*-oxide **107** being synthesized without the presence of the bis-*N*-oxide **44**. Having been undertaken with 5 equivalents of hydrogen peroxide, doubling the equivalents of oxidant did not affect the selectivity of the reaction. Contrary to the selective TFA reaction, when substituting TFA for acetic acid, both mono **107** and bis-*N*-oxide **44** are observed when only one equivalent was used. Therefore, the selectivity must come from the trifluoroperacetic acid that is formed in the reaction and must be due to the electronegativity of the CF_3- group present compared to the methyl group in the peracetic acid lowering the pK_a of the peracid.

2.5.2 Synthesis of 4-Nitro-2,2'-bipyridine *N*-oxide

Nitration of the *N*-oxide **107** at the 4-position was the next step in the synthesis, the procedure by Hirose[107] was first studied for the nitration, because of its familiarity to the Harwood group.
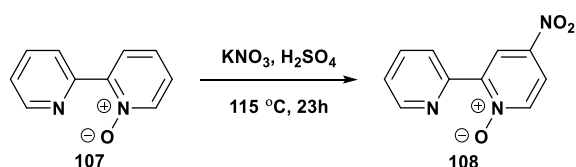
Scheme 2.12: Nitration of Bipyridine *N*-oxide using Hirose's method.

The reaction gave a 50% yield of **108**, but the crude product was only about 90% pure, still containing starting material. This reaction was repeated several times, modifying the reaction conditions and work-up in attempts to increase the yield. The yield was found to vary quite significantly from 21-75% over 12 reactions.[108] Clearly, the consistency of this reaction will need to be improved to allow for future-proofing when scaling up.

The lack of repeatability led to attempting another procedure developed by Zalas' group.[109] This pathway uses the same reagents; however, the reaction is performed at a lower temperature of 80°C but for 7 hours longer. The reaction led to the formation of **108** in 81% yield, but contrary to our previous results, the product was determined to be 99% pure by ^{1}H NMR analysis (Figure 2.8).
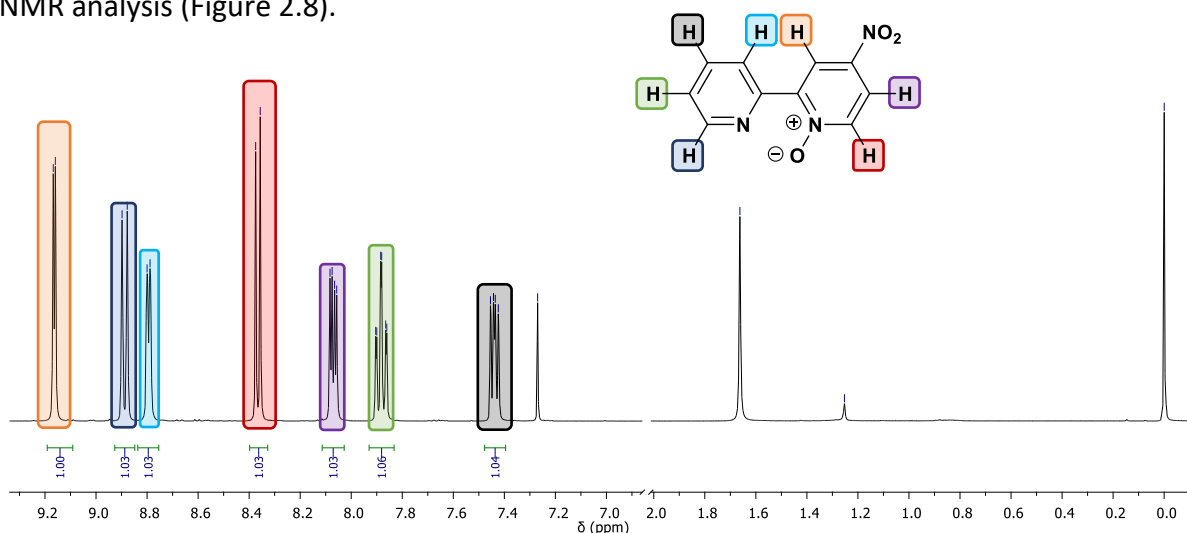
Figure 2.8: NMR of 4-Nitro-2,2'-bipyridine-*N*-oxide 108 using Zalas' procedure.

Interestingly, it was observed that this reaction was reversible dependent on the pH of the reaction medium. Upon scale-up of the reaction to 50 g, 500 mL of concentrated sulfuric acid

was required and, to reduce the hazards involved, the amount of acid was decreased but the equivalents of potassium nitrate remained unchanged. After the 30 h a small aliquot was removed and analysed (Figure 2.9); the NMR showed 1:2 conversion of the starting material to the desired product by comparing signals at 8.78 ppm and 8.72 ppm as they correspond to the same proton on each molecule. It was then decided to add another equivalent of potassium nitrate to the reaction as this had previously driven the reaction to completion. Surprisingly, rather than driving the reaction to completion, the opposite occurred, with conversion of the desired product back into the starting material now with a ratio of 1.5:1 of starting material to product. It was proposed that, like sulfonations, nitrations are also reversible and mediated by pH' therefore, concentrated sulfuric acid was added in excess to drive the reaction to completion resulting in 100% conversion yielding 69% of the product.
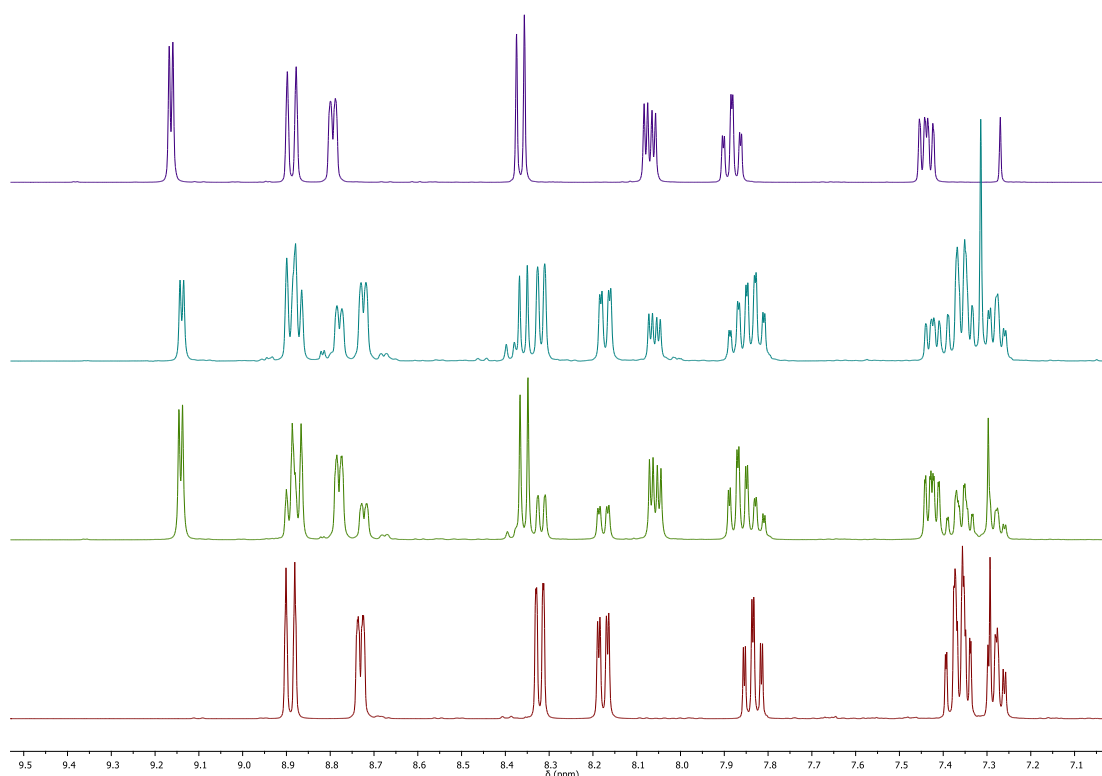
Figure 2.9: NMR Spectra showing reversible nitration of 2,2'-bipyridine-*N*-oxide 108. Red = Starting Material, Green = After 30 h, Teal = After addition of one equivalent of KNO₃, Purple = Desired product after addition of conc. Sulfuric acid.

2.5.3 Synthesis of 4-Bromo-2,2'-bipyridine *N*-oxide

Following the nitration, a substitution reaction to furnish 4-bromo-2,2'-bipyridine *N*-oxide **109**

was undertaken. The procedure involved using acetyl bromide and acetic acid, giving a 59%

yield of the desired product **109**; however, only 90% conversion of the starting material was

observed, and the product was contaminated and difficult to purify (Scheme 2.13).
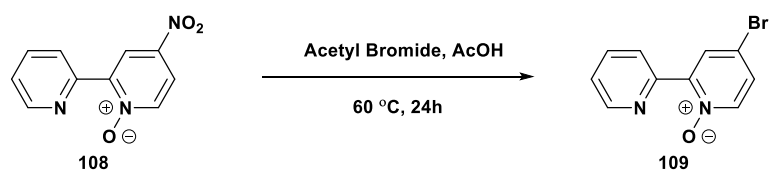
Scheme 2.13: Synthesis of 4-Bromo-2,2'-bipyridine *N*-oxide.
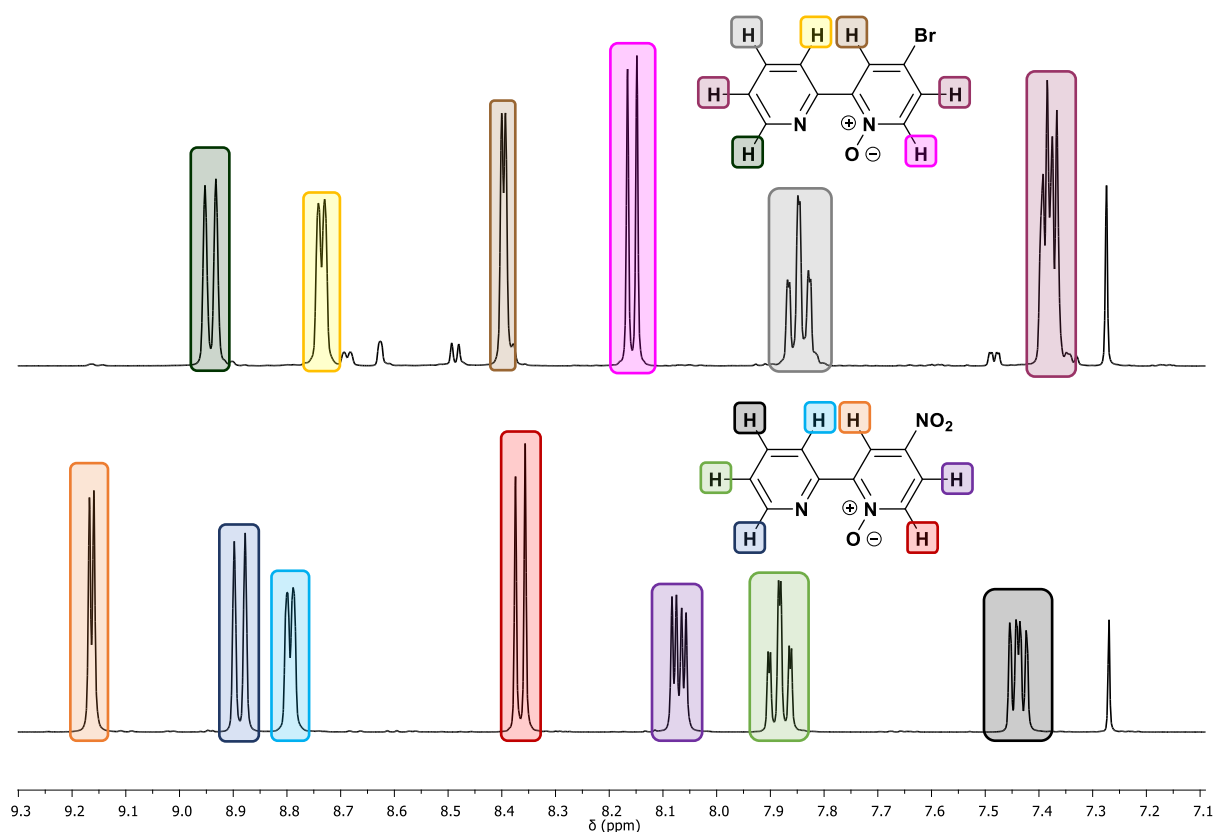
Figure 2.10: Stacked NMR of impure 4-bromo-2,2'-bipyridine-*N*-oxide 108.

It was thought that simply adding another equivalent of acetyl bromide and acetic acid to the

isolated impure product would complete the reaction, which resulted in 100% conversion of

the starting materials with a yield of 40%.

54

Attempts were made to synthesize 4-bromo-2,2'-bipyridine **118**, and the first procedure attempted was documented by Adeloye *et al.*[110] which showed that the reaction between 2,2'-bipyridine **44**, hydrogen peroxide and hydrobromic acid would yield 4-bromo-2,2'-bipyridine **118** using a modified procedure developed by Bedekar *et al.*[111] (Scheme 2.14). However, the procedure did not form **118** and only starting material **44** was isolated.

i) AgOOCF₃, Br₂, TFA, 24 h, r.t.; ii) NBS, H₂SO₄, CHCl₃, 24 h, r.t.
iii) TFA, H₂O₂, Br₂, 16 h, 75 °C
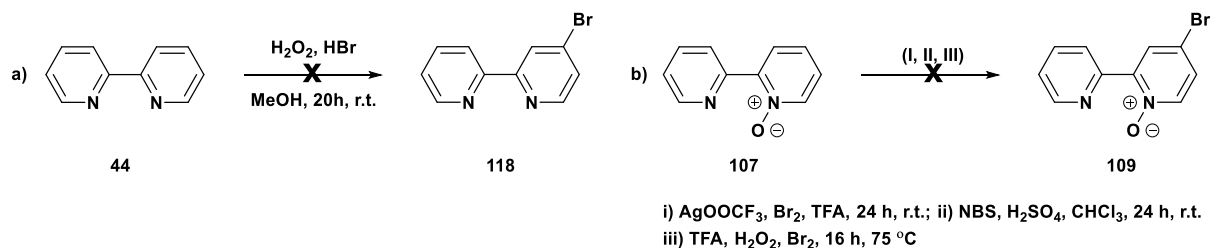
Scheme 2.14: Attempted synthesize for formation of brominated bipyridine.

The conversion is proposed to occur by oxidising the bromide to bromonium ions that would undergo electrophilic aromatic substitution. However, the 4-position on pyridine is electron deficient due to mesomeric and inductive effects, which make it unfavourable for electrophilic substitution. Thus, it is possible that the 4-position on the pyridine ring is not reactive enough, or that the intermediate bromonium ion is not forming as expected and thus yielding no product. It was theorised that using 2,2'-bipyridine *N*-oxide **107** as starting material could facilitate the desired reaction, because the 4-position is more reactive to electrophilic substitution due to increased stabilization of reaction intermediates as a result of the N-oxide lone pair donating into the ring. However when attempted, ^{1}H-NMR analysis showed the starting material was not consumed.

Scheme 2.14b(i) depicts a little-known reaction where the idea was to form trifluoroacetyl hypobromite and to test its feasibility as a brominating reagent. However, this procedure was never going to be scaled up due to the cost of the silver triflate used. The reaction converted

the starting material to an unknown material that was not the desired product. Scheme 2.14b(ii) was designed to deduce if *N*-bromosuccinamide could be used as a suitable brominating agent, but no conversion was observed. This most likely due to the minor difference in electronegativity of the Br-N bond where nitrogen is slightly more electronegative compared to bromine on the Pauling scale (N 3.0, Br 2.8)[112] and therefore the dipole moment across the bond is not as great. The pathway in Scheme 2.14b(iii) was designed to emulate reaction in pathway 2.14b(i), forming the trifluoroacetyl hypobromite, but again this was unsuccessful and only starting material **107** was isolated.

It was later found that the first procedure previously used by the Harwood group was repeated under a nitrogen atmosphere and adding excess acetyl bromide whilst at room temperature, rather than at 60 °C, increased the yield from 59% to 95% with increased purity. We proposed that this was due to increased [Br$^-$] in solution and the nitrogen atmosphere slowing the formation of HBr gas, maintaining a high [Br$^-$] for the duration of the reaction.

2.5.4 Attempts at the Iodination of 2,2'-Bipyridines

In tandem with the bromination, iodination of 2,2'-bipyridine *N*-oxide **107** was proposed to alleviate the slow kinetics and poor yields later in the synthesis when undergoing lithiation with respective ketones.[80] It was then realised that an activated pyridine *N*-oxide could undergo electrophilic substitution with an iodonium ion which could be provided by iodine monochloride and iodine monobromide. Of the two reagents, Iodine monochloride has a stronger dipole moment than iodine monobromide due to the increased electronegativity of the chloride.

Having found very little information in the literature on this topic, it was decided to examine the electrophilic substitution reaction with iodine monochloride and 2,2-bipyridine *N*-oxide

107 (Scheme 2.15). The reaction was carried out in ethanol to ensure a homogenous mixture whilst varying the temperature and base (Table 2).
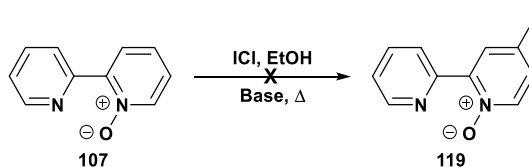
Scheme 2.15: Iodination reactions using ICl, whilst varying the temperature and base.

Table 2: Iodination reactions varying base and temperature.

Reaction	Base	Temperature (°C)	Conversion
A	-	20	0
B	-	40	0
C	-	80	0
D	Potassium Carbonate	20	0
E	Potassium Carbonate	40	0
F	Potassium Carbonate	80	0
G	Triethylamine	20	0
H	Triethylamine	40	0
I	Triethylamine	80	0

However, none of the reactions yielded any product. It was noticed that the reactions at higher temperatures produced more by-products, the colour of the reactions changed from a transparent yellow to an opaque brown. Reactions G-I, were brown in colour and a gas was given off when the triethylamine was added to the solution.

2.5.5 Synthesis of 4-Bromo-2,2'-bipyridine-*N,N'-bis*-oxide

Originally, the Harwood group synthesized 4-Bromo-2,2'-bipyridine-*N,N'-bis*-oxide **110** by reacting the mono-*N*-oxide **109** with *m*-CPBA in chloroform with low yields of 36% as result of the work-up procedure.[80] The *bis*-oxide **110** has a high solubility in water resulting in significant losses during the bicarbonate washes required to remove the excess *m*-CPBA and the acid by-product.
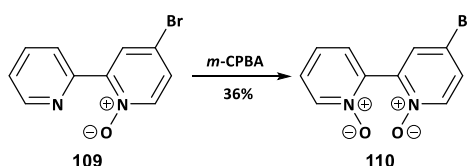
Scheme 2.16: Synthesis of 4-Bromo-2,2'-bipyridine-*N,N'-bis*-oxide using *m*-CPBA.

Changing the solvent to DCM facilitated the removal of the carboxylic acid by-product by cooling the reaction mixture to -10°C and filtering off the precipitate. However, the resultant product still contained *m*-CPBA which could not be removed by washing and the product adhered to both normal phase and reverse phased silica. Therefore, an alternate method was employed, utilising acetic acid and hydrogen peroxide under the same conditions to those where 2,2'-bipyridine **44** is *bis*-oxidized. However, this protocol proved not to be not ideal as it produced low yields and often resulted in a viscous red oil that, when triturated with THF at -20°C, resulted in the product as an off-white solid.
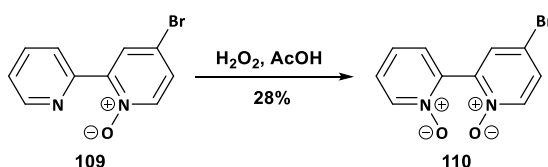
Scheme 2.17: Synthesis of 4-bromo-2,2'-bipyridine-*N,N'-bis*-oxide using hydrogen peroxide and acetic acid.

A different method of synthesizing the *bis*-oxide **110** was needed, with the previous attempts resulting in low yields. Upon further reading, Swager's group at MIT synthesized the above

bis-oxide **110** by oxidizing the mono-nitro **109** compound and subsequent bromination (Scheme 2.18).[113,114] The synthesis of the nitro *bis*-oxide **120** proceeded with high yields and purity, but the bromination resulted in a mixture of products wherein oxidized and reduced by-products were present. Lowering the temperature of the reaction from 60°C to room temperature resulted in no conversion of the starting material after 24 h.
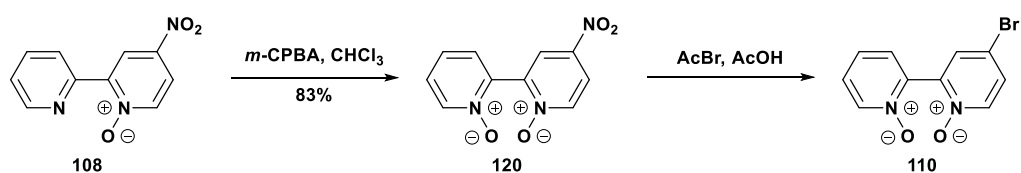
Scheme 2.18: New synthesis of 4-Bromo-2,2'-bipyridine-*N,N'*-bis-oxide *via* 4-nitro-2,2'-bipyridine-*N,N'*-bis-oxide 120.
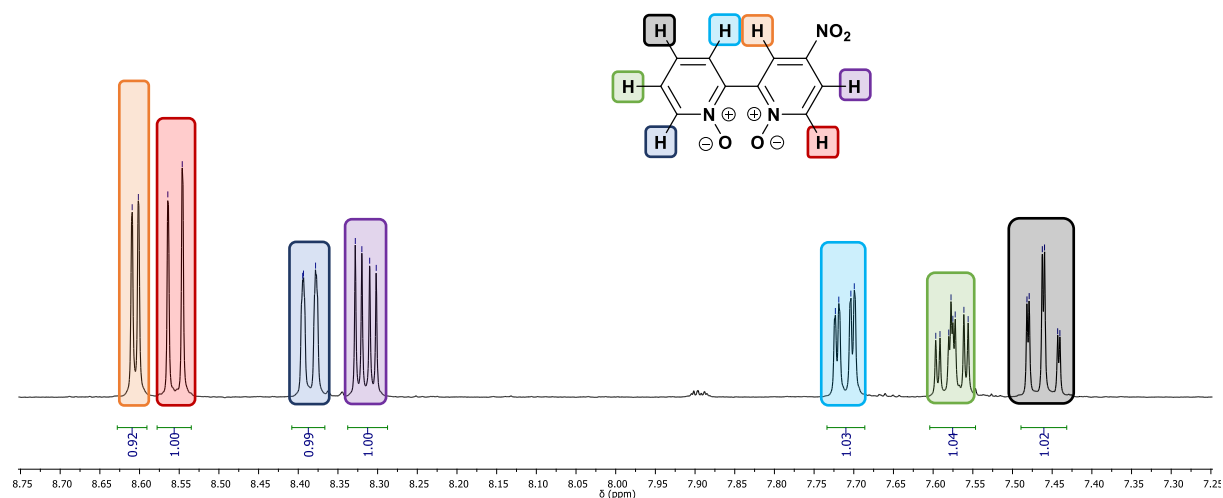
Figure 2.11: NMR spectrum of 4-nitro-2,2'-bipyridine-*N,N'*-bis-oxide 120.

After these failed attempts, it was decided to proceed with the material on hand to the next step of the synthesis.

2.5.6 Synthesis of 4-bromo-2,2'-bipyridine-6,6'-dicarbonitrile

The next step in the synthesis was the cyanation of the *bis*-oxide **110** using trimethylsilyl cyanide and benzoyl bromide in a modified Reissert-Henze reaction (Scheme 2.19). Fife

proposed the that the *N*-oxide attacks the benzoyl bromide followed by attack by the trimethylsilyl cyanide at the 2-position on the pyridine ring, breaking and reforming the aromaticity on elimination of the benzoyl group, reducing the *N*-oxide.
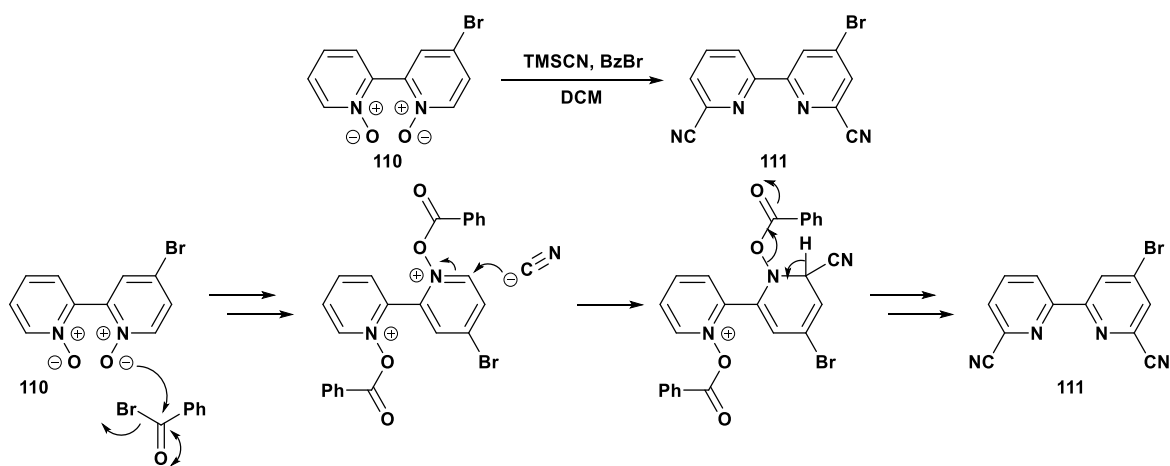
Scheme 2.19: Synthesis and mechanism of formation of 4-bromo-2,2'-bipyridine-6,6'-dicarbonitrile.

Unfortunately, after multiple attempts at synthesizing the dicarbonitrile, the reaction never progressed to completion resulting in benzoic acid contaminated product. The majority of the benzoic acid was removed by rapid washing with 1M NaOH so as to not hydrolyse the nitrile groups. It was later discovered that trituration with cold methanol would remove the benzoic acid from the remaining material. However, the tan solid material that remained was determined to be starting material.

The second method used a modification of work previously published by the Harwood group, where 4-nitro-2,2'-bipyridine-*N*,*N*'-bis-oxide underwent both chlorination and cyanation in a single step (Scheme 2.20).[80]
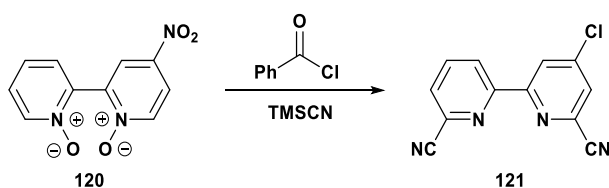
Scheme 2.20: Alternative cyanidation, from 4-nitro-2,2'-bipyridine-*N*,*N*'-bis-oxide.

However, in our case the bromo form **111** was required and therefore, benzoyl bromide was used. As before, when the crude product was isolated, the major impurity was benzoic acid, which was removed by 1M NaOH wash followed by trituration with MeOH. After removal, the residue was again found to be starting material. With the small quantity of material remaining, it was decided to shift focus to the *bis*-solvated degradation adducts.

2.6 Synthesis of *bis*-solvated CyMe$_4$-BTBP Degradation Adducts

The proposed synthetic route to synthesize the *bis*-solvated adducts was similar to the that of the mono-adducts (Scheme 2.21). Oxidation of 2,2'-bipyridine **44** to the *bis*-oxide **46** using acetic acid and hydrogen peroxide, followed by nitration at the 4-positions facilitated by potassium nitrate and sulfuric acid. The following nucleophilic aromatic substitution reaction to produce 4,4'-dibromo-2,2'-bipyridine-*bis-N,N'*-oxide **122** was carried out using acetyl bromide and acetic acid. As previously, trimethylsilyl cyanide and benzoyl bromide introduced the nitrile groups at the 2- and 11- positions. Following this, treating the dinitrile **123** with hydrazine hydrate resulted in the *bis*-(aminohydrazide) **124** that was condensed with CyMe$_4$-diketone to produce the dibromo-CyMe$_4$-BTBP. This underwent lithiation facilitated by using 2 equivalents of *n*-BuLi or other lithiating agent and either cyclohexanone or 1-octanal to form the desired degradation adduct.
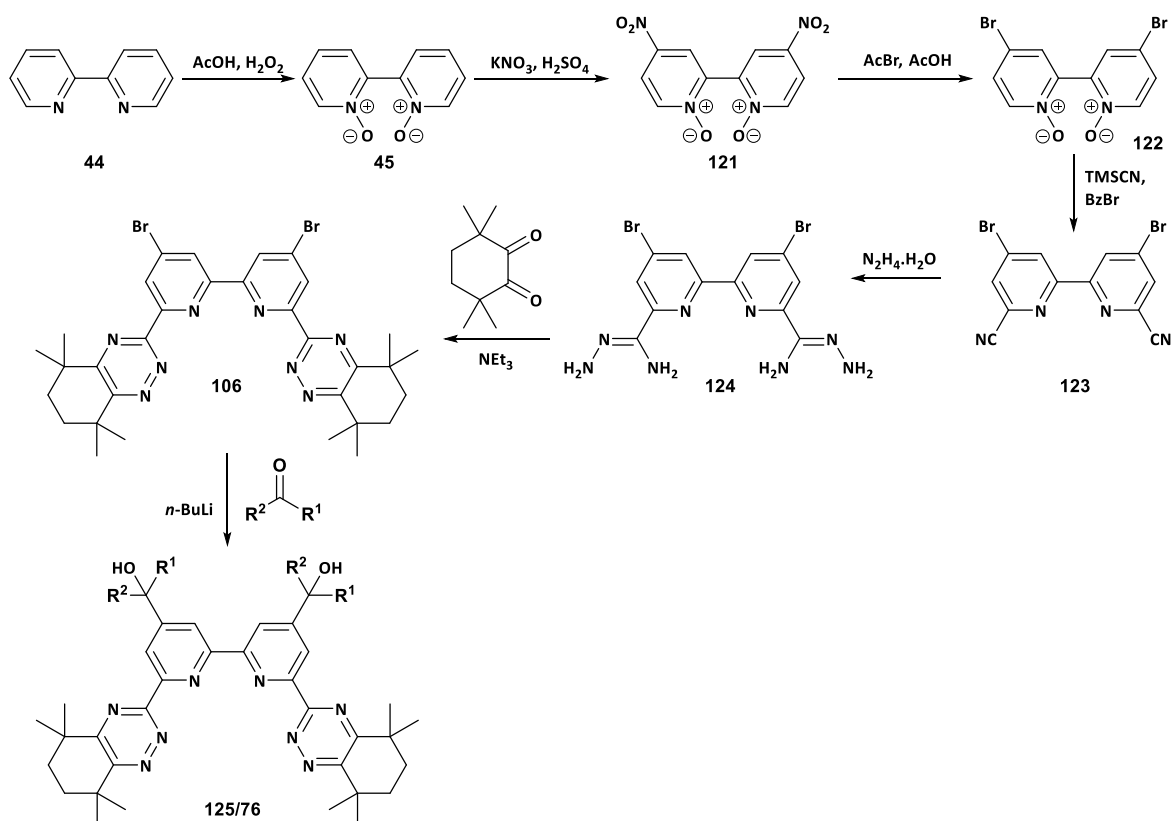
Scheme 2.21. Proposed synthetic route to the *bis*-solvated degradation adducts of CyMe$_4$-BTBP.

2.6.1 Synthesis of 2,2'-Bipyridine-*bis-N,N*-oxide

2,2'-Bipyridine-*bis-N,N*-oxide **45** was successfully synthesized according to Clennan *et al.*[115] utilizing hydrogen peroxide and acetic acid to generate peracetic acid *in situ* which oxidized the 2,2'-bipyridine in in 76% yield (Scheme 2.22).
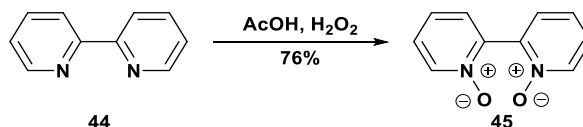
Scheme 2.22: Synthesis of 2,2'-bipyridine-*N,N'*-oxide.

The reaction showed 100% conversion to the *bis*-oxide **45** and the low isolated yield was attributed to the loss of product from the work-up procedure, which entailed precipitation of the product by addition of acetone to the reaction. Changing the work-up to removing most of the aqueous acetic acid mixture *in vacuo* and triturating the resulting residue with acetone led to a 99% yield of the desired *bis-N*-oxide **45**. The trituration also acted to remove any

remaining starting material and *mono-N*-oxide **107**, resulting in a high purity of final product (Figure 2.12).
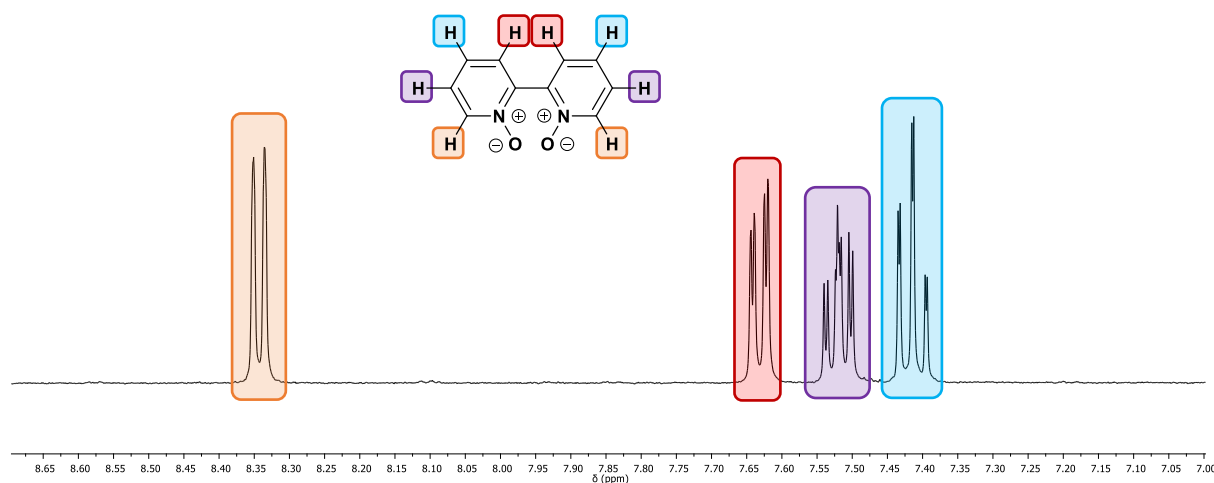
Figure 2.12: NMR spectrum of 2,2'-bipyrine-*bis-N,N'*-oxide 45.

2.6.2 Synthesis of 4,4'-Dinitro-2,2'-bipyridine-*bis-N,N'*-oxide

4,4'-Dinitro-2,2'-bipyridine-*bis-N,N'*-oxide **121** was synthesized as before from the *mono*-nitro bipyridine **108** precursor using potassium nitrate and concentrated sulfuric acid. However, the procedure resulted in low yields of *circa* 23-35% because of the high solubility of the product in water compared to organic solvents (Scheme 2.23).
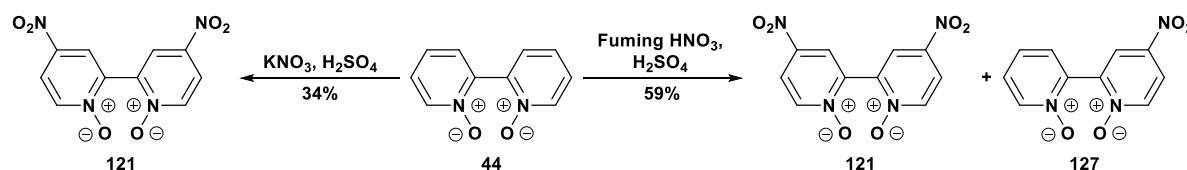
Scheme 2.23: Synthesis of 4,4'-dinitro-2,2'-bipyridine-*bis-N,N'*-oxide.

To limit the volume of water in the reaction, fuming nitric acid was used in place of the potassium nitrate as described by Leech *et al.*[116] In addition, the workup procedure was altered so that when the acidic mixture was poured onto ice, the mixture was cooled to -40 °C, resulting in precipitation of the product. This resulted in a crude yield of 59% but the

63

product was impure and difficult to purify with an unknown mono-4-substituted bipyridine being present (Figure 2.13).
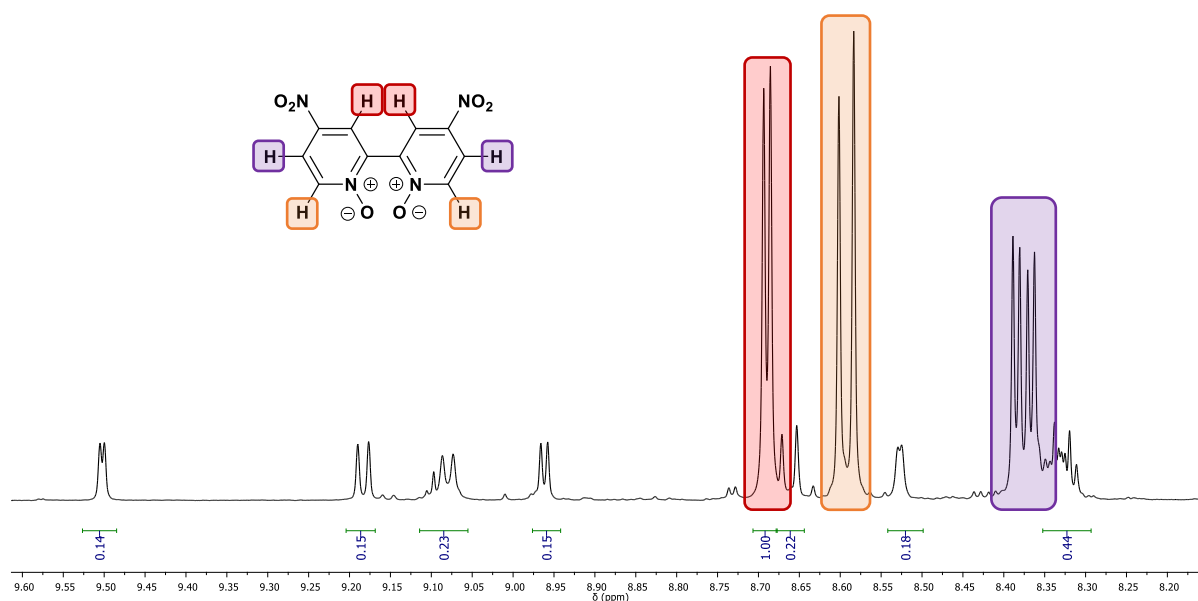
Figure 2.13: NMR spectrum of 4,4'-dinitro-2,2'-bipyridine-*bis-N,N'*-oxide with unknown 4-substituted bipyridine.

After some success by limiting the use of water in the second protocol, this workup was applied to the first protocol using potassium nitrate. As a result, 4,4'-dinitro-2,2'-bipyridine-*bis-N,N'*-oxide **121** was synthesized in 52% yield with high purity (Figure 2.14). This reaction was repeated on 10 g and 25 g quantities and enough material was therefore synthesized to continue to the bromination step.
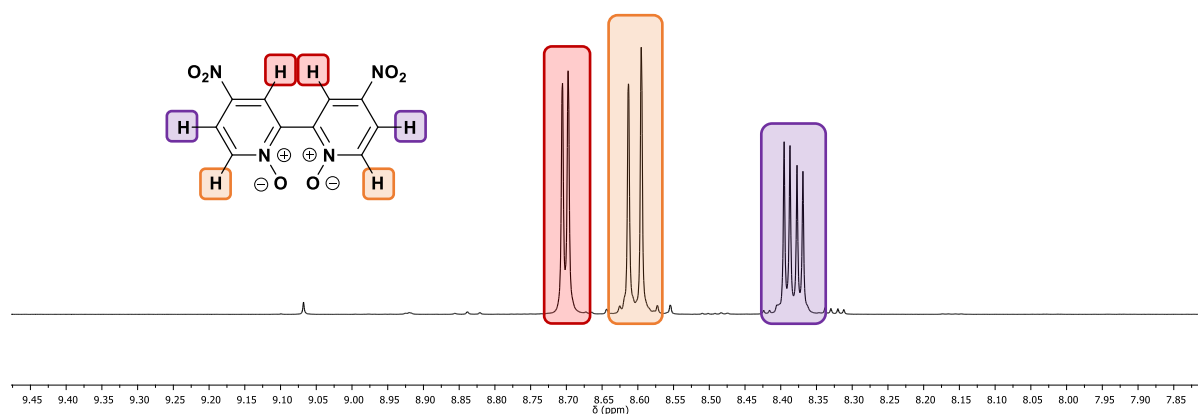
Figure 2.14: NMR of new synthesis of 4,4'-dinitro-2,2'-bipyridine-*bis-N,N'*-oxide 121.

2.6.3 Synthesis of 4,4'-dibromo-2,2'-bipyridine-*bis-N,N'*-oxide

4,4'-Dibromo-2,2'-bipyridine-*bis-N,N'*-oxide **122** was successfully synthesized from the dinitro-compound **121** in 90% yield as before from the *mono*-bromo bipyridine **109** compound under a nitrogen atmosphere with excess acetyl bromide in acetic acid (Scheme 2.24).
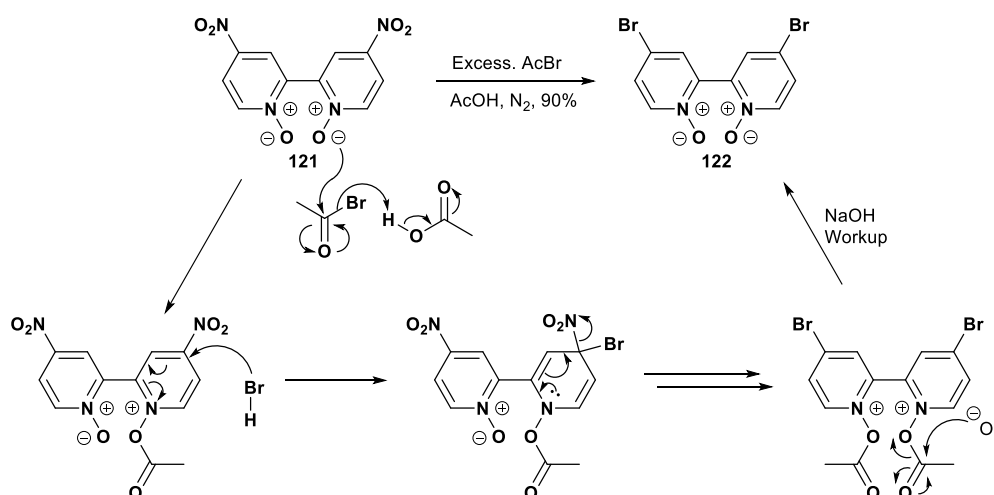
Scheme 2.24: Synthesis and mechanism of formation of 4,4'-dibromo-2,2'-bipyridine-*bis-N,N'*-oxide.

The reaction proceeds by the reaction between acetic acid and acetyl bromide forming acetic anhydride and hydrogen bromide in solution followed by S$_N$Ar reaction at the 4-position by the HBr, displacing nitrous acid. The acetic anhydride formed in the reaction is quenched during the workup when basifying with 12.5M sodium hydroxide. After the base wash the precipitated product was washed with cold water to remove any inorganic salts to furnish the pure product (Figure 2.15).
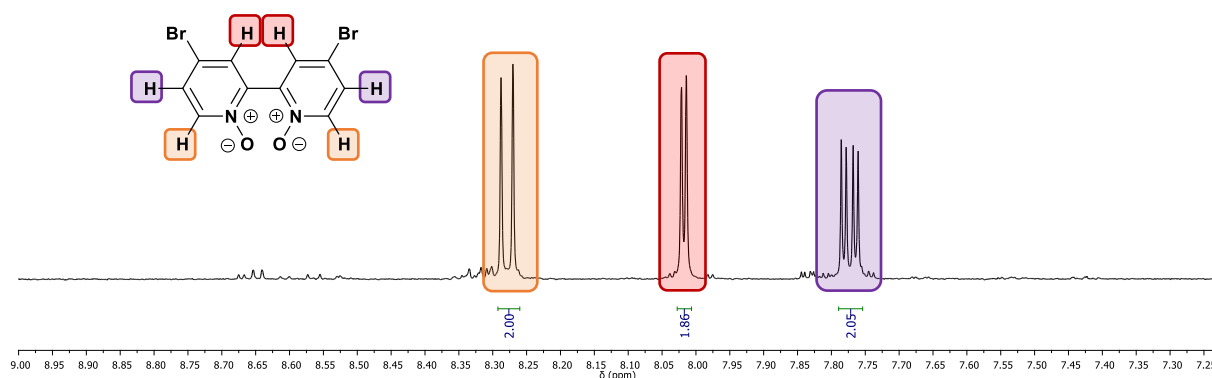
Figure 2.15: NMR spectrum of 4,4'-dibromo-2,2'-bipyridine-*bis-N,N'*-oxide.

65

2.6.4 Synthesis of 4,4'-dibromo-2,2'-bipyridine-dicarbonitrile

The proposed synthetic route to the dicarbonitrile **123** was to follow the modified Reissert-Henze reaction as before, using trimethylsilyl cyanide and benzoyl bromide. However, attempting this reaction with the dibromo- compound **122** resulted in no conversion to desired product, despite multiple attempts.
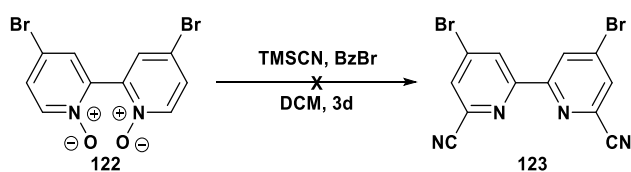
Scheme 2.25: Synthesis of 4,4'-dibromo-2,2'-bipyridine-dicarbonitrile using the modified Reissert-Henze reaction.

At first, we suspected that either the TMSCN or BzBr were no longer usable; therefore, the benzoyl bromide was distilled under vacuum to remove trace amounts of HBr and NMR analysis after showed 98% purity. Due to the hazardous nature of trimethylsilyl cyanide, direct analysis by conventional means (NMR, IR, MS) was not an option therefore, the product as purchased was reacted with 2,2'-bipyridine-*bis-N,N'*-oxide and benzoyl chloride, which furnished the dicarbonitrile product in 66% yield, proving neither purchased chemical was impure.

Therefore, it was thought that understanding the products formed by the reaction could lead to the necessary adjustments required to improve the reaction. Mass spectrometric analysis of the mixture of products obtained showed several different compounds to be present (Figure 2.16). The analysis showed that the major ion peaks were found to be $[M+H]^+ = 121$, 263, 339, 344, 353, 448, 521 Da.
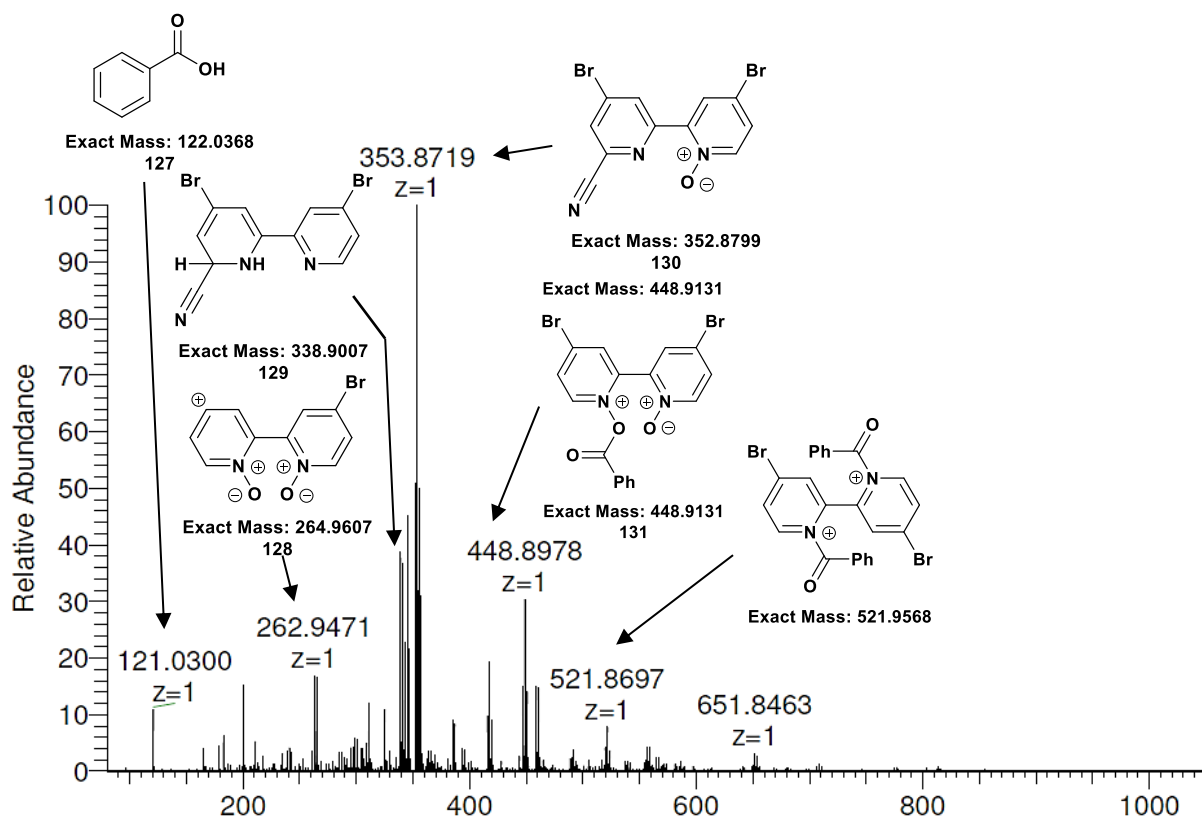
Figure 2.16: Mass spectrum of the product obtained from the Reissert-Henze reaction.

The signal at 121 corresponds to benzoic acid **127**, a by-product of the reaction. The ion at 263, corresponds to the cleavage of a bromine **128**, from the lack of isotope signals from the corresponding $^{81}Br^{81}Br$ isotope, from the starting *bis*-oxide **122**, this is likely to have occurred in the mass spectrometer and not in the reaction. The signal at 339 is proposed to correspond to single cyanation of dibromo-dihydrobipyridine **129**, the mechanism of how the reduction occurs is not described, but attack at the 2-position is documented by Fife.[117] The peak at 344 relates to the starting material, 4,4'-dibromo-2,2'-bipyridine-*bis-N,N'*-oxide **122**. The most abundant signal at 353, corresponds to a molecule where only one ring has undergone the reaction. It is proposed that the ion at 448 corresponds to the addition of benzoyl bromide to the starting material to form the *mono*-benzoyloxy-bipyridine **131**. Interestingly, the signal at

521 suggests the formation of dibenzoylbipyridine **132** where the reduced bipyridine attacks the benzoyl bromide.

A common fragmentation pathway for *N*-oxides is the elimination of hydroxy radicals[118] however, this would not explain the formation of the benzoylated by-products therefore, the reduction of the *N*-oxides must occur during the reaction and before the addition of the CN. Whilst this phenomenon is not documented we propose that attack of a nucleophile, possibly benzoate, onto the benzoylated N-oxide facilitates the reduction (Scheme 2.26).
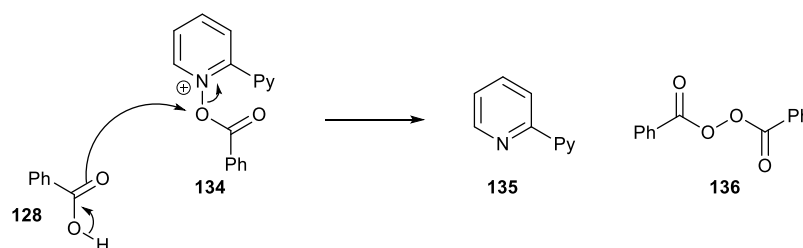
Scheme 2.26: Potential mechanism of reduction of pyridine-*N*-oxides during the cyanation.

This would suggest that the addition of the benzoyl bromide is occurring before the attack of the cyanide, to avoid this, TMSCN should be added to the starting material and the mixture allowed to stir at room temperature for 24 h to ensure the attack is facilitated, before adding in the benzoyl bromide dropwise. Unfortunately, due to time limitations at the end of this project, this experiment was not carried out.

2.6.5 Design of a new synthetic route to the *bis*-solvated degradation adducts using homocoupling

In tandem with the above approach to synthesize the *bis*-solvated adducts, a different synthetic approach was explored as a result of the issues faced with the low yield in the *bis*-nitration and issues with the cyanation. The desired product from this route was 4,4'-dibromo-2,2'-bipyridine-dicarbonitrile **123**, which is symmetrical and therefore, homocoupling two

pyridine rings forms the basis for this synthetic route (Scheme 2.27). 4-bromopyridine **137** is commercially available as its hydrochloric salt, which underwent carboxamidation with formamide and potassium persulfate to furnish 4-bromopicolinamide **138** as described by Bhat *et al.*[119] Following oxidation with phosphorous oxychloride to yield the cyanopyridine **139** and selective iodination following work by Gros and Caubere[120] at the 2-position, homocoupling the 2-iodopyridine using a nickel-zinc system designed by Duan *et al.*[121] should furnish the desired dicarbonitrile **123**.
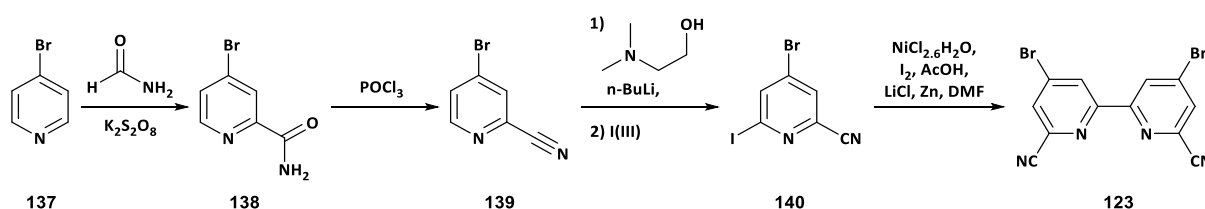
Scheme 2.27: Proposed synthetic route to 4,4'-dibromo-2,2'-bipyridine-dicarbonitrile 123 using homocoupling.

The carboxamidation using potassium persulfate and formamide was unsuccessful and resulted in no conversion of the starting material. The issue was thought to be the low solubility of the potassium persulfate in formamide and so this was replaced by ammonium persulfate which dissolved in the formamide but also resulted in no conversion of the starting material. Further reading on the reaction revealed similar papers using sodium formate and silver nitrate under an oxygen atmosphere in conjunction with the persulfate to facilitate the picolinamide.[122] The issue here however, was that the stochiometric amount of silver nitrate required was uneconomical to contemplate scaling this reaction to the necessary quantity required.

The next avenue considered was to use chemistry familiar to the group by oxidizing the pyridine **137** to the *N*-oxide and using the modified Reissert-Henze reaction to furnish the cyanopyridine **138** (Scheme 2.28). However, instead of using benzoyl bromide the literature

suggested using triethylamine[123] proceeding by a proposed mechanism where the *N*-oxide **137** attacks the silane releasing cyanide, which in turn attacks the pyridine at the 2-position breaking the aromaticity, followed by deprotonation and the reforming of aromaticity by loss of trimethylsilanol.
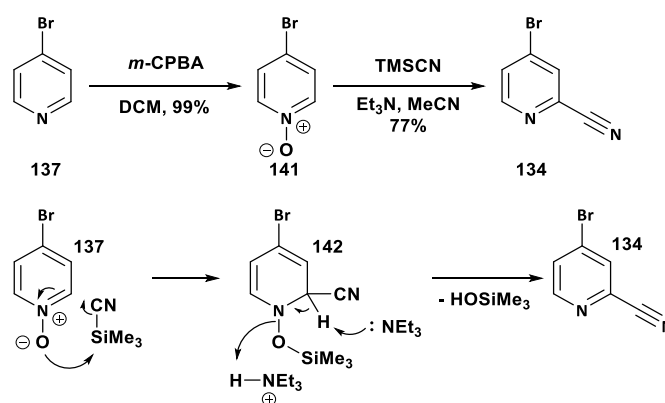
Scheme 2.28: Synthesis of 2-cyano-4-bromopyridine and mechanism for the cyanidation using triethylamine.

The oxidation of the pyridine was successful with complete conversion to 4-bromopyridine *N*-oxide **141** in 99% yield with high purity as evidenced by NMR analysis (Figure 2.17). The by-product of the reaction, *m*-chlorobenzoic acid precipitated out of DCM after 16 h and was filtered off, giving a filtrate containing only the desired product.
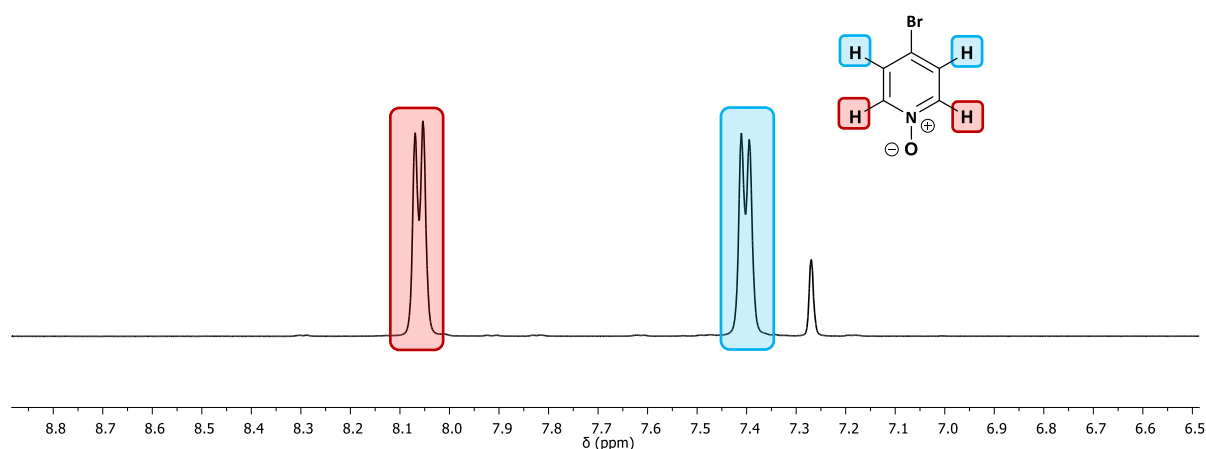
Figure 2.17: NMR of 4-bromopyridine-*N*-oxide 141.

2-cyano-4-bromopyridine **139** was successfully synthesized using the triethylamine-modified Reissert-Henze reaction in 77% yield on a 3 g scale reaction. Following the workup there was no evidence of reduction before the addition of the cyanide, nor any unwanted side products as evidenced by NMR analysis (Figure 2.18).
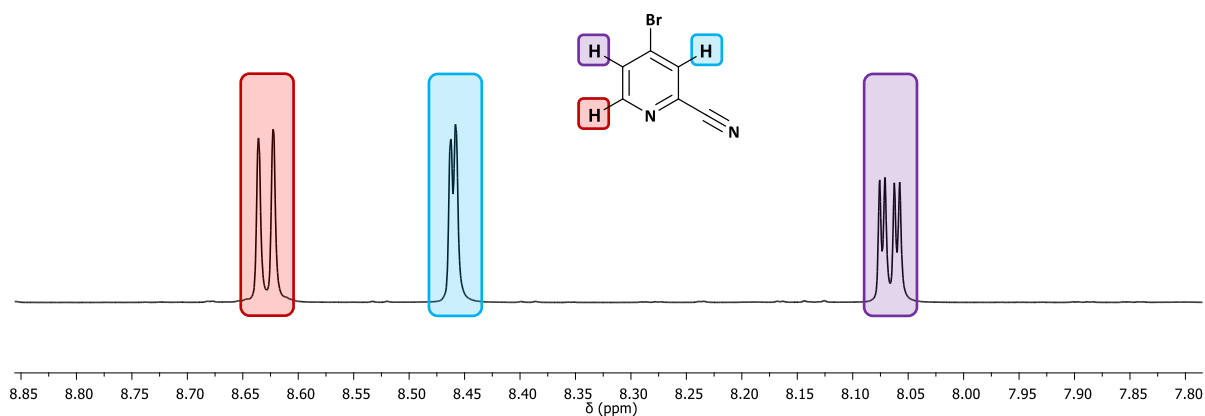
Figure 2.18: NMR spectrum of 2-cyano-4-bromo-pyridine.

The subsequent iodination using lithium dimethylaminoethanol (LiDMAE) and iodine monochloride was unsuccessful and the desired product was not isolated. However, we propose that, on addition of the LiDMAE, lithiation of the bromine occurred resulting in the homocoupling with another cyanopyridine **139** at the 4-positions to furnish 2,2'-dicyano-4,4'-bipyridine **144** as confirmed by NMR analysis. The reaction was repeated in the absence of iodine monochloride to confirm that that it had no effect on the reaction, and indeed resulted in the formation of the 4,4'-bipyridine **144**.
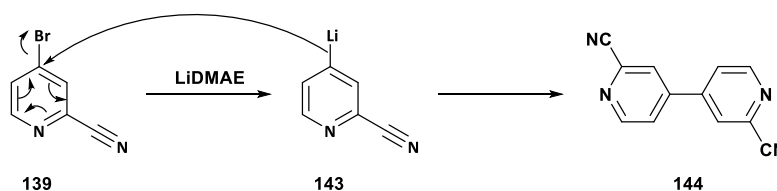
Scheme 2.29: Proposed mechanism for formation of 2,2'-dicyano-4,4'-bipyridine.

Without the ability to iodinate the 2-cyano-4-bromopyridine **139** or perform a coupling on the 2-position from the pyridine this route was abandoned.
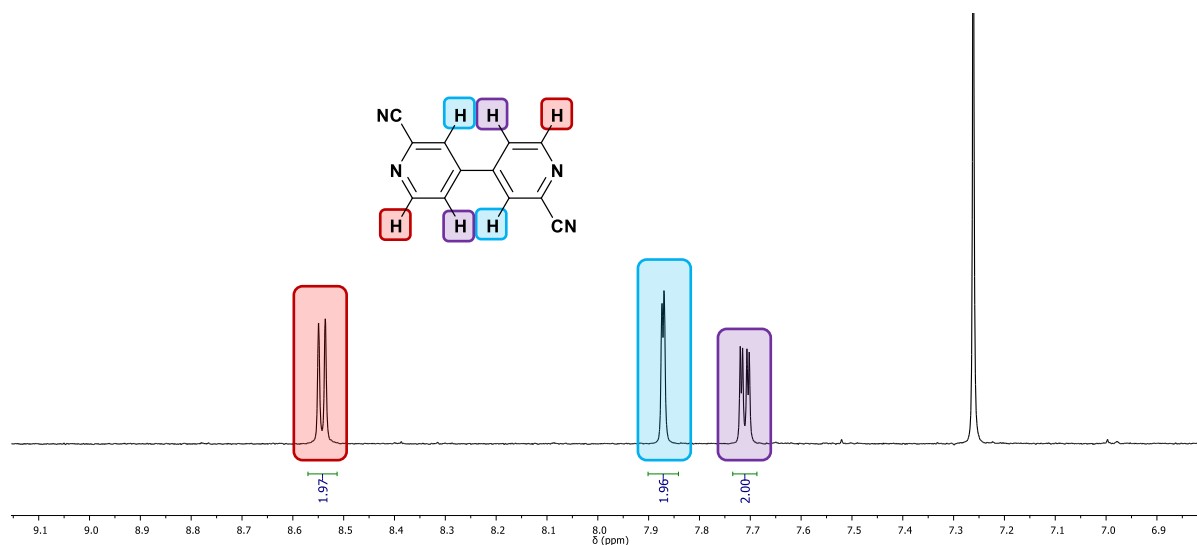
Figure 2.19: NMR spectrum of 2,2'-dicyano-4,4'-bipyridine.

2.6.6 Design of a new synthetic route using 6,6'-dimethyl-2,2'-bipyridine

After the failed attempts at synthesizing the degradation adducts, and with time of the essence one last ditch attempt was made at synthesizing the adducts. 6,6'-Dimethyl-2,2'-bipyridine **145** was used the starting material for this new route that merged the synthetic routes used to prepare bromo-BTBP **106** and BTPhens **72**. The proposed route was to oxidize the dimethylbipyridine **145** using acetic acid and hydrogen peroxide, followed by nitration with potassium nitrate and bromination with acetyl bromide and acetic acid as above, followed by reducing the *N*-oxides **148** with phosphorous tribromide to furnish 4,4'-dibromo-6,6'-dimethyl-2,2'-bipyridine **149**. The methyl groups were then to be oxidized using selenium dioxide to the *bis*-aldehyde **150** as before and treating with hydroxylamine hydrochloride to produce the *bis*-oxime **151**. Reacting with tosyl chloride in the presence of pyridine would give the 4,4'-dibromo-2,2'-bipyridine-dicarbonitrile **123**. Treating the dicarbonitrile with hydrazine

hydrate would then lead to the bis-(aminohydrazide) **124** and the resultant condensation would provide the desired dibromo-CyMe₄-BTBP **106** in 9 steps.
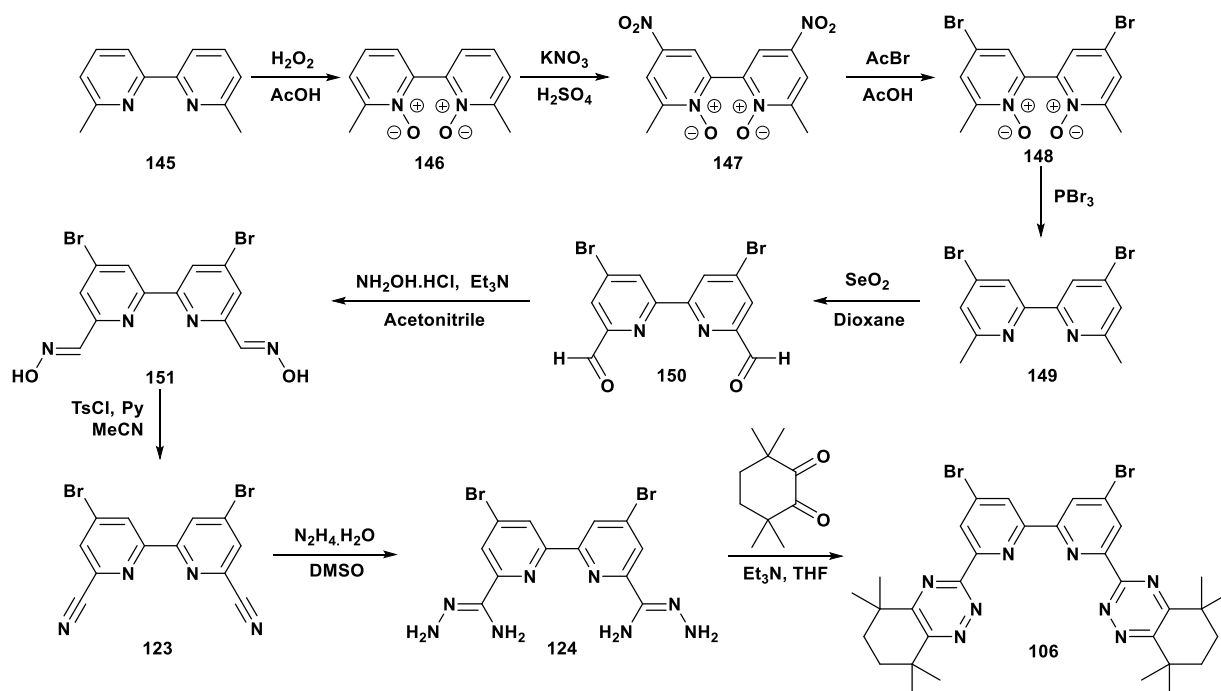
Scheme 2.30: Proposed synthetic route towards dibromo-BTBP for synthesis of the Degradation adducts.

The oxidation of the 6,6'-dimethyl-2,2'-bipyridine **145** was successful generating a colourless powder in 95% yield using acetic acid and hydrogen peroxide (Scheme 2.31). Interestingly, when attempting to synthesize the *mono*-bromobipyridine **152** there was no conversion of the starting material.
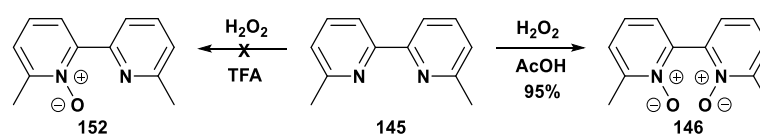
Scheme 2.31: Synthesis of 6,6'-dimethyl-2,2'-bipyridine-*bis-N,N'*-oxide.
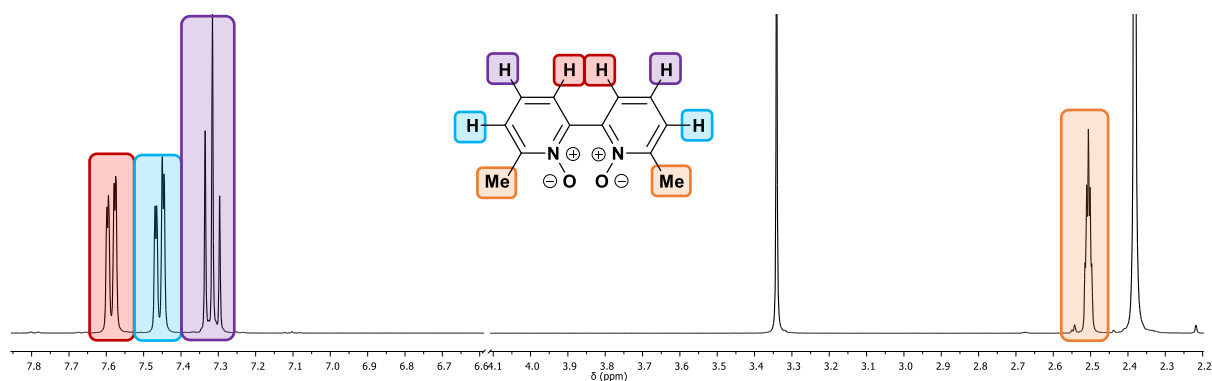
Figure 2.20: NMR spectrum of 6,6'-dimethyl-2,2'-bipyridine-*bis-N,N'*-oxide 146.

The subsequent nitration of the oxide proceeded well; however the reaction resulted in a low yield (36%) on a 11 mmol scale. As before, the low yield can be attributed to the high solubility of the product in water over organic solvents, although NMR analysis indicated that the product was pure.
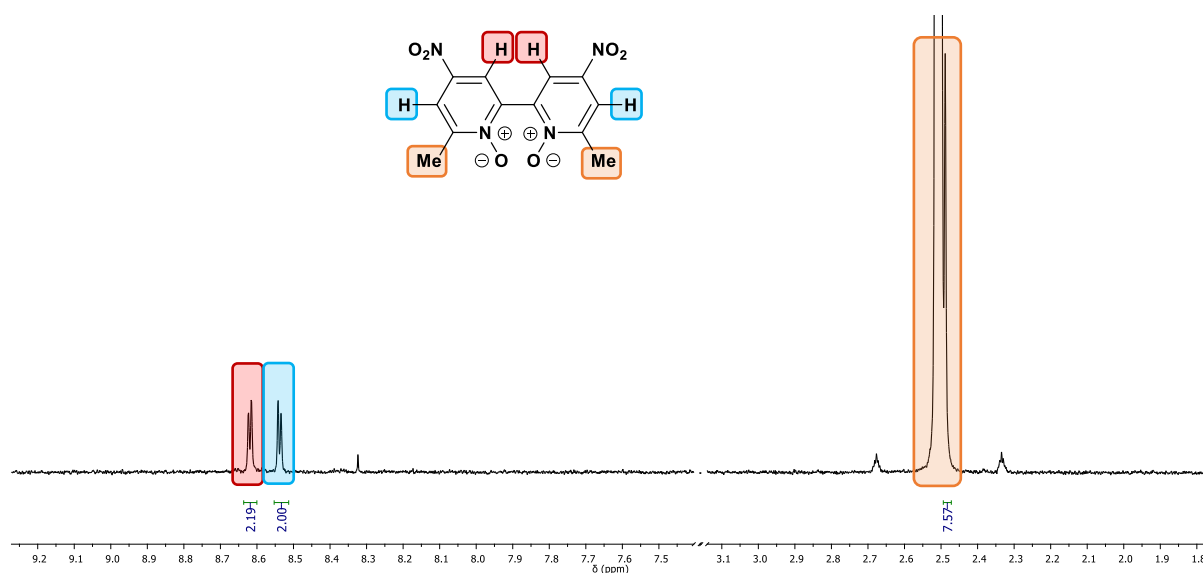
Figure 2.21: NMR spectrum of 4,4'-dinitro-6,6'-dimethyl-2,2'-bipyridine-*bis-N,N'*-oxide 147.

Bromination of the dinitrobipyridine **147** using acetyl bromide and acetic acid was unsuccessful resulting in a complex mixture of products that were difficult to separate. NMR analysis showed that no starting material remained and, by comparison with the literature,[124] there were three singlet resonances at 7.92, 7.84 and 2.36 ppm, none of which were present in the spectrum (Figure 2.22). Due to time constraints, repeating this reaction could not be undertaken to obtain the product and proceed with the remaining steps of the synthesis.
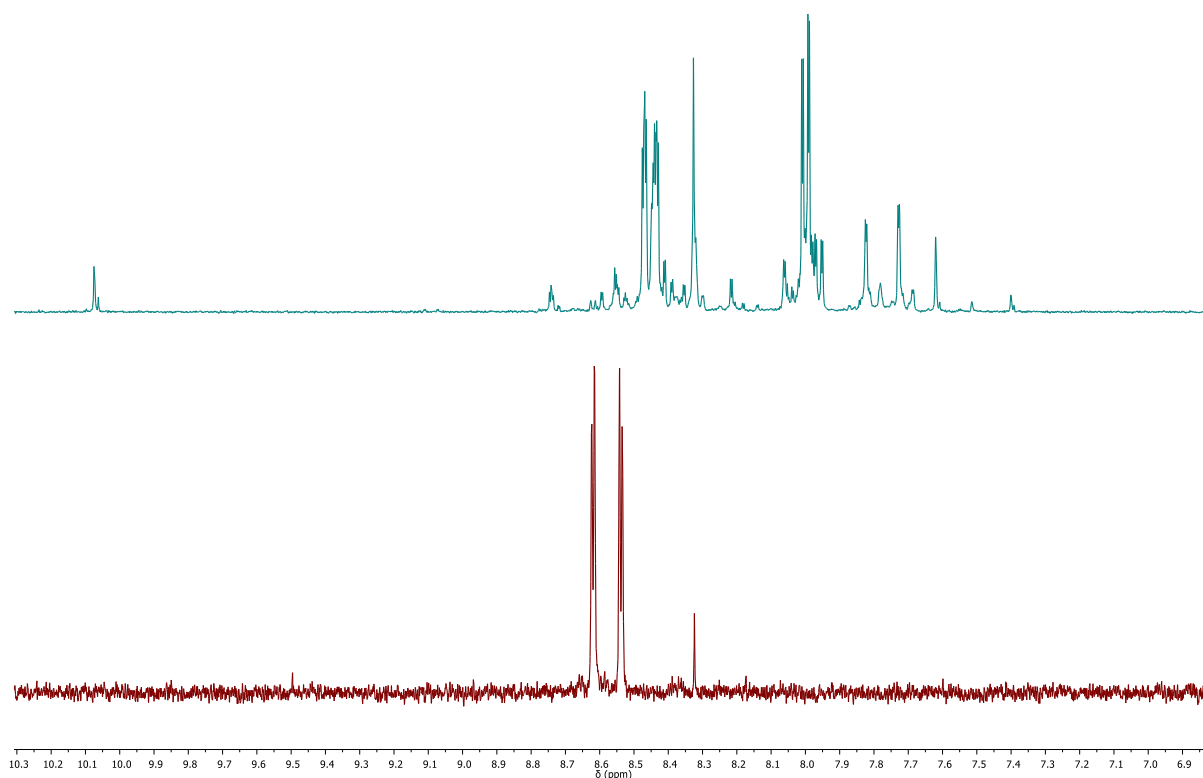
Figure 2.22: Stacked NMR spectra showing the product of the bromination of 4,4'-dinitro-6,6'-dimethyl-2,2'-bipyridine-

bis-N,N'-oxide 148.

2.7 Synthesis of CyMe$_4$-Diketone

Previous work by Harwood *et al.*[31] disclosed an improved and scalable synthetic procedure to obtain CyMe$_4$-diketone **43**. The synthesis involved the alkylation of ethyl isobutyrate **40** with ethane-1,2-ditoluenesulfonate, followed by a Ruhlmann-modified acyloin condensation to give trimethylsilyl-protected ketone **42**.[125] This, on oxidation with bromine yielded the diketone **43** in 45% overall yield.
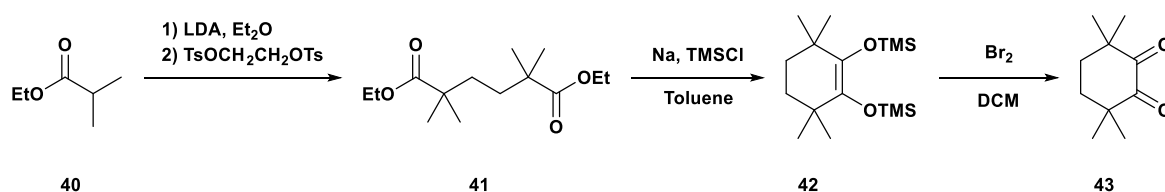
Scheme 2.32: Synthesis of CyMe$_4$-Diketone.

This synthetic route was attempted multiple times to try to synthesize the diketone **43**. The first step requires specific timing for the yields and purity to be acceptable. The diester **41** was synthesized in 52% yield, the procedure states that it should be purified by vacuum distillation, but the product was deemed to be pure enough to be taken forward as it was. The second step is less specific on timing; however, the reaction yielded only 35% of product after vacuum distillation. The distillation must be completed quickly within 2-3 hours or the product **42** starts to decompose into inseparable by-product. Subsequently, on repeating the procedure, it was found that the distillation was not needed, resulting in a higher 55% yield. However, **42** readily degrades at 4 °C to the unprotected alcohol and ketone and subsequent mixtures of each, and therefore must be used immediately after synthesis. Finally, the oxidative deprotection yielded 77% of pure CyMe₄-diketone **43** (22% overall).

Adapting Synthetic Routes to Synthesising CyMe₄-Diketone

Although better than previous approaches to the target molecule, the published synthetic route still has room for improvement. As an estimate, the diketone **43** costs £44 per gram to prepare, not including approximately two weeks of time to synthesize it.[126] The significant cost is the price of ethylene di(*p*-toluenesulfonate) (£175 per 50 g) and solvent cost. Therefore, if the disulfonate can be eliminated the procedure could become economically scalable and hopefully require less experimental time.

The first approach was to submit pivalic acid **153** to UV irradiation (hv = 354 nm) in the presence of hydrogen peroxide. The hypothesis was that the light would generate hydroxyl radicals that would abstract a hydrogen from a methyl group on the pivalic acid, which would undergo a termination reaction by reacting with another radical to produce the 2,2,5,5-tetramethyladipic acid **154**. This reaction was attempted in both a batch reactor and flow

reactor. The reaction in the batch seemed to perform better yielding more product but saw many other products being formed, as well as unreacted starting material remaining. The reaction in the flow reactor did not convert the starting material to the desired product, but only to unidentified by-products.
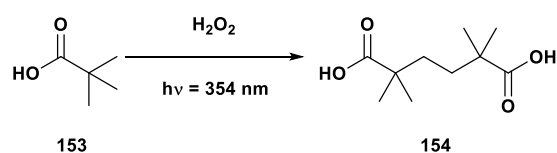
Scheme 2.33: UV reaction to synthesize 2,2,5,5-tetramethyladipic acid.

After the reaction failed to yield pure **154** another approach was considered. The symmetry of diester **41** led to the idea of a homocoupling reaction and a synthetic route was developed to synthesize the key intermediate methyl 3-bromopivalate **156** from hydroxypivalic acid **155.**
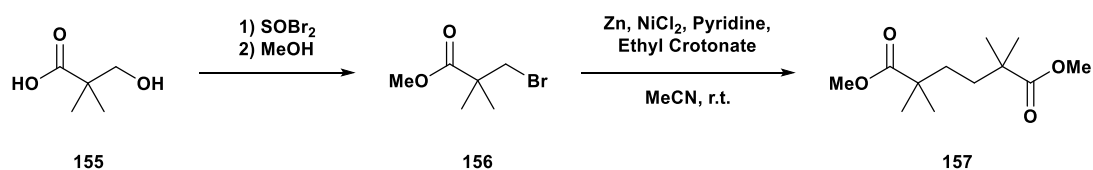
Scheme 2.34: Synthesis of methyl 3-bromopivalate and homocoupling reaction.

The first step of the synthetic route used thionyl bromide as brominating reagent, because hydroxypivalic acid **155** is neopentylic in nature. These groups do not undergo S$_N$1 reactions because the position is primary and S$_N$2 is disfavoured due to steric hinderance. However, thionyl bromide would follow an S$_N$I pathway that is more favourable for neopentylic groups.

However, when hydroxypivalic acid was treated with thionyl bromide, NMR spectroscopic and mass spectrometric analysis did not indicate presence of the desired homo-coupling product and high mass ion peaks in the mass spectrum were seen, suggesting polymerisation had occurred. Therefore, it was decided to separate the bromination and esterification steps. It was imperative that the acid bromide could not form, or this could result in polymerization as

before. Hence, the procedure described by Sandoz *et al.* was used, utilising hydrobromic acid

at 100 °C to convert the neopentylic alcohol to the bromide (Scheme 2.35).[127]
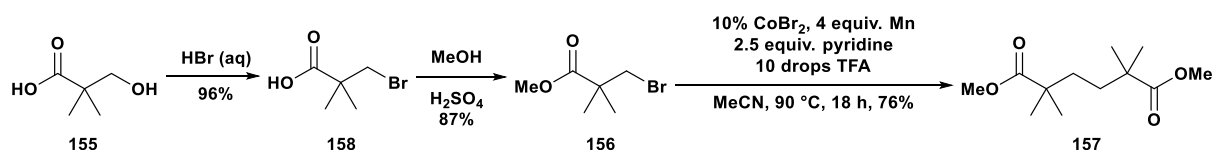
Scheme 2.35: Synthesis of methyl diester using homocoupling.

It was noted that at 100 °C the bromination did not result in 100% conversion of the starting

material after 18 h, but when the temperature was raised to 120 °C the reaction proceeded

to completion and was higher yielding, giving 96% of desired bromide **158** compared to 66%

yield at 100 °C. We propose that the reaction propose that reaction proceeds via formation

an intermediate β-lactone **160** (Scheme 2.36); aided by the Thorpe-Ingold effect due to the

presence of *gem*-dimethyl substituents.[128]
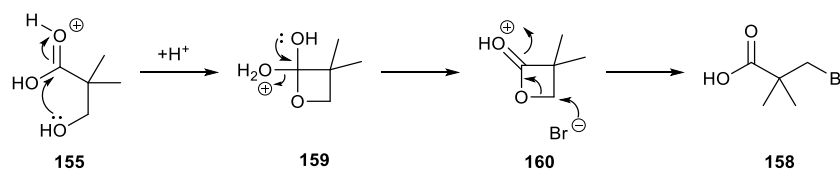
Scheme 2.36: Mechanism for the bromination of hydroxypivalic acid *via* the β-lactam intermediate.

After considering the literature on sp³-sp³ homocoupling reactions, two different catalyst

systems, nickel[129] and cobalt,[130] looked promising. The nickel system (Scheme 2.34) utilised

zinc to chelate to the bromoester and pyridine, and ethyl crotonate to ligate to the nickel

catalyst. However when attempted, the reaction did not yield the desired product, possibly

due to hydrodehalogenation of the bromoester **156** and loss of the methyl pivalate upon

removal of the acetonitrile solvent. The cobalt system (Scheme 2.35) used manganese-

activated by TFA with pyridine as a ligand for the Co(II). When tested on the methyl ester the

reaction proceeded with 100% conversion of the starting material **156** by TLC but again did not yield the desired diester instead no product was isolated. However, activating the manganese powder by sonicating bath in pre-dried acetonitrile resulted in a yield of 76% of the diester **157**. The following acyloin condensation and oxidative deprotection progresses as previously resulting in a 25 % overall yield of the diketone **43**; a slight improvement over the previously reported procedure.

2.8 Synthesis of Ligands used for Collaborators

As part of the conditions of my funding various groups within the GENIORS project and also other collaborators would often require ligands to be synthesized for a variety of analytical experiments.

2.8.1 Synthesis of Tetraethyldiglycolamide and Tetraethylmalonamide

The following section led to the publication: A. J. Canner, L. M. Harwood, J. Cowell, J. S. Babra, S. F. Brown and M. D. Ogden, *J. Solution Chem.*, 2020, **49**, 52–67.

Tetraethyldiglycolamide (TEDGA) **164** and tetraethylmalonamide (TEMA) **166**, similar to TODGA **5** mentioned earlier, can be used in the DIAMEX process. These ligands were synthesized for Dr. Mark Ogden's group at the University of Sheffield. Researchers at the University of Sheffield investigated the interactions between monoamides, diamides, and digylcolamides with uranium oxide in pseudo-aqueous media. The diglycolamides were shown to produce 104 different species with the uranium oxide leading extremely complex solution chemistries. The diglycolamides were shown to produce stronger complexes with uranium than the monomides and diamides.[131]

Synthesis of the ligands involved using an EDCI.HCl amide coupling of diglycolic acid **162** malonic acid **165** and diethylamine **163** in the presence of hydroxybenztriazole and triethylamine, yielding 86% and 84% yield for TEDGA **164** and TEMA **166** respectively (Scheme 2.37).

Scheme 2.37: Synthesis of TEDGA and TEMA.
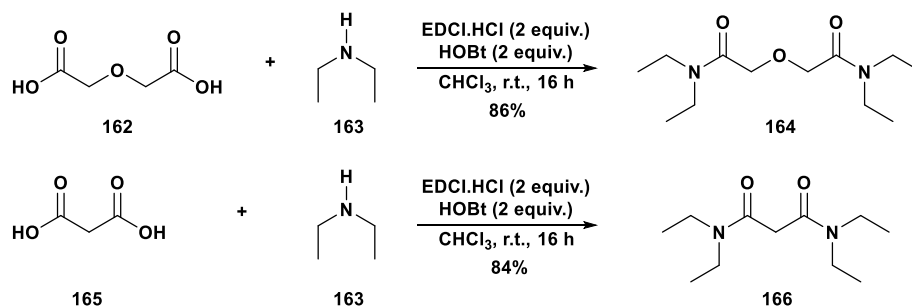
2.8.2 Synthesis of Tetra(*m*-sulfonylphenyl)-BTBP

The Mount group from the University of Edinburgh requested a bipyridyl ligand that was water soluble so that they could measure the transfer kinetics of ligated metals in solution as part of the GENIORS framework. The most common water-soluble ligand in our field is the tetra(*m*-sulfonylphenyl)-BTBP **167** (Figure 2.23) which has undergone extensive testing for use in the proposed *i*-SANEX process, where the minor actinides are retained in the aqueous phase, rather than being extracted into the organic phase.[60,61,132]
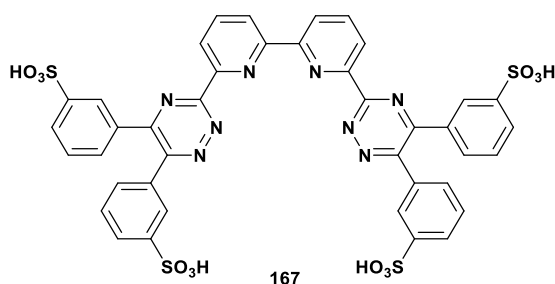
Figure 2.23: Structure of Tetra(*m*-sulfonylphenyl)-BTBP

The ligand was synthesized according to the procedure reported by Harwood and Lewis *et al.*[132] (Scheme 2.38), where bipyridine *N*-oxide **44** was synthesized as described in section 2.6.1 and the following cyanidation was completed with 70% yield. Treatment with hydrazine

hydrate in DMSO furnished the *bis*-(aminohydrazide) **47**. The condensation reaction with benzil in dioxane successfully produced tetraphenyl-BTBP **168** as a fine bright yellow powder in 40% yield. Higher yields (59%) were achieved when a vigorous reflux was used.
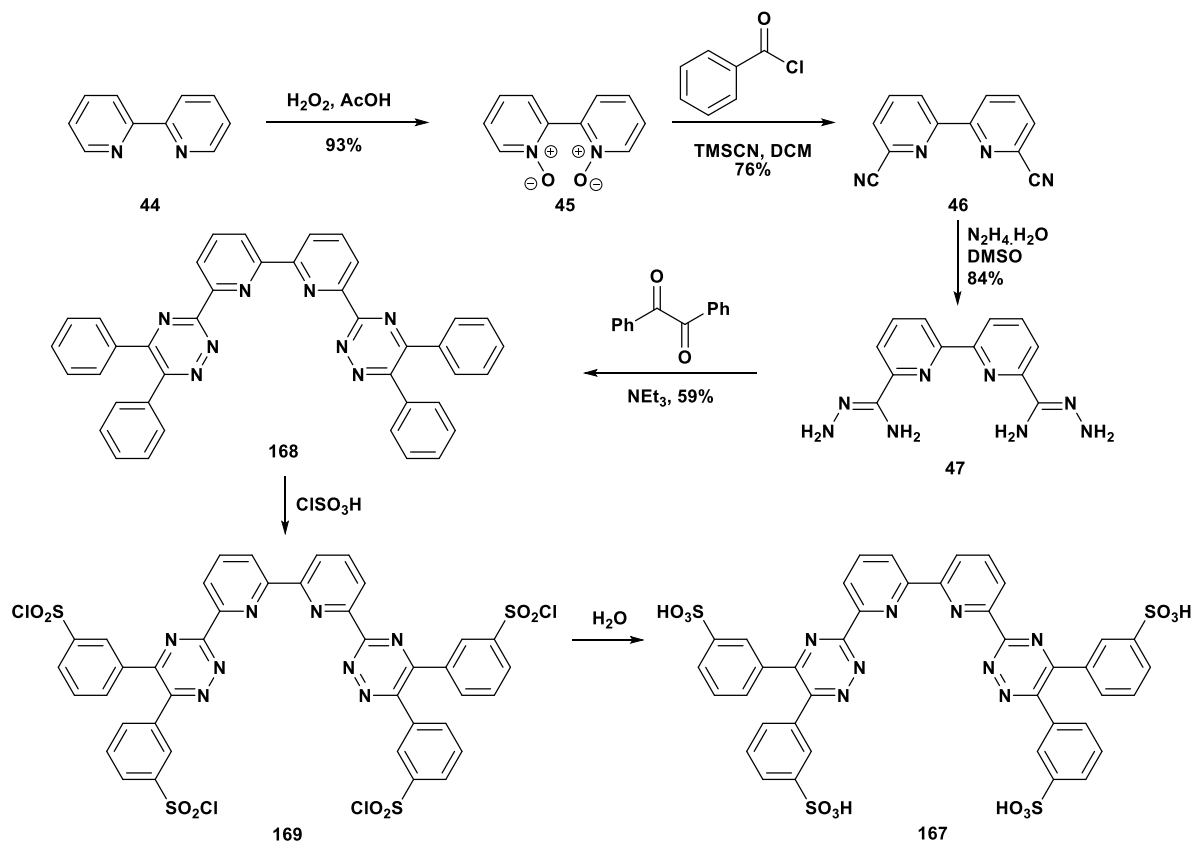
Scheme 2.38: Synthesis of Tetra(*m*-sulfonylphenyl)-BTBP 170.
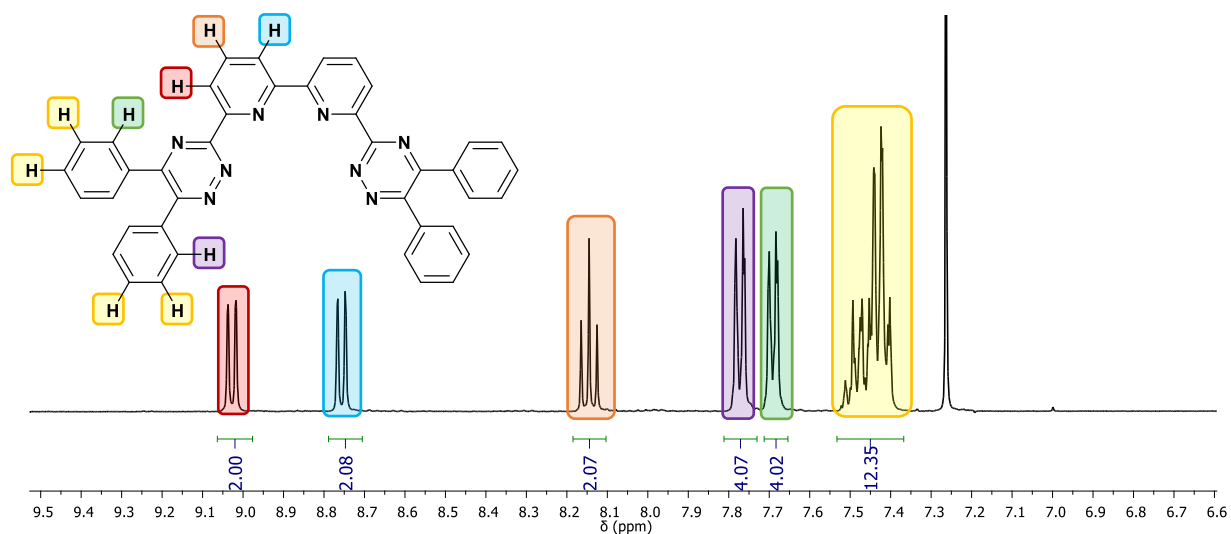
Figure 2.24: NMR spectrum of Tetraphenyl-BTBP.

81

The sulfonation of the tetraphenyl rings was potentially hazardous, using chlorosulfonic acid, resulting in what was initially proposed to be the tetra-chlorosulfonylated product. However, the procedure stated by Lewis *et al.* displayed the same splitting patterns and shifts as with our product and mass spectrometry confirmed the lack of a chlorine atom in the parent ion. Therefore, we propose that whilst the chlorosulfonyl acid is formed in the reaction, it is quicky quenched when the reaction is poured onto ice during the workup. Ultimately, Tetra(*m*-sulfonylphenyl)-BTBP was synthesized in a 7 g quantity, which was sent to Edinburgh for analysis.

Chapter 3 – Conclusions and Future Work

3.1 Conclusions

The introduction to this thesis summarized the current proposed processes for the future of nuclear power and the role of synthetic chemistry in the decommissioning of older generation nuclear reactors and the reprocessing. The timeline of the development of actinide selective ligands was discussed from BTPs **36** to BTPhens **72** was discussed. A short review on the radiolytic degradation of BTBPs **53** and BTPhens **72** was also covered.

Following the irradiation of CyMe$_4$-BTBP **53** in cyclohexanone and CyMe$_4$-BTPhen **72** in octanol the samples were analysed by mass spectrometry. The analysis showed little to no degradation of the ligands in isolation but indicated that adducts were being formed with both cyclohexanone and octanol solvents and structures have been proposed to match the ion signals. For CyMe$_4$-BTBP **53** the degradation adducts were separated into two categories of *mono-* and *bis-*solvated degradation adducts. However, mass spectrometry alone is not a quantitative technique and therefore, the degradation adducts needed to be synthesized, and compared against the degradation data.

To retrieve more data of the irradiated adducts, CyMe$_4$-BTBP **53** and CyMe$_4$-BTPhen **72** were synthesized in good yields 42% over 4 steps and 24% over 6 steps, respectively. The samples were sent to external groups to be irradiated. However, the irradiated samples were never received as a result of the COVID-19 pandemic and the analysis was therefore not completed. Thus, attempts at synthesizing the degradation adducts suggested by the results by Schmidt were designed.

83

The reported synthesis of 4-bromo-CyMe$_4$-BTBP **113** was followed, and several steps were altered to improve the yields and reliability of the synthetic pathway.[80] Improvements to the *N*-oxidation resulted in an increase from the literature yield of 30% literature to 96%; lowering the temperature of the nitration resulting in increased reliability of previous yields from 12-80% to consistently >80% yields. The subsequent bromination step was improved by performing the reaction under inert atmosphere with excess acetyl bromide and resulted in a yield of 95% compared to the previous yield of 70%. The bis-*N*-oxidation resulted in a modest increase in yield from the 30% literature yield to 53% using acetic acid and hydrogen peroxide. The following cyanation caused issues that are yet to be resolved. Over the first 4 steps the overall yield has increased significantly from a minimum 1.8% yield to 39%, with a 73% overall yield over the first 3 steps.

The synthesis of the *bis*-solvated adducts was undertaken with the *bis*-oxidation of 2,2'-bipyridne, by modification to the workup procedure resulting in an improved yield of 93%. The following nitration was increased to 52% from the previous 30% by reducing the volume of water used in the work up and by cooling the reaction to - 40 °C. The subsequent bromination resulted in a 90% yield using a shorter reaction time to limit the reduction of the *N*-oxide. The cyanation proved troublesome here too; however, further investigation indicated that the reduction of the *N*-oxide moieties before the addition of the cyanide to the pyridine ring. Additionally, a new procedure suggested delaying the addition of benzoyl bromide to the reaction.

To combat the problems with the cyanation reactions, a new synthetic route was designed. 4-Bromopyridine **137** was used as the initial building block and was oxidized to the *N*-oxide in 99% yield using *m*-CPBA, before undergoing a basic cyanation with TMSCN and NEt$_3$ in a yield

of 77%. However, when attempting to perform an iodination at the 2-position, 2-cyano-4-bromopyridine **139** underwent lithiation from LiDMAE in solution to result in dimerization, producing 2,2'-cyano-4,4'-bipyridine as the only product.

The second attempt at circumventing the cyanation approach used 6,6'-dimethylbipyridine **145** as starting material, which was oxidized and nitrated as above with yields of 95% and 36% respectively. However, bromination of the dinitrobipyridine **147** did not result in conversion to desired product and resulted in an inseparable mixture.

As part of this work, ligands were synthesized, on request, for a variety of analytical experiments. Tetraethyldiglycolamide **164** and tetraethylmalonamide **166** were synthesized using EDC.HCl amide coupling for the Ogden group at the University of Sheffield in 86% and 84% yield for TEDGA **164** and TEMA **166** respectively and were tested for speciation with uranium oxides by the Sheffield researchers.

The Mount group in Edinburgh requested a water-soluble ligand to test transfer kinetics of ligated metals in solution. Tetra(*m*-sulfonylphenyl)-BTBP **167** was chosen and synthesized according to the literature procedure in 29% yield over 5 steps, wherein 2,2'-bipyridine **44** was oxidized in 93% yield, following the cyanation in 70% yield and treatment with hydrazine hydrate to furnish the bis-(aminohydrazide) **47** in 78% yield. Condensing with benzil gave moderate a yield of 59% and sulfonation using chlorosulfonic acid furnished the target tetra(*m*-sulfonylphenyl)-BTBP **167** in 97% yield.

3.2 Future Work

Further work into synthesizing the proposed degradation adducts is necessary, to obtain as much knowledge regarding the extraction process and the life-cycle of the ligands used. To

that end, revisiting the cyanation reaction of 4-bromo- **110** and 4,4'-dibromo-bipyridine-*bis-N*-oxide **122** would be beneficial to test the effect of delaying the addition of the benzoyl bromide to the reaction. In addition, using different sources of cyanide to increase the rate of addition to the pyridine ring should be investigated.

A new pathway could be developed using selective iridium borylation developed by the Hartwig group.[133,134] This route would involve applying this methodology to the CyMe$_4$-BTBP **53** where the 4-position would be selectively borylated. However, these procedures are sensitive to water and dissolved oxygen in the reaction, so dry inert samples would need to be used, and the iridium catalyst would need to be handled under inert atmosphere when making the stock solutions. This has issues with scale-up but could be a useful laboratory-scale approach. From the borylation, the boron-derivative could be converted to the 4-iodo compound **171** using *N*-iodosuccinamide (Scheme 3.1).[135]
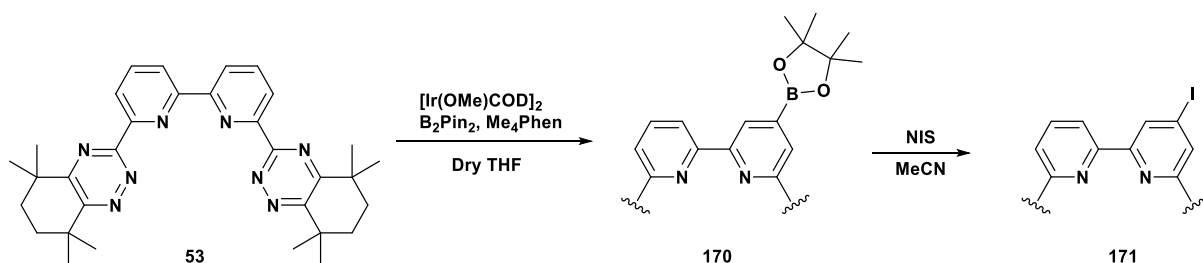
Scheme 3.1: Proposed Synthesis of 4-Iodo-CyMe4-BTBP.

A third potential method for synthesizing the iodo-CyMe$_4$-BTBP **171** would be to synthesize the chloro-CyMe$_4$-BTBP according to literature[80] and perform an aromatic Finkelstein reaction as described by Buchwald *et al.*[136] using 5 mol% of copper(I) iodide and sodium iodide. Due to the nature of the ligand, it is likely 1.1 equivalents of CuI might be required to ensure not all of the copper is ligated to the ligand.

Another method to determine the degradation adducts would be to irradiate larger quantities of CyMe$_4$-BTBP **53** and CyMe$_4$-BTPhen **72** and, after concentrating the samples, separating them by preparative scale HPLC to isolate all the degradation adducts. Following collection of the isolated degradation adducts, analysis by a combination of techniques, particularly NMR spectroscopy, should lead to determination of the exact structures of the ligands. This is dependent on receiving degradation mixtures from our collaborators – something that has proven impossible during the COVID-19 pandemic.

Chapter 4 – Experimental
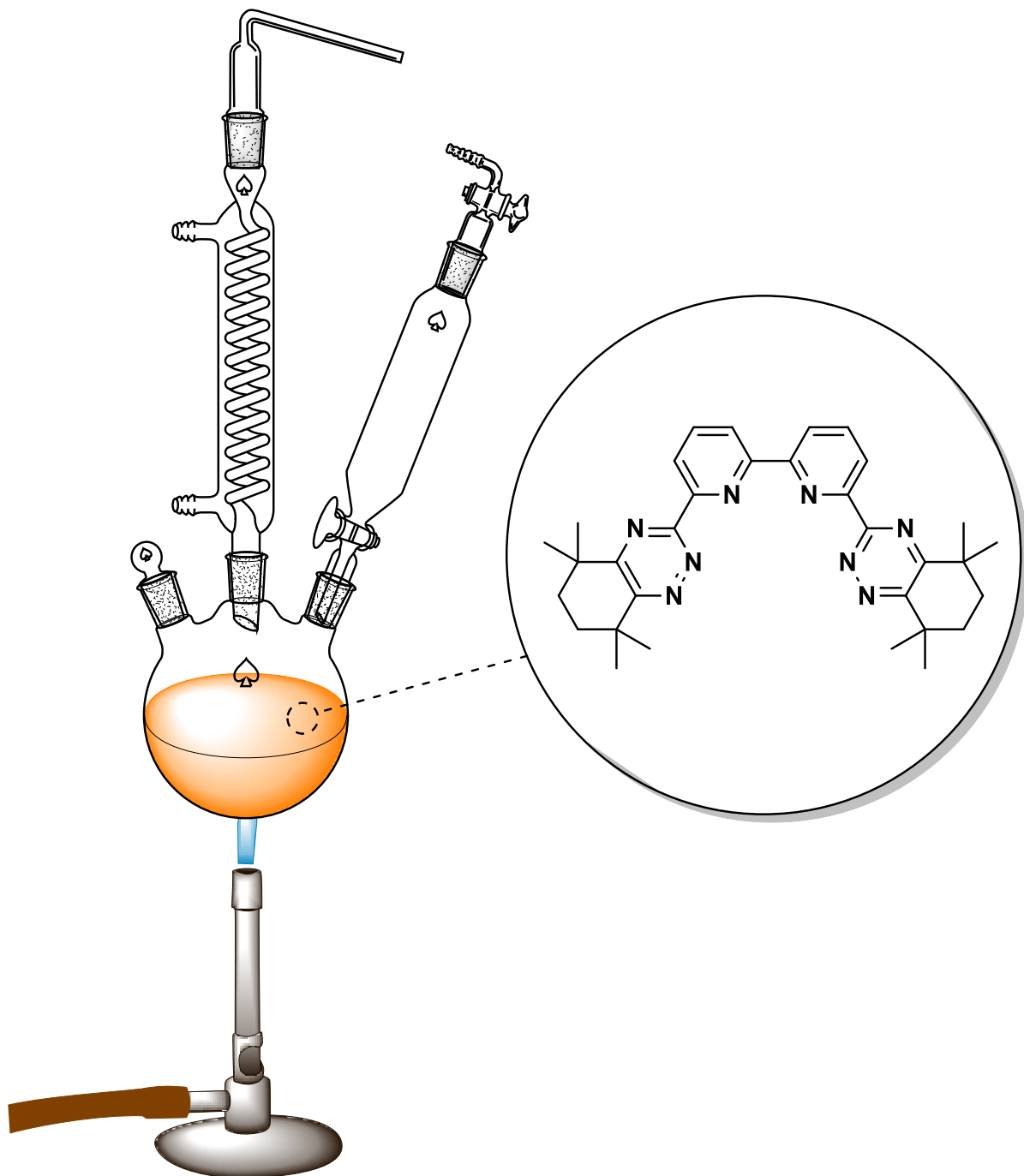
Experimental Details

All reagents and solvents were used as received without further purification from Sigma-Aldrich, Fisher Scientific UK, Fluorochem UK, Tokyo Chemical Industries UK, or Scientific Laboratory Supplies unless specified. Anhydrous solvents were purified using procedures from Armarego and Chai.[137]

The majority of NMR spectroscopic analyses were recorded on either a Bruker DPX-400 or a Bruker Nanobay spectrometer. In specific cases the Bruker Avance III 700 MHz spectrometer was used. ^{1}H NMR spectra were recorded at 400 MHz using deuterated chloroform with tetramethylsilane (δH = 0.00 ppm); or the central resonance of dimethyl sulfoxide (DMSO-$d6$, δH = 2.50 ppm) as internal references. ^{13}C NMR spectra were recorded at 101 MHz using deuterated chloroform (δC = 77.00 ppm); or the central resonance of dimethyl sulfoxide (δC = 39.43 ppm) as internal reference.

Coupling constants are quoted to the nearest 0.5 Hz. Splitting patterns are abbreviated as follows: singlet (s), doublet (d), triplet (t), quartet (q), quintet (quin.), multiplet (m), (ap.) apparent, (b) broad. Chemical shifts are quoted in parts per million (ppm). Multiplets are quoted as a range.

Infrared spectra were recorded as a thin film using a Perkin-Elmer Spectrum One FT-IR spectrometer or Thermofisher Id7 ATR Spectrometer with absorption intensity indicated by: w, weak, < 40%; m, medium, 41-74%; s, strong >75%; and br, broad.

Mass spectrometric analyses were recorded using a Thermo Scientific LTQ-Orbitrap XL using 1 mgL^{-1} samples and diluted 30-fold in MS grade solvents.

Melting points were obtained using a Stuart SMP10 melting point apparatus and are uncorrected.

Analytical thin layer chromatography (TLC) was performed using pre-coated Merck aluminium-backed silica gel plates (Silica gel 60 F254) unless specified. Visualization was by 6W 254 or 356 nm UV light and/or staining with iodine, potassium permanganate, or *p*-anisaldehyde.

Synthesis of 2,2'-Bipyridine *N*-oxide
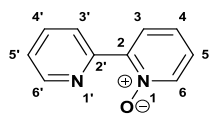
2,2'-Bipyridine *N*-Oxide[2] (**107**)

2,2-Bipyridine **44** (10 g, 64 mmol) was dissolved in trifluoroacetic acid (45 mL, 590 mmol) at 0 °C and hydrogen peroxide (30%, 10 mL, 323.5 mmol) was added to the solution dropwise over 15 minutes. The reaction was allowed to warm to room temperature over 24 h and cooled to 0 °C, basified with 12.5M NaOH until pH 11 and extracted with chloroform (3x100 mL). The combined extracts were dried over magnesium sulfate, filtered and the residual solvent was removed *in vacuo* to afford a colourless oil that solidified after 24 h (10.56 g, 96%).

Mpt. 55-57 °C (lit.[138] 56-57 °C); FTIR (ATR − Thin Film) v/cm^{-1} = 3068 (C$_{Aryl}$-H), 1612 (C$_{Aryl}$=C$_{Aryl}$),1416 (N^{+}-O^{-}); δ$_H$ (400 MHz, CDCl$_3$) 8.89 (1 H, d, *J* 8.0 Hz, **6'**), 8.73 (1 H, ddd, *J* 4.5, 2.0, 0.5 Hz, **3'**), 8.32 (1 H, dd, *J* 6.5, 0.5 Hz, **6**), 8.18 (1 H, dd, *J* 8.0, 2.0 Hz, **3**), 7.83 (1 H, td, *J* 8.0, 2.0 Hz, **4'**), 7.41 − 7.31 (2 H, m, **5, 5'**), 7.31 − 7.22 (1 H, m, **4**); δ$_C$ (101 MHz, CDCl$_3$) 149.6 (C, **2**), 149.4 (CH, **3'**), 147.4 (C, **2'**), 140.7 (CH, **6**), 136.3 (CH, **4'**), 127.9 (CH, **3**), 125.8 (CH, **4**), 125.5 (CH, **5**), 125.3 (CH, **6**), 124.3 (CH, **5'**); HRMS ESI^{+} [M+H]$^{+}$ calculated for C$_{10}$H$_9$N$_2$O = 173.0709 found 173.0705.

Synthesis 4-Nitro-2,2'-Bipyridine *N*-oxide
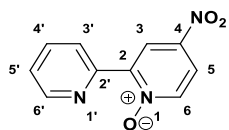
4-Nitro-2,2'-Bipyridine *N*-Oxide (**108**)

2,2'-bipyridine *N*-oxide **107** (10 g, 58 mmol) and potassium nitrate (32.6 g, 322 mmol) were dissolved in concentrated sulfuric acid (100 mL) and the mixture stirred at 80 °C for 30 h. The reaction was poured onto ice and basified to pH 11 with 25% NaOH solution. The precipitate formed was filtered off, washed with cold water and dissolved in DCM. The insoluble material was filtered off, and the filtrate was dried over magnesium sulfate, filtered and the solvent removed *in vacuo*. The precipitate was dried under vacuum at 40 °C for 16 h, to afford a yellow solid (10.1 g, 80%).

Mpt. 184-186 °C (lit.[107] 184-186); FTIR (ATR – Thin Film) v/cm^{-1} = 3064 (C$_{Aryl}$-H), 1604 (C$_{Aryl}$=C$_{Aryl}$),1583 (N-O), , 1416 (N$^+$-O$^-$); δ_H (400 MHz, CDCl$_3$) 9.17 (1 H, d, *J* 3.5 Hz, **3**), 8.89 (1 H, d, *J* 8.0 Hz, **6'**), 8.80 (1 H, d, *J* 4.5 Hz, **3'**), 8.36 (1 H, d, *J* 7.0 Hz, **6**), 8.07 (1 H, dd, *J* 7.0, 3.5 Hz, **5**), 7.88 (1 H, td, *J* 8.0, 2.0 Hz, **5'**), 7.44 (1 H, dd, *J* 8.0, 4.5 Hz, **4'**); δ_C (101 MHz, CDCl$_3$) 149.9 (CH, **3'**), 148.3 (C, **2**), 147.6 (C, **2'**), 142.5 (C, **4**), 142.0 (CH, **6**), 136.7 (CH, **5'**), 125.4 (CH, **4'**), 125.1 (CH, **1'**), 122.5 (CH, **3'**), 118.9 (CH, **5**); HRMS ESI$^+$ [M+H]$^+$ calculated for C$_{10}$H$_8$O$_3$N$_3$ = 218.0560, found 218.0567.

Synthesis of 4-Bromo-2,2'-Bipyridine *N*-oxide
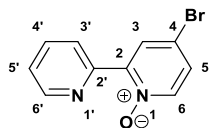
4-Bromo-2,2'-Bipyridine *N*-oxide[139] (**109**)

4-Nitro-2,2'-bipyridine N-oxide **108** (10 g, 46 mmol) was dissolved in glacial acetic acid (100 mL) and acetyl bromide (50 mL, excess) under a nitrogen atmosphere and the mixture heated to reflux for 16 h. After this time, the reaction was poured onto ice and basified with potassium hydroxide until the pH was 11. The reaction was extracted with chloroform (3 x 100 mL) and the combined organic phases were washed with cold water and dried over magnesium sulfate. After filtration, the solvent was removed *in vacuo* to give an orange solid (10.96 g, 95%).

Mpt. 106-108 °C (lit.[107] 107-108 °C); FTIR (ATR – Thin Film) v/cm^{-1} = 3050 (C$_{Aryl}$-H), 1664 (C$_{Aryl}$=C$_{Aryl}$), 1436 (N$^+$-O$^-$), 666s (C-Br); δ_H (400 MHz, CDCl$_3$) 8.94 (1 H, d, *J* 8.0 Hz, **6'**), 8.74 (1 H, d, *J* 4.5 Hz, **3'**), 8.40 (1 H, d, *J* 2.5 Hz, **3**), 8.16 (1 H, d, *J* 7.0 Hz, **6**), 7.85 (1 H, td, *J* 8.0, 1.5 Hz, **4'**), 7.41 – 7.35 (2 H, m, **5, 5'**); δ_C (101 MHz, CDCl$_3$) 149.5 (CH, **3'**), 148.4 (C, **2**), 148.0 (C, **2'**), 141.5 (CH, **6**), 136.5 (CH, **4'**), 130.7 (CH, **3**), 128.3 (CH, **5**), 125.6 (CH, **6'**), 124.8 (CH, **5'**), 119.2 (C, **4**); HRMS ESI$^+$ [M+H]$^+$ calculated for C$_{10}$H$_8$ON$_2$Br = 250.9815, found 250.9820.

Synthesis of 4-Bromo-2,2'-bipyridine-bis-*N,N'*-oxide
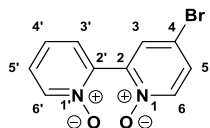
4-Bromo-2,2'-bipyridine-*N,N'*-oxide (**110**)

4-Bromo-2,2'-bipyridine-*N*-oxide **109** (7.5 g, 30 mmol mmol) was dissolved in acetic acid (75 mL, 1.3 mol) and hydrogen peroxide (20 mL, 650 mmol) was added and the mixture heated to 70 °C for 16h. After this time, the reaction was cooled to room temperature and the solvent removed *in vacuo*. The resulting residue was triturated in 1:1 THF:acetone at -20 °C until a precipitate formed. The resultant solid was filtered and washed with cold 1:1 THF:acetone to furnish the product (4.21g, 53%).

Mpt. 114-116 °C (lit.[140] <260 °C); FTIR (ATR – Thin Film) v/cm^{-1} = 3066 (C$_{Aryl}$-H), 1584 (C$_{Aryl}$-H), 1461 (N$^+$-O$^-$), 655s (C-Br); δ_H (400 MHz, DMSO) 8.80-8.74 (2 H, m, **6'**, **3'**), 8.31 (1 H, d, *J* 7.0, **6**), 8.29 (1 H, d, *J* 3.0, **3**), 7.97 (1 H, td, *J* 8.0, 2.0, **4'**), 7.72 (1 H, dd, *J* 7.0, 3.0, **5**), 7.53 (1 H, ddd, *J* 8.0, 5.0, 1.0, **5'**); δ_C (101 MHz, DMSO) 149.6 (CH, **3'**), 148.3 (C, **2'**), 147.0 (C, **2**), 141.9 (CH, **6**), 136.6 (CH, **4'**), 129.8 (CH, **5**), 128.9 (CH, **3**), 125.0 (CH, **5**), 125.0 (CH, **6'**), 117.3 (C, **4**); HRMS ESI$^+$ [M+H]$^+$ calculated for C$_{10}$H$_8$O$_2$N$_2$Br = 266.9764, found 266.9764.

Synthesis of 4-Nitro-2,2'-bipyridine-bis-*N,N'*-oxide
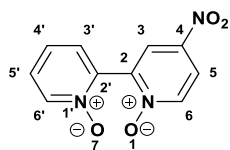
4-Nitro-2,2'-bipyridine-bis-*N,N'*-oxide[113] (**120**)

A solution of *m*-CPBA (12 g, 55 mmol) in chloroform (150 mL) was added dropwise to a solution of 4-nitro-2,2'-bipyridine-*N*-oxide **108** (5 g, 29 mmol) in 150 mL at 0 °C over 10 minutes and the mixture allowed to warm to room temperature for 40h. After this time, the reaction was cooled to -20 °C and the precipitate formed was filtered off. The filtrate was concentrated *in vacuo* and the resulting solid was dissolved in DCM and then purified by passing the solution through a basic alumina plug to furnish a yellow solid (5.62 g, 83%).

Mpt. 232-234 °C (lit.[113] 234-238); FTIR (ATR – Thin Film) v/cm^{-1} = 3013 (C_{Aryl}-H), 1618 (C_{Aryl}=C_{Aryl}), 1516 (N-O), 1431 (N$^+$-O$^-$); δ_H (400 MHz, CDCl$_3$) 8.60 (1 H, d, *J* 3.0, **3**), 8.55 (1 H, d, *J* 7.0, **6**), 8.39 (1 H, dd, *J* 6.5, 1.0, **6'**), 8.31 (1 H, dd, *J* 7.0, 3.0, **5**), 7.71 (1 H, ddd, *J* 8.0, 2.0, 0.5, **3'**), 7.58 (1 H, ddd, *J* 8.0, 6.5, 2.0, **5'**), 7.46 (1 H, td, *J* 8.0, 1.0, **4'**); δ_C (101 MHz, CDCl$_3$) 143.7 (CH, **4**), 141.2 (CH, **2**), 140.8 (C, **2'**), 140.5 (CH, **6**), 139.2 (CH ,**6'**), 128.8 (CH, **3'**), 127.7 (CH, **5'**), 124.8 (CH, **4'**), 123.2 (CH, **3**), 121.3 (CH, **5**); HRMS ESI$^+$ [M+H]$^+$ calculated for C$_{10}$H$_7$O$_4$N$_3$Na = 256.0329, found 256.0325.

Synthesis of 2,2'-Bipyridine *bis-N*-oxide
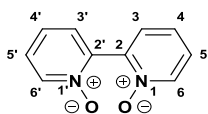
2,2'-Bipyridine *bis-N*-oxide (**45**)

2,2'-Bipyridine **44** (12 g, 75 mmol) was dissolved in acetic acid (75 mL) and the solution cooled to 0 °C, before hydrogen peroxide (30%, 12.5 mL, 40 mmol) was added dropwise over 15 mins. The solution was then heated to 75 °C for 8 h before cooling to room temperature for 16 h. After this time, the solvent was removed *in vacuo* and triturated with acetone to give a white solid (13.37 g, 93%).

Mpt. 297-300 °C (lit.[113] 295-298); FTIR (ATR – Thin Film) v/cm^{-1} = 3037 (C$_{Aryl}$-H), 1585 (C$_{Aryl}$=C$_{Aryl}$),, 1425 (N$^+$-O$^-$); δ_H (400 MHz, DMSO) 8.35 (2 H, dd, *J* 6.0, 0.5, **6, 6'**), 7.64 (2 H, dd, *J* 8.0, 2.0, **3, 3'**), 7.53 (2 H, ddd, *J* 8.0, 6.0, 2.0, **5, 5'**), 7.42 (2 H, td, *J* 8.0, 1.0, **4, 4'**); δ_C (101 MHz, DMSO) 139.7 (CH, **6, 6'**), 128.9 (CH, **3, 3'**), 127.5 (CH, **5, 5'**), 125.0 (CH, **4, 4'**); HRMS ESI$^+$ [M+H]$^+$ calculated for C$_{10}$H$_8$N$_2$O$_2$ = 189.0659, found 189.0657.

Synthesis of 4,4'-Dinitro-2,2'-bipyridine-bis-*N,N'*-oxide
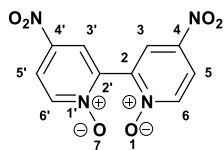
4,4'-Dinitro-2,2'-bipyridine-bis-*N,N'*-oxide[116] (**121**)

2,2-Bipyridine-*bis-N,N'*-oxide **45** (10 g, 53 mmol) was dissolved in conc. H_2SO_4 (200 mL) and potassium nitrate (63 g, 623 mmol) was added, and the reaction was heated to 80 °C for 30h. After this time, the reaction was cooled to room temperature poured onto ice and cooled to -78 °C. The precipitate was filtered off whilst cold and washed with diethyl ether to afford an orange solid (7.62 g, 52%).

Mpt. 272-275 °C (lit.[141] 273-274 °C); FTIR (ATR – Thin Film) v/cm^{-1} = 3060 (C_{Aryl}-H), 1616 (C_{Aryl}=C_{Aryl})1514 (N-O), 1420 (N$^+$-O$^-$); δ_H (400 MHz, DMSO) 8.69 (2H, dd, *J* 3.5, 0.5, **3**, **3'**), 8.60 (2H, dd, *J* 7.0, 0.5, **6**, **6'**), 8.36 (2H, dd, *J* 7.0, 3.5, **5**, **5'**); δ_C (101 MHz, DMSO) 142.1 (C, **2**, **2'**), 141.2 (C, **4**, **4'**), 140.5 (CH, **6**, **6'**), 123.8 (CH, **3**, **3'**), 121.9 (CH, **5**, **5'**); HRMS submitted, calculated [M+H]$^+$ = 279.0360, no corresponding mass ion observed; [M-NO$_2$] = 234.0506 observed.

Synthesis of 4,4'-Dibromo-2,2'-bipyridine-*bis-N,N'*-oxide
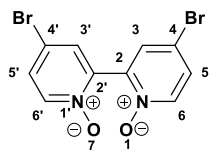
4,4'-Dibromo-2,2'-bipyridine-*bis-N,N'*-oxide[142] (**122**)

4,4'-Dinitro-2,2'-bipyridine-bis-*N,N'*-oxide **121** (3g, 11 mmol) was suspended in acetic acid (48 mL) and acetyl bromide (31.8 mL, 430 mmol) was added under a nitrogen atmosphere and the mixture was heated to 100 °C for 3 h. The mixture was then cooled to 0 °C, poured onto ice and neutralised with 12.5M NaOH. The resulting precipitate was filtered, washed with cold water and allowed to dry in air to afford a tan solid (3.35g, 90%).

Mpt. 251-256 °C Decomposition (lit.[113] 260 °C, decomposition); FTIR (ATR – Thin Film) ν/cm^{-1} = 3090 (C_{Aryl}-H), 1591 (C_{Aryl}=C_{Aryl}),1444 (N^+-O^-), 649 (C-Br); δ_H (400 MHz, DMSO) 8.28 (1 H, d, *J* 7.0, **6, 6'**), 8.02 (1 H, d, *J* 3.0, **3, 3'**), 7.77 (1 H, dd, *J* 7.0, 3.0, **5, 5'**); δ_C (101 MHz, DMSO) 142.7 (C, **2, 2'**), 140.3 (CH, **6, 6'**), 131.2 (CH, **3, 3'**), 130.1 (CH, **5, 5'**), 116.1 (C, **4, 4'**); HRMS ESI$^+$ [M+H]$^+$ calculated for $C_{10}H_7N_2O_2Br_2$ = 344.8869, found 344.8867.

Synthesis of 6,6'-Dimethyl-2,2'-Bipyridine *bis-N,N'*-oxide
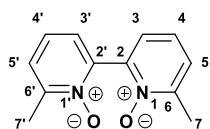
6,6'-Dimethyl-2,2'-Bipyridine-*bis-N*-oxide (**146**)

6,6'-Dimethyl-2,2'-Bipyridine **145** (5 g, 27 mmol) was dissolved in acetic acid (30 mL), hydrogen peroxide (10 mL, 350 mmol) was added at room temperature and the mixture was heated to 70 °C for 16 h. After this time, the mixture was allowed to cool, concentrated *in vacuo* and the residue was triturated with acetone to give the product as colourless powder (5.6 g, 95%).

Mpt. 185-187 °C (lit.[143] 181-182 °C); FTIR (ATR – Thin Film) v/cm^{-1} = 3037 (C_{Aryl}-H), 1701 (C_{Aryl}=C_{Aryl}),, 1425 (N$^+$-O$^-$); δ_H (400 MHz, DMSO) 7.59 (1 H, dd, *J* 8.0, 1.5, **3, 3'**), 7.46 (1 H, dd, *J* 8.0, 1.5, **5, 5'**), 7.32 (1 H, t, *J* 8.0, **4, 4'**), 2.49 (6 H, s, **7, 7'**); δ_C (101 MHz, DMSO) 148.5 (C, **6, 6'**), 143.6 (C, **2, 2'**), 127.7 (CH, **3, 3'**), 126.3 (CH, **5, 5'**), 124.1 (CH, **4, 4'**), 17.8 (CH$_3$, **7, 7'**); HRMS ESI$^+$ [M+H]$^+$ calculated for $C_{12}H_{12}N_2O_2$ = 217.0972, found 217.0975.

99

Synthesis of 4,4'-Dinitro-6,6'-dimethyl-2,2'-Bipyridine *bis-N,N'*-oxide
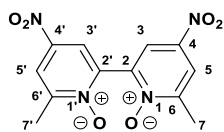
4,4'-Dinitro-6,6'-dimethyl-2,2'-Bipyridine *bis-N*-oxide (**147**)

6,6'-Dimethyl-2,2'-bipyridine *bis-N*-oxide **146** (2.35 g, 11 mmol) was dissolved in a mixture of concentrated sulfuric acid (100 mL) and potassium nitrate (15.3 g, 150 mmol) and heated to 80 °C for 30 h. After this time, the reaction was allowed to cool to room temperature, poured onto ice and basified with 12.5M NaOH. The precipitate formed was filtered and the product extracted with chloroform. The filtrate was concentrated *in vacuo* to allow an orange solid (1.2 g, 36%).

Mpt. >300 °C Decomposition (lit.[143] >300 °C Decomposition); 3086 (C_{Aryl}-H), 1601 (C_{Aryl}=C_{Aryl}) 1572 (N-O), 1483 (N^+-O^-); δ_H (400 MHz, DMSO) 8.63 – 8.61 (2 H, d, *J* 3.0, **3, 3'**), 8.54 (2 H, d, *J* 3.0, **5, 5'**), 2.49 (6 H, s. **7, 7'**); δ_C (101 MHz, DMSO) 150.4 (C, **4, 4'**), 142.9 (C, **6, 6'**), 140.6 (C, **2, 2'**), 121.8 (CH, **3, 3'**), 121.4 (CH, **5, 5'**), 17.7 (CH_3, **7, 7'**); HRMS ESI$^+$ [M+H]$^+$ calculated for $C_{12}H_{11}N_4O_6$ = 307.0673, found 307.0671 within 0.7739 ppm.

Synthesis of 2,2'-Bipyridine-6,6'-dicarbonitrile
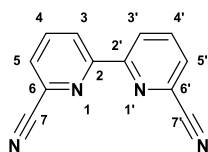
2,2'-Bipyridine-6,6'-dicarbonitrile[144] (**46**)

2,2'-Bipyridine-*bis-N,N'*-oxide **45** (10.3 g, 55 mmol) was suspended in DCM (200 mL) and trimethylsilyl cyanide (20.4 mL, 168 mmol) was added in one portion. Benzoyl chloride (19.4 mL, 170 mmol) was added dropwise over 15 mins to the mixture, and it was stirred at room temperature for 3 days before heating to reflux for 24 h. The mixture was allowed to cool and quenched with 10% aqueous potassium carbonate (200 mL). The insoluble material was filtered off and the precipitate was washed with water (100 mL) and diethyl ether (100 mL). The biphasic filtrate was separated, and the organics were extracted with DCM (3 x 50 mL). The combined phases were dried *in vacuo* and the resultant solids triturated with methanol to furnish an off-white solid (7.85 g, 70%).

Mpt. 256-258 (lit.[145] 255-258); FTIR (ATR – Thin Film) v/cm^{-1} = 3069 (C_{Aryl}-H), 2236 (C≡N), 1575 ($C_{Aryl}=C_{Aryl}$), 1080 (C-N); δ_H (400 MHz, DMSO) = 8.64 (2 H, dd, *J* 8.0, 1.0, **3, 3'**), 8.27 (2 H, t, *J* 8.0, **4, 4'**), 8.19 (2 H, dd, *J* 8.0, 1.0, **5, 5'**); δ_C (101 MHz, DMSO) 154.8 (C, **2, 2'**), 139.9 (CH, **4, 4'**), 132.5 (C, **6, 6'**), 130.1 (CH, **5, 5'**), 124.9 (CH, **3, 3'**), 117.3 (CN, **7, 7'**); HRMS ESI$^+$ [M+H]$^+$ calculated for $C_{12}H_7N_4$ = 207.0665, found 207.

Synthesis of 2,2'-Bipyridine-6,6'-*bis*(carbohydrazonamide)
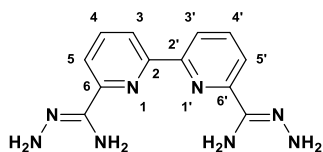
2,2'-Bipyridine-6,6'-*bis*(carbohydrazonamide)[46] (**47**)

2,2'-Bipyridine-6,6'-dicarbonitrile **46** (4.95g, 24 mmol) was suspended in DMSO (100 mL), hydrazine hydrate (45 mL 1.4 mol) was added slowly, and the reaction was left to stir overnight. The mixture was then poured onto water (250 mL), the resultant precipitate was filtered off and washed with deionised water (200 mL) and diethyl ether (200 mL) and dried with suction to afford a yellow solid (5.05 g, 78%).

Mpt. >300 °C (lit.[46] >300 °C); FTIR (ATR – Thin Film) v/cm^{-1} = 3446 (N-H Stretch), 3193 (C$_{Aryl}$-H), 1659 (N-H Bend), 1618 (C$_{Aryl}$=C$_{Aryl}$), 1073 (C-N); δ_H (400 MHz, DMSO) = 8.62 (2 H, d, J 8.0, **3**, **3'**), 7.98 (2 H, dd, J 8.0, 1.0, **5**, **5'**),k 7.90 (2 H, t, J 8.0, **4**, **4'**), 6.00 (4 H, s, **NH₂**), 5.56 (4 H, s, **NH₂**); δ_C (101 MHz, DMSO) 153.7 (CH), 137.7 (CH), 120.0 (CH); HRMS ESI$^+$ [M+H]$^+$ calculated for C$_{12}$H$_{15}$N$_8$ = 271.1414, found 271.1413.

NB. ^{13}C NMR spectrum not obtained due to low solubility of the product in deuterated solvents.

Synthesis of CyMe$_4$-BTBP
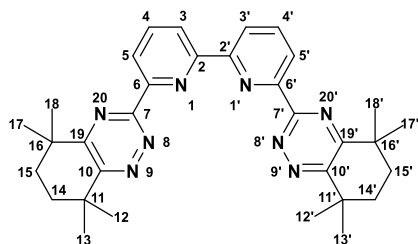
CyMe$_4$-BTBP[146] (**53**)

2,2'-Bipyridine-6,6'-*bis*(carbohydrazonamide) **46** (0.525 g, 2 mmol) and CyMe$_4$-Diketone **43** (0.718 g, 4.2 mmol) were suspended in THF (75 mL) and triethylamine (3.42 mL, 25 mmol) was added. The reaction mixture was heated to reflux for 72 h. After this time, the reaction was allowed to cool to room temperature and the precipitate formed was filtered and the solid washed with DCM (50 mL). The filtrate was concentrated *in vacuo* and the solid was triturated with cold Et$_2$O to afford the product as a pale-yellow solid (0.856 g, 82%).

Mpt. 263-265 °C (lit.[146] 261-262); FTIR (ATR – Thin Film) v/cm^{-1} = 3675 (C$_{Aryl}$-H), 2967 (C$_{Alkyl}$–H), 2080 (N=N), 1145 (C-N); δ$_H$ (400 MHz, CDCl$_3$) 8.95 (2 H, d, *J* 7.5, **3, 3'**), 8.54 (2 H, d, *J* 7.5, **5, 5'**), 8.05 (2 H, t, *J* 7.5, **4, 4'**), 1.90 (8 H, s, **14, 14', 15, 15'**), 1.53 (12 H, s, **12, 12', 13, 13'**), 1.48 (12 H, s, **17, 17', 18, 18'**); δ$_C$ (101 MHz, CDCl$_3$) 164.4 (C, **19, 19'**), 163.0 (C, **10, 10'**), 160.9 (C, **6, 6'**), 156.1 (C, **2, 2'**), 152.8 (C, **7, 7'**), 137.9 (CH, **4, 4'**), 123.9 (CH, **3, 3'**), 122.9 (CH, **5, 5'**), 37.3 (C, **16, 16'**), 36.5 (C, **11, 11'**), 33.8 (CH$_2$, **14, 14', 15, 15'**), 33.3 (CH$_2$, **14, 14', 15, 15'**), 29.8 (CH$_3$, **12, 12', 13, 13'**), 29.3 (CH$_3$, , **17, 17', 18, 18'**); HRMS ESI+ [M+H]$^+$ calculated for C$_{32}$H$_{39}$N$_8$ = 535.3292, found 535.3301.

Synthesis of Diethyl 2,2,5,5-tetramethylhexanedioate
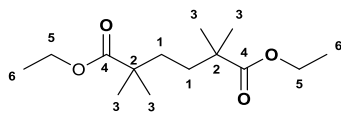
Diethyl 2,2,5,5-tetramethylhexanedioate[31] (**41**)

Dry diethyl ether (500 mL) was cooled to -78 °C and di*iso*propylamine (41 mL, 293 mmol) was added. After 30 minutes, *n*-butyl lithium (122 mL, 1320 mmol) was added dropwise over 2 h at -78 °C. After 3 h, ethyl isobutyrate **40** (35 mL, 260.mmol) was added dropwise over 30 minutes and the mixture then allowed to warm to room temperature. Upon reaching room temperature, ethylene di(*p*-toluenesulfonate) (55 g, 149 mmol) was added in small aliquots over 10 minutes and then the reaction was heated to reflux. After 48 h, the mixture was allowed to cool to room temperature, the precipitate was filtered off and washed with diethyl ether (300 mL) and dichloromethane (300 mL). The filtrate was washed with sat. aq. ammonium chloride (200 mL) and the phases separated. The aqueous phase was extracted with diethyl ether (100 mL). The combined organic extracts were washed with water and dried over magnesium sulfate. After filtration, the solvent was removed *in vacuo* to allow a pale-yellow oil (35 g, 52%).

FTIR (ATR – Thin Film) v/cm^{-1} = 2976 (C$_{Alkyl}$-H), 1730 (C=O), 1176 (C–O); δ_H (400 MHz, CDCl$_3$) = 4.12 (4 H, q, J = 7.0 Hz, **5**), 1.44 (4 H, s, **1**), 1.25 (6 H, t, J = 7.0 Hz, **6**), 1.15 (12 H, s, **3**); δ_C (101 MHz, CDCl$_3$) = 177.7 (C, **4**), 60.3 (CH, **5**), 41.9 (C, **2**), 35.3 (CH, **1**), 25.1 (CH, **3**), 14.3 (CH, **6**); HRMS ESI$^+$ [M+Na]$^+$ calculated for C$_{14}$H$_{26}$O$_4$Na = 281.1723, found 281.1725.

Synthesis of 1,2-Bis(trimethylsilyloxy)-3,3,6,6-tetramethylcyclohex-1-ene
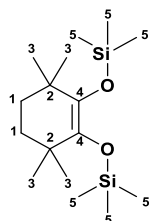
1,2-Bis(trimethylsilyloxy)-3,3,6,6-tetramethylcyclohex-1-ene[31] (**42**)

Dry toluene (200 mL) was added to an oven-dried 3-neck round bottom flask, sealed under a nitrogen atmosphere. Sodium (6.2 g, 270 mmol) was added, and the flask heated to 123 °C until the sodium melted. The diester **41** (14 g, 54 mmol) and chlorotrimethylsilane (34.4 mL, 270 mmol) were added dropwise at a rate such that the sodium did not solidify, and the mixture was kept at 123 °C for 72 h. After this time, the reaction mixture was cooled to room temperature and filtered through a bed of Celite® under nitrogen. The Celite® bed was washed with toluene (300 mL) and tetrahydrofuran (400 mL) and remaining sodium particulates were quenched by adding small amounts of the bed to large volumes of water. The filtrate was concentrated *in vacuo* to afford yellow oil. The product was purified using vacuum distillation (9.5 g, 55%).

Bpt. 110 °C, 7.2 mbar; δ_H (400 MHz, CDCl$_3$) = 1.24 (4 H, s, **1**), 0.83 (12 H, s, **3**), -0.00 (18 H, s, **5**); NB. Full characterisation not possible due to significant product degradation at 4 °C.

Synthesis of 3,3,6,6-tetramethylcyclohexane-1,2-dione (CyMe$_4$-diketone)
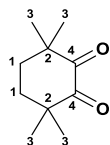
3,3,6,6-tetramethylcyclohexane-1,2-dione[31] (**43**)

1,2-Bis(trimethylsilyloxy)-3,3,6,6-tetramethylcyclohex-1-ene **42** (9.5 g, 28 mmol) was dissolved in dichloromethane (100 mL). Bromine (1.55 mL, 24 mmol) was added dropwise over 5 minutes and the mixture stirred at room temperature for 2 h. The solution was diluted with dichloromethane (100 mL) and washed with water (2 x 50 mL) and sat aq. sodium sulfite (75 mL). The solution was dried over magnesium sulfate, filtered and the solvent removed *in vacuo* to afford a yellow solid, the solid was triturated with hexane at -20 °C to afford a yellow powder (3.92 g 77%).

Mpt. 114-115 °C (lit.[147] 113.5-115 °C); FTIR (ATR – Thin Film) v/cm^{-1} = 2970 (C$_{Alkyl}$-H), 1705 (C=O); δ$_H$ (400 MHz, CDCl$_3$) = 1.87 (4 H, s, **1**), 1.15 (12 H, s, **3**); δ$_C$ (101 MHz, CDCl$_3$) = 207.4 (CO, **4**), 48.7 (s, **2**), 34.7 (CH, **1**), 23.0 (CH, **3**); HRMS ESI$^+$ [M+Na]$^+$ calculated for C$_{10}$H$_{16}$O$_2$Na = 191.1043, found 191.1038.

Synthesis of 3-Bromopivalic acid
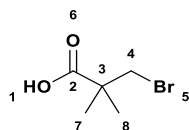
3-Bromopivalic acid[127] (156)

3-Hydroxypivalic acid **155** (10 g, 84.7 mmol) was dissolved in 47% aqueous hydrobromic acid (150 mL) and heated to reflux (120 °C) for 18h. After this time, the reaction was allowed to cool to room temperature and the mixture was poured onto water with external cooling (ice-bath) and the product extracted with diethyl ether (4 x 100 mL). The combined organics were dried over magnesium sulfate, filtered (passed through activated charcoal if the solution was coloured) and concentrated *in vacuo* to allow a glassy solid on standing (14.7 g, 96%).

FTIR (ATR – Thin Film) v/cm^{-1} = 3368 (O-H), 2974 (C_{Alkyl}-H), 1711 (C=O), 1655 (C_{Alkyl}=C_{Alkyl}), 1158 (C-O); δ_H (400 MHz, CDCl$_3$) = 3.52 (2 H, s, **4**), 1.36 (6 H, s, **7**, **8**); δ_C (101 MHz, CDCl$_3$) = 181.5 (CO, **2**), 44.2 (C, **3**), 40.8 (CH$_2$, **4**), 24.3 (CH$_3$, **7**, **8**); HRMS submitted but no ion found, suspected decarboxylation.

Synthesis of Methyl 3-Bromopivalate
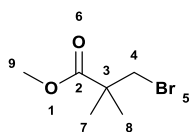
Methyl 3-bromopivalate (**156**)

3-Bromopivalic acid **155** (6.0 g, 33.1 mmol) was dissolved in methanol (100 mL) and concentrated sulfuric acid (6 mL) was added slowly to the solution before heating the mixture to reflux for 18 h. The mixture was allowed to cool to room temperature and neutralized with sat. aq. Na_2CO_3 and the remaining methanol was removed *in vacuo*. The residue was diluted with H_2O (50 mL) extracted with Et_2O (3 x 50 mL). The combined organic fractions were dried over magnesium sulfate, filtered and the solvent removed *in vacuo* to furnish a colourless oil (5.6 g, 87%).

FTIR (ATR – Thin Film) v/cm^{-1} = 2978 (C_{Alkyl}-H), 1733 (C=O), 1169 (C-O), 660 (C-Br); δ_H (400 MHz, CDCl$_3$) = 3.72 (3 H, s, **9**), 3.51 (2 H, s, **4**), 1.32 (6 H, s, **7**, **8**); δ_C (101 MHz, CDCl$_3$) = 175.4 (CO, **2**), 52.3 (CH$_3$, **9**), 44.2 (C, **3**) 41.4 (CH$_2$, **4**), 24.2 (CH$_3$, **7**, **8**). HRMS submitted but no corresponding ion found; [M+H]$^+$ calculated for $C_6H_{12}BrO_2$ = 195.0015 found 553.2115, 653.2636, 721.5059.

Synthesis of Dimethyl 2,2,5,5-tetramethylhexanedioate
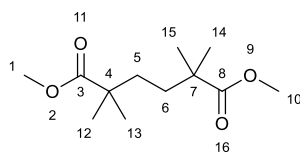
Dimethyl 2,2,5,5-tetramethylhexanedioate (**157**)

Manganese powder (516 mg, 9.4 mmol) was placed in a round bottomed flask under a nitrogen atmosphere and preheated using a heat gun for 5 mins, before adding dry acetonitrile (10 mL) and then placed in a sonicating bath for 30 mins. After this time, TFA (10 drops) was added to activate the manganese further and the mixture stirred for 15 mins. A concentrated solution of $CoBr_2$ (113 mg, 0.52 mmol) in dry acetonitrile was added to the activated manganese solution, followed by methyl 4-bromopivalate **156** (0.5 g, 2.56 mmol) and pyridine (0.51 mL, 6.3 mmol), dropwise. The gas evolved was allowed to dissipate, and the mixture heated to reflux for 24 h. After this time, the mixture was allowed to cool to room temperature and filtered through a Celite® bed (approx. 2 cm) and washed with EtOAc (150 mL). The filtrate was quenched with 2M HCl (50 mL) for 30 mins, the organic layer was separated, and the aqueous fraction extracted with EtOAc (2 x 25 mL). The combined organic extracts were washed with brine, dried over magnesium sulfate, filtered and the solvent removed *in vacuo* to furnish an off-white waxy solid. (0.223 g, 76%).

FTIR (ATR – Thin Film) v/cm^{-1} = 2951 (C_{Alkyl}-H), 1728 (C=O), 1193 (C-O); δ_H (400 MHz, CDCl$_3$) = 3.66 (6H, s, **1**, **10**), 1.44 (4H, s, **5**, **6**), 1.17 (12H , s, **12**, **13**, **14**, **15**); δ_C (101 MHz, CDCl$_3$) = 178.3 (CO, **3**, **8**), 51.8 (CH$_3$, **1**, **10**), 42.2 (C, **4**, **7**), 35.8 (CH$_2$, **5**, **6**), 25.2 (CH$_3$, **12**, **13**, **14**, **15**); HRMS ESI$^+$ [M+H]$^+$ calculated for $C_{12}H_{23}O_4$ = 231.1591, found 231.1596.

Synthesis of 5,6-Dibromoneocuproine
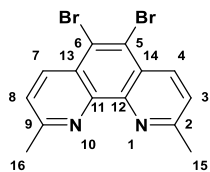
5,6-Dibromoneocuproine[148] (**172**)

Neocuproine **58** (5 g, 24 mmol) was added to fuming sulfuric acid (40 mL), bromine (3 mL, 62 mmol) was added slowly, and the mixture was heated to 135 °C for 3 days. An upside-down funnel trap (sodium thiosulfate) was used to trap the HBr/Br$_2$ fumes emitted. The mixture was allowed to cool to room temperature and slowly poured onto 2M NaOH with external cooling (ice bath). NaOH pellets were added slowly until the pH was 8-9 and the product extracted with chloroform (10 x 100 mL). The combined organics were separated, dried over magnesium sulfate and filtered before removing the solvent *in vacuo* to afford a tan solid (4.3g, 49%).

Mpt. 145-146 °C (lit.[149] 163-166 °C); FTIR (ATR – Thin Film) v/cm^{-1} = 3060 (C$_{Aryl}$-H), 1588 (C$_{Aryl}$=C$_{Aryl}$ Stretching), 820 (C$_{Aryl}$=C$_{Aryl}$ Bending); δ$_H$ (400 MHz, CDCl$_3$) 8.64 (2 H, d, *J* 8.5, **3**, **8**), 7.57 (2 H, d, *J* 8.5, **4**, **7**), 2.96 (6 H, s, **15**, **16**). δ$_C$ (101 MHz, CDCl$_3$) 160.6 (C, **2**, **9**), 144.9 (C, **11**, **12**), 137.4 (CH, **3**, **8**), 126.9 (CBr, **5**, **6**), 125.0 (CH, **4**, **7**), 124.1 (C, **13**, **14**), 25.7 (CH$_3$, **15**, **16**); HRMS ESI$^+$ [M+H]$^+$ calculated for C$_{14}$H$_{11}$N$_2$Br$_2$ = 364.9284, found 364.9280.

Synthesis of Phenanthroline-5,6-epoxide
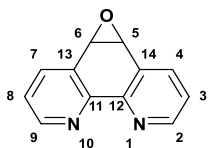
Phenanthroline-5,6-epoxide[150] (**173**)

14% aq. Sodium hypochlorite (500 mL) was diluted with deionised water (2 L) and the pH adjusted with conc. Hydrochloric acid to pH = 9 with a cooling water bath. A solution of phenanthroline (10 g, 55 mmol) and tetrabutylammonium hydrogen sulfate (8.7 g, 26 mmol) in chloroform (800 mL) was added and the reaction stirred vigorously for 30 mins. The organic phase was separated, and the aqueous phase extracted with chloroform (3 x 300 mL). The combined phases were washed with brine, dried over magnesium sulfate, filtered and the solvent removed *in vacuo*. The resulting solid was recrystallized from 1 : 1 DCM : hexane to give a white powder (8.26 g, 75%).

Mpt. 161-164 °C (lit.[151] 160-162); FTIR (ATR – Thin Film) ν/cm^{-1} = 3001 (C_{Aryl}-H), 1578 (C_{Aryl}=C_{Aryl}), 1428 (C-O); δ_H (400 MHz, CDCl$_3$) 8.92 (2 H, dd, J 4.5, 1.5, **2**, **9**), 8.02 (2 H, dd, J 7.5, 1.5, **4**, **7**), 7.41 (2 H, dd, J 7.5, 4.5, **3**, **8**), 4.63 (2 H, s, **5**, **6**); δ_C (101 MHz, CDCl$_3$) 151.0 (CH, **2**, **9**), 149.7 (C, **11**, **12**), 138.3 (CH, **4**, **7**), 129.3 (C, **13**, **14**), 123.8 (CH, **3**, **8**), 55.3 (CH, **5**, **6**); HRMS ESI$^+$ [M+H]$^+$ calculated for $C_{12}H_9N_2O$ = 197.0709, found 197.0705.

Synthesis of 2,9-Bis(trichloromethyl)-1,10-phenanthroline
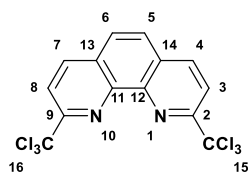
2,9-Bis(trichloromethyl)-1,10-phenanthroline[152] (**59**)

2,9-Dimethyl-1,10-phenanthroline **58** (7 g, 16.1 mmol) was dissolved in chloroform (100 mL) and *N*-chlorosuccinamide (31.42 g, 133.5 mmol) (recrystallised from hot acetic acid) and *m*-chloroperbenzoic acid (2.32 g, 17.3 mmol) was added. The reaction was heated to reflux for 18 h. After this time, the reaction mixture was cooled to room temperature and washed with 2M aq. NaOH (50 mL) and brine 50 mL. The organic phase was dried over magnesium sulfate, filtered and the remaining solvent removed *in vacuo* to allow a pale-yellow solid (10.45 g, 75%).

Mpt. 210-212 °C (lit.[153] 210-212 °C); FTIR (ATR – Thin Film) v/cm^{-1} = 2987 (C_{Aryl}-H), 1581 (C_{Aryl}=C_{Aryl}), 720 (C-Cl); δ_H (400 MHz; CDCl$_3$) 8.44 (2H, d, *J* = 8.5, **4**, **7**), 8.32 (2H, d, *J* = 8.5, **3**, **8**), 7.96 (2H, s, **5**, **6**); δ_C (101 MHz; CDCl$_3$) 158.0 (C, **11**, **12**), 143.2 (C, **13**, **14**), 138.2 (CH, **4**, **7**), 129.2 (C, **2**, **9**), 127.6 (CH, **5**, **6**), 120.5 (CH, **3**, **8**), 98.2 (CCl$_3$, **15**, **16**); HRMS ESI$^+$ [M+H]$^+$ calculated for $C_{14}H_7N_2Cl_6$ = 412.8735, found 412.8734.

Synthesis of Dimethyl 1,10-phenanthroline-2,9-dicarboxylate
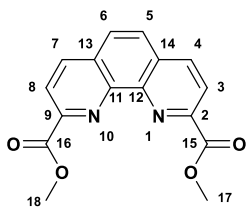
Dimethyl 1,10-phenanthroline-2,9-dicarboxylate[152] (**60**)

2,9-Bis(trichloromethyl)-1,10-phenanthroline **59** (10 g, 24 mmol) was dissolved in concentrated sulfuric acid (80 mL) and the solution heated to 110 °C for 4 h. The solution was allowed to cool to room temperature and methanol (200 mL) was added slowly over 30 mins. After complete addition, the reaction was heated to reflux for 18 h. The solution was allowed to cool to room temperature and the excess methanol was removed *in vacuo*. The acidic residue was poured onto ice water and the precipitate was filtered off, washed with deionised water, and dried in at 40 °C under vacuum to afford a beige solid (4.99 g, 70%).

Mpt. 194-196 °C (lit.[46] 195-198 °C); FTIR (ATR – Thin Film) v/cm^{-1} = 2958 (C_{Aryl}-H), 1720 (C=O), 1639 (C_{Aryl}=C_{Aryl}), 1146 (C-O); δ_H (400 MHz, CDCl$_3$) 8.51 (2 H, d, *J* 8.5, **4, 7**), 8.45 (2 H, d, *J* 8.5, **3, 8**), 7.97 (2 H, s, **5, 6**), 4.14 (6 H, s, **17, 18**); δ_C (101 MHz, CDCl$_3$) 166.0 (CO, **15, 16**), 148.3 (C, **11, 12**), 145.5 (C, **2, 9**), 137.5 (CH, **3, 8**), 130.7 (C, **13, 14**), 128.3 (CH, **5, 6**), , 123.9 (CH, **4, 7**), 53.1 (CH$_3$, **17, 18**); HRMS ESI$^+$ [M+Na]$^+$ calculated for $C_{16}H_{12}N_2O_4Na$ = 319.0689, found 319.0680.

Synthesis of 1,10-Phenanthroline-2,9-dicarboxamide
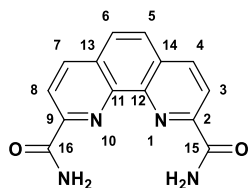
1,10 Phenathroline-2,9-dicarboxamide[152] (**61**)

Dimethyl 1,10-phenanthroline-2,9-dicarboxylate **60** (5.7 g, 19.24 mmol) was suspended in ammonium hydroxide (115 mL, 2.89 mol) and ammonium chloride (3.65 g, 68 mmol) was added and stirred at room temperature for 18 h. The resultant solid was filtered off, washed with deionized water (250 mL) and diethyl ether (250 mL), and dried at 40 °C under vacuum to give an off-white solid (4.8 g, 94%).

Mpt. 310 °C Decomposition (lit.[46] >300 °C); FTIR (ATR – Thin Film) v/cm^{-1} = 3189 (N-H), 1674 (C=O), 1581 ($C_{Aryl}=C_{Aryl}$), 1393 (C-N); δ_H (400 MHz, DMSO) = 8.96 (2 H, s, N**H₂**), 8.71 (2 H, d, J 8.5, **4**, **7**), 8.46 (2 H, d, J 8.5, **3**, **8**), 8.17 (2 H, **5**, **6**), 7.88 (2 H, s, N**H₂**); δ_C (101 MHz, DMSO) 166.6 (CO, **15**, **16**), 150.5 (C **2**, **9**), 144.4 (C, **11**, **12**), 138.5 (CH, **4**, **7**), 130.6 (C, **13**, **14**), 128.4 (CH, **5**, **6**), 121.5 (CH, **3**, **8**); HRMS ESI⁺ [M+Na]⁺ calculated for $C_{14}H_{10}N_4O_2Na$ = 289.0686, found 289.0694.

Synthesis of 1,10-Phenanthroline-2,9-dicarbonitrile
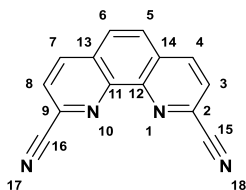
1,10-Phenanthroline-2,9-dicarbonitrile[152] (**62**)

1,10-Phenanthroline-2,9-dicarboxamide **61** (3.79 g, 18.03 mmol) was dissolved in phosphorus oxychloride (20 mL, 214 mmol) and the solution heated to reflux for 18 h. The solution was allowed to cool to room temperature and poured on to ice-water, with external cooling. The slurry was diluted with water and the resulting precipitate was filtered and washed with deionised water (250 mL) and diethyl ether (250 mL). The solid was dried at 40 °C *in vacuo* to afford a brown solid (2.90 g 88%).

Mpt. 281-285 °C (lit.[152] 280-283); FTIR (ATR – Thin Film) v/cm^{-1} = 3055 (C$_{Aryl}$-H), 2236 (C≡N), 1616 (C$_{Aryl}$=C$_{Aryl}$); δ_H (400 MHz, DMSO) = 8.82 (1 H, d, *J* 8.5, **4**, **7**), 8.40 (1 H, d, *J* 8.5 **3**, **8**), 8.25 (1 H, s, **5**, **6**). δ_C (101 MHz, DMSO) = 145.3 (C, **11**, **12**), 139.1 (CH, **4**, **7**), 133.4 (C, **2**, **9**), 131.0 (C, **13**, **14**), 129.7 (CH, **5**, **6**), 128.0 (CH, **3**, **8**), 118.1 (CN, **15**, **16**). HRMS ESI$^+$ [M+H]$^+$ calculated for C$_{14}$H$_7$N$_4$ = 231.0665, found 239.0662.

Synthesis of 1,10-Phenanthroline-2,9-bis(carbohydrazonamide)
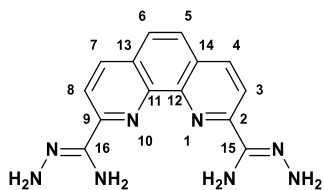
1,10-Phenanthroline-2,9-bis(carbohydrazonamide)[152] (**63**)

1,10-Phenanthroline-2,9-dicarbonitrile **62** (2.9 g, 12.6 mmol) was dissolved in DMSO (35 mL) and hydrazine hydrate (35 mL, 720 mmol) was added slowly over 5 minutes. The resulting solution was stirred at room temperature for 18 h. After this time, the reaction was poured onto deionized water (250 mL). The resulting the precipitate was isolated by filtration and washed with deionized water (250 mL) and diethyl ether (250 mL) and then dried with suction to afford a brown solid (2.65 g, 72%).

Mpt. >300°C (lit.[154] >300 °C); FTIR (ATR – Thin Film) v/cm^{-1} = 3308 (N-H), 1616 (C_{Aryl}=C_{Aryl}); δ_H (400 MHz, DMSO) 8.39 (2 H, d, J 8.5, **4**, **7**), 8.29 (2 H, d, J 8.5, **3**, **8**), 7.95 (2 H, s, **5**, **6**), 6.16 (4 H, s, N**H₂**), 5.70 (4 H, s N**H₂**); δ_C (101 MHz, DMSO) 151.7 (C, **11**, **12**), 143.9 (C, **13**, **14**), 136.5 (CH, **4**, **7**), 128.6 (C, **2**, **9**), 126.5 (CH, **5**, **6**), 119.4 (CH, **3**, **8**), 40.9 (C, **15**, **16**); HRMS ESI$^+$ [M+Na]$^+$ calculated for $C_{14}H_{14}N_8Na$ = 317.1234, found 317.1234.

Synthesis of CyMe₄-BTPhen
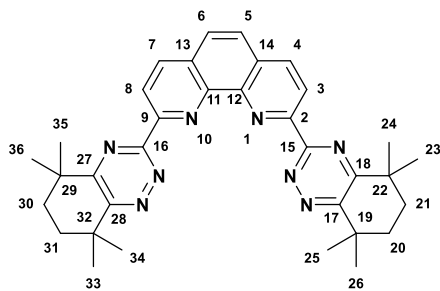
CyMe$_4$-BTPhen[152] (**72**)

1,10-Phenanthroline-2,9-bis(carbohydrazonamide) (0.56 g, 1.90 mmol) was suspended in THF (75 mL). Triethylamine (3.35 mL, 24.03 mmol) and CyMe$_4$-diketone (0.704 g, 4.18 mmol) were added, and the mixture was heated to reflux over 3 days. After this time, the reaction was allowed to cool to room temperature and the insoluble material was filtered off. The filtrate was concentrated *in vacuo* and the resultant solid was triturated with cold diethyl ether and allowed to dry under suction to allow a pale-yellow solid (0.827 g, 78%).

Mpt. 245-248 °C (lit.[155] 247-250 °C);

FTIR (ATR – Thin Film) v/cm^{-1} = 2960(C$_{Alkyl}$-H), 2932(C$_{Aryl}$-H), 1151 (C-N); δ_H (400 MHz, CDCl$_3$) 8.90 (2 H, d, *J* 8.5, **3**, **8**), 8.48 (2 H, d, *J* 8.5, **4**, **7**), 7.95 (2 H, s, **5**, **6**), 1.92 (8 H, s, **20**, **21**, **30**, **31**), 1.58 (12 H, s, **25**, **26**, **34**, **33**), 1.54 (2 H, s, **23**, **24**, **35**, **36**); δ_C (101 MHz, DMSO) 165.1 (C), 163.3 (C), 161.4 (C), 153.9 (C), 146.5 (C), 137.3 (CH, **3**, **7**), 129.8 (C), 127.7 (CH, **5**, **6**), 123.5 (CH, **3**, **8**), 37.5 (C), 36.7 (C), 33.7 (CH$_2$, **20**, **21**, **30**, **31**), 29.8 (CH$_3$, **25**, **26**, **34**, **33**), 29.3 (CH$_3$, **23**, **24**, **35**, **36**); HRMS ESI$^+$ [M+H]$^+$ calculated for C$_{34}$H$_{39}$N$_8$ = 559.3292, found 559.3293.

Synthesis of Tetraethyldiglycolamide (TEDGA)
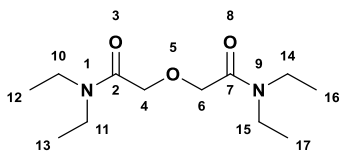
Tetraethyldiglycolamide (TEDGA)[131] (164)

Diglycolic acid **162** (4.02 g, 30 mmol) was suspended in chloroform (120 mL). To the solution, EDC.HCl (11.49 g, 60 mmol), triethylamine (8.4 mL, 60 mmol), diethylamine (6.3 mL, 60 mmol) and hydroxybenztriazole (9.18 g, 60 mmol) were added at 0 °C. The reaction mixture was allowed to warm to room temperature and stirred for 24 h. After this time, the mixture was washed with 1 M HCl (500 mL) and 1 M NaOH (500 mL). The combined organics were dried over magnesium sulfate, filtered and the solvent removed *in vacuo* to give a colourless oil (6.27 g, 86%).

FTIR (ATR – Thin Film) v/cm^{-1} = 2971 (C$_{Alkyl}$-H), 1624 (C=O), 1428 (C-O), 1218 (C-N); δ_H (400 MHz, CDCl$_3$) 4.30 (4 H, s, **4**, **6**), 3.35 (8 H, dq, *J* 21.0, 7.0, **10**, **11**, **14**, **15**), 1.15 (12 H, dt, *J* 21.0, 7.0, **12**, **13**, **16**, **17**); δ_C (101 MHz, CDCl$_3$) = 168.1 (CO, **2**, **7**), 69.4 (CH$_2$, **4**, **6**), 41.1 (CH$_2$, **11**, **15**), 40.0 (CH$_2$, **14**, **10**), 14.2 (CH$_3$, **13**, **17**), 12.9 (CH$_3$, **12**, **16**); HRMS ESI$^+$ [M+H]$^+$ calculated for C$_{12}$H$_{25}$N$_2$O$_3$ = 245.1860, found 245.1860.

Synthesis of N^1,N^1,N^3,N^3-Tetraethylmalonamide (TEMA)
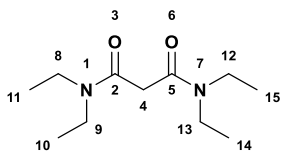
N^1,N^1,N^3,N^3-Tetraethylmalonamide (TEMA)[131] (**166**)

Malonic acid **165** (4.16 g, 40 mmol) was suspended in chloroform (160 mL). To the solution, EDC.HCl (15.32 g, 80 mmol), triethylamine (11.2 mL, 80 mmol), diethylamine (8.4 mL, 80 mmol) and hydroxybenztriazole (12.24 g, 80 mmol) were added at 0 °C. The reaction mixture was allowed to warm to room temperature and stirred for 24 h. After this time, the mixture was washed with 1 M HCl (500 mL) and 1 M NaOH (500 mL). The combined organics were dried over magnesium sulfate, and the solvent removed *in vacuo* to allow a colourless oil (7.2 g, 84%).

FTIR (ATR – Thin Film) v/cm^{-1} = 2973 (C$_{Alkyl}$-H), 1635 (C=O), 1435 (C-O), 1116 (C-N); δ_H (400 MHz, CDCl$_3$) 3.46-3.37 (10 H, m, **4**, **12**, **13**, **8**, **9**), 1.14 (12 H, dt, *J* 21.0, 7.0 Hz, **10**, **11**, **14**, **15**); δ_C (101 MHz, CDCl$_3$) 166.4 (CO, **2**, **5**), 42.6 (CH$_2$, **4**), 40.7 (CH$_2$, **9**, **13**), 40.3 (CH$_2$, **8**, **12**), 14.2 (CH$_3$, **10**, **14**), 12.9 (CH$_3$, **11**, **15**); HRMS ESI$^+$ [M+H]$^+$ calculated for C$_{11}$H$_{23}$N$_2$O$_2$ 215.1754, found 215.1753.

Synthesis of 1,10-Phenanthroline *N*-oxide
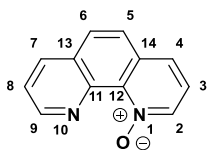
1,10-Phenanthroline *N*-oxide[156] (**174**)

1,10-Phenanthroline (3 g, 16.65 mmol) was dissolved in acetic acid (20 mL), deionized water (1.2 mL) and hydrogen peroxide (2 mL, 65 mmol) and the mixture was heated to 70 °C for 2 h. After this time, another equivalent of hydrogen peroxide (2 mL, 65 mmol) was added. After 1 h, a third aliquot of hydrogen peroxide (1.4 mL, 46 mmol) was added to the mixture and was allowed to cool to room temperature. The mixture was then diluted with water and neutralized with solid sodium carbonate, extracted with chloroform (3 x 75 mL) and the combined organic phases were dried over magnesium sulfate filtered and the solvent was removed *in vacuo* to afford a pale green solid (1.7 g, 52%).

Mpt. 175-176 °C (lit.[105] 178-179 °C); FTIR (ATR – Thin Film) v/cm^{-1} = 3073 (C$_{Aryl}$-H), 1567 (C$_{Aryl}$=C$_{Aryl}$), 1433 (N$^+$-O$^-$), 1245 (C-N); δ_H (400 MHz, CDCl$_3$) 9.32 (1 H, d, *J* 8.0 Hz, **9**), 8.76 (1 H, d, *J* 6.5 Hz, **2**), 8.25 (1 H, dd, *J* 8.0, 2.0 Hz, **7**), 7.82 (1 H, d, *J* 9.0 Hz, **6**), 7.78 – 7.73 (2 H, m, **4, 5**), 7.67 (1 H, dd, *J* 8.0, 4.5 Hz, **8**), 7.47 (1 H, dd, *J* 8.0, 6.5 Hz, **3**); δ_C (101 MHz, CDCl$_3$) = 150.1 (CH, **9**), 142.7 (C, **12**), 140.8 (CH, **2**), 138.4 (C, **11**), 135.9 (CH, **7**), 133.3 (C, **13**), 129.1 (CH, **6**), 128.9 (C, **14**), 126.5 (CH, **5**), 124.6 (CH, **4**), 123.2 (CH, **8**), 122.9 (CH, **3**); HRMS ESI$^+$ [M+H]$^+$ calculated for C$_{12}$H$_9$ON$_2$= 197.0709, found 197.0714.

Synthesis of Tetraphenyl-BTBP
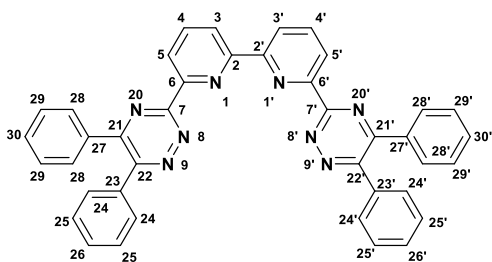
Ph$_4$-BTBP[132] (**168**)

Bipyridine *bis*-aminohydrazide **47** (5.2 g, 19 mmol) was suspended in dioxane (700 mL) and stirred vigorously. Benzil (8.9 g, 42 mmol) and triethylamine (93.6 mL, 671 mmol) was added before the reaction was heated to reflux over 3 days. After this time, the reaction was cooled to 0 °C and the resulting precipitate was filtered off and washed with Et$_2$O (200 mL) and allowed to dry in air to give a bright yellow solid (7.0 g, 59%).

Mpt. >300 °C (lit.[132] >300 °C); FTIR (ATR – Thin Film) ν/cm^{-1} = 3050 (C$_{Aryl}$-H), 1573 (C$_{Aryl}$=C$_{Aryl}$); δ$_H$ (400 MHz, CDCl$_3$) = 9.03 (2 H, d, *J* 8.0, **5, 5'**), 8.76 (2 H, d, *J* 8.0, **3, 3'**), 8.14 (2 H, t, *J* 8.0, **4, 4'**), 7.77 (4 H, d, *J* 7.0, **24, 24'**), 7.69 (4 H, d, *J* 7.0, **28, 28'**), 7.54 – 7.37 (12 H, m, **25, 25', 26, 26', 29, 29', 30, 30'**); δ$_C$ (101 MHz, CDCl$_3$) 165.4 (C), 160.9 (C), 156.3 (C), 156.2 (C), 156.0 (C), 138.1 (CH, **4, 4'**), 128.7 (CH, 4 × *o*-**ArC**), 128.6 (CH, 4 × *m*-**ArC**), 124.5 (CH, **3, 3'**), 123.4 (**5, 5'**); HRMS ESI$^+$ [M+H]$^+$ calculated for C$_{40}$H$_{27}$N$_8$= 619.2353, found 619.2345.

Synthesis of *m*-Sulfonyl-tetraphenyl-BTBP
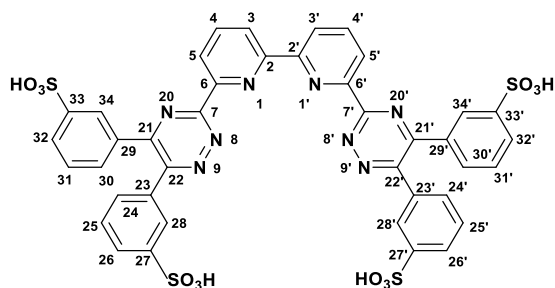
$(SO_3HPh)_4$-BTBP[132] (**167**)

Tetraphenyl-BTBP **168** (7 g, 11 mmol) was dissolved in chlorosulfonic acid (100 mL), and the solution heated to 170 °C for 24 h. After this time, the reaction mixture was allowed to cool to room temperature and carefully poured onto ice (CAUTION EXTREME EXOTHERM). The resultant precipitate was washed with cold water (200 mL), diethyl ether (200 mL) and chloroform (200 mL) and the solid was allowed to dry under vacuum (40 °C) to afford a pale-green solid (11.1 g, 97%).

Mpt. >300 °C (lit.[132] >300 °C); FTIR (ATR – Thin Film) v/cm^{-1} =3364 (O-H), 1620 (C_{Aryl}=C_{Aryl}), 1365 (S=O); δ_H (400 MHz, DMSO) 8.87 (2 H, d, *J* 8.0, **5, 5'**), 8.68 – 8.62 (2 H, m, **3, 3'**), 8.42 – 8.30 (4 H, m, **4, 4', 28, 28' or 34, 34'**), 8.24 (2 H, t, *J* 1.5, **28, 28' or 34, 34'**), 7.77 – 7.59 (6 H, m, ArSO$_3$H 2x *m*-**H**, 4x *o*-**H**), 7.38 – 7.24 (6 H, m, ArSO$_3$H 2x *m*-**H**, 4x *p*-**H**); δ_C (101 MHz, DMSO) 160.3 (C), 156.3 (C), 155.8 (C), 155.4 (C), 152.4 (C), 148.9 (C), 148.8 (C), 139.1 (CH, **4, 4'**), 135.1 (C), 134.9 (C), 130.0 (CH), 129.9 (C), 128.0 (CH), 127.8 (CH), 127.5 (CH, **28, 28' or 34, 34'**), 127.9 (CH), 126.5 (CH, **28**, **28' or 34, 34'**), 125.9 – 125.7 (m), 124.7 (CH, **4, 4'**), 122.7 (CH, **5, 5'**); HRMS ESI$^+$ [M+H]$^+$ calculated for $C_{40}H_{27}N_8S_4O_{12}$= 939.0626, found 939.0619.

Synthesis of 4-Bromopyridine-*N*-oxide
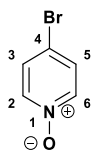
4-Bromopyridine-*N*-oxide[157] (**141**)

4-Bromopyridine hydrochloride **137** (5 g, 25 mmol) was dissolved in DCM (100 mL) and potassium carbonate (4.25 g, 30 mmol) was suspended. After 2h, *m*-CPBA (8.8 g, 50 mmol) and the mixture stirred at room temperature overnight. The precipitate was filtered off, washed with ethyl acetate (100 mL) and the filtrate was concentrated *in vacuo*. The residue was triturated with 1:1 Et_2O:Hexane to furnish a colourless solid (4.45 g, 99%).

Mpt. 143-145 °C decomposition (lit.[158] 143-144 °C decomposition); FTIR (ATR – Thin Film) v/cm^{-1} = 2997 (C_{Aryl}-H), 1633 (C_{Aryl}=C_{Aryl}), 1474 (N$^+$-O$^-$), 633 (C-Br); δ_H (400 MHz, CDCl$_3$) 8.06 (1 H, d, *J* 6.5, **2**, **6**), 7.40 (1 H, d, *J* 6.5, **3**, **5**); δ_C (101 MHz, DMSO) 140.4 (CH, **2**, **6**), 133.2 (C, **4**), 131.1 (CH, **3**, **5**); HRMS ESI$^+$ [M+H]$^+$ calculated for C_5H_4NOBr= 172.9476, found 172.9475.

Synthesis of 2-Cyano-4-bromopyridine
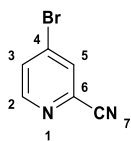
2-Cyano-4-bromopyridine[123] (**137**)

4-Bromopyridine-*N*-oxide **141** (3 g, 17 mmol) was dissolved in acetonitrile (20 mL), trimethylsilyl cyanide (7.2 mL, 58 mmol) and trimethylamine (5 mL, 36 mmol) were added, and the reaction heated to reflux for 2 h. After this time, the reaction was allowed to cool to room temperature and concentrated *in vacuo*. The residue was basified with sat. aq. sodium carbonate and extracted with DCM (3 x 50 mL). The combined extracts were dried over magnesium sulfate, filtered and the solvent removed *in vacuo* to afford a brown solid (2.65 g, 77%).

Mpt. 142-144 °C; FTIR (ATR – Thin Film) v/cm^{-1} = 3076 (C$_{Aryl}$-H), 2240 (C≡N), 1556 (C$_{Aryl}$=C$_{Aryl}$), 848 (C-Br); δ_H (400 MHz, CDCl$_3$) 8.63 (1 H, d, *J* 5.5, **2**), 8.46 (1 H, d, *J* 2.0, **5**), 8.07 (1 H, dd, *J* 5.5, 2.0, **3**); δ_C (101 MHz, CDCl$_3$) 152.1 (CH, **2**), 133.6 (CBr, **4**), 133.3 (C, **6**), 132.0 (CH, **5**), 131.2 (CH, **3**), 116.2 (CN, **7**); HRMS ESI$^+$ [M+H]$^+$ calculated for C$_6$H$_4$N$_2$Br= 182.9552, found 182.9552.

Chapter 5 – References

1   M. Höök and X. Tang, *Energy Policy*, 2013, **52**, 797–809.

2   *2017 World Population Data Sheet*, Washington D.C., 2017.

3   T. R. Anderson, E. Hawkins and P. D. Jones, *Endeavour*, 2016, **40**, 178–187.

4   M. Rieth, S. L. Dudarev, S. M. Gonzalez De Vicente, J. Aktaa, T. Ahlgren, S. Antusch, D. E. J. Armstrong, M. Balden, N. Baluc, M. F. Barthe, W. W. Basuki, M. Battabyal, C. S. Becquart, D. Blagoeva, H. Boldyryeva, J. Brinkmann, M. Celino, L. Ciupinski, J. B. Correia, A. De Backer, C. Domain, E. Gaganidze, C. García-Rosales, J. Gibson, M. R. Gilbert, S. Giusepponi, B. Gludovatz, H. Greuner, K. Heinola, T. Höschen, A. Hoffmann, N. Holstein, F. Koch, W. Krauss, H. Li, S. Lindig, J. Linke, C. Linsmeier, P. López-Ruiz, H. Maier, J. Matejicek, T. P. Mishra, M. Muhammed, A. Muñoz, M. Muzyk, K. Nordlund, D. Nguyen-Manh, J. Opschoor, N. Ordás, T. Palacios, G. Pintsuk, R. Pippan, J. Reiser, J. Riesch, S. G. Roberts, L. Romaner, M. Rosiński, M. Sanchez, W. Schulmeyer, H. Traxler, A. Ureña, J. G. Van Der Laan, L. Veleva, S. Wahlberg, M. Walter, T. Weber, T. Weitkamp, S. Wurster, M. A. Yar, J. H. You and A. Zivelonghi, *J. Nucl. Mater.*, 2013, 432, 482–500.

5   R. Karki, in *Encyclopedia of Sustainable Technologies*, Elsevier, 2017, pp. 217–230.

6   History of Nuclear Energy - World Nuclear Association, https://world-nuclear.org/information-library/current-and-future-generation/outline-history-of-nuclear-energy.aspx, (accessed 21 June 2021).

7   Marie Curie - Article on Radium and Radioactivity, https://history.aip.org/exhibits/curie/article.htm, (accessed 21 June 2021).

8   M. Tubiana, *Bull Acad Natl Med.*, 1996, **180**, 97–108.

9   E. Tretkoff, A. Chodos and J. Ouellette, This Month in Physics History, https://www.aps.org/publications/apsnews/200803/physicshistory.cfm, (accessed 21 June 2021).

10   T. J. Trenn, *Isis*, 1976, **67**, 61–75.

11   F. Soddy, *Annu. Reports Prog. Chem.*, 1913, **10**, 262–288.

12   J. Ch, *Proc. R. Soc. London. Ser. A, Contain. Pap. a Math. Phys. Character*, 1932, **136**, 692–708.

13   J. Chadwick, *Nature*, 1932, 129, 312.

14   *Nature*, 1933, 131, 91.

15   Weart. Spencer R., *The Rise of Nuclear Fear* , Harvard University Press, 2012, vol. 1.

16   C. J. Hardy, *Atomic Rise and Fall : The Australian Atomic Energy Commission, 1953-1987*, Glen Haven, 1st edn., 1999.

17   C. E. Housecroft and A. G. Sharpe, *Inorganic Chemistry*, Prentice Hall, Harlow, 3rd ed., 2008.

18   V. S. Yemel'Yanov and A. I. Yevstyukhin, *The Metallurgy of Nuclear Fuel*, Pergamon, 1969.

19   D. D. Sood and S. K. Patil, *J. Radioanal. Nucl. Chem.*, 1996, 203, 547–573.

20   J. E. Birkett, M. J. Carrott, O. D. Fox, C. J. Jones, C. J. Maher, C. V. Roube, R. J. Taylor and D. A. Woodhead, *Chim. Int. J. Chem.*, 2005, **59**, 898–904.

21   IAEA., Energy and I. Atomic, *Nuclear Power Reactors in the World*, 40th edn., 2020, vol. Reference.

22   N. I. Shumkov, in *Nuclear Submarine Decommissioning and Related Problems*, Springer Netherlands, 1996, pp. 3–5.

23   P. L. Ølgaard, in *Nuclear Submarine Decommissioning and Related Problems*, Springer Netherlands, 1996, pp. 7–16.

24   I. Poro, *Handbook of Generation IV Nuclear Reactors*, Woodhead Publishing - Elsevier , 1st edn., 2016.

25   C. Behar, *Technology Roadmap Update for Generation IV Nuclear Energy Systems*, 2014.

26   R. Scheele and A. Casella, *Assessment of the Use of Nitrogen Trifluoride for Purifying Coolant and Heat Transfer Salts in the Fluoride Salt-Cooled High-Temperature Reactor*, Richland, WA (United States), 2010.

27   *A Technology Roadmap for Generation IV Nuclear Energy Systems*, 2002.

28   The Royal Society, *Fuel cycle stewardship in a nuclear renaissance*, 2011.

29   F. A. Settle, *J. Chem. Educ.*, 2009, **86**, 316.

30   F. W. Lewis, M. J. Hudson and L. M. Harwood, *Synlett*, 2011, 2609–2632.

31   F. W. Lewis, L. M. Harwood, M. J. Hudson, M. G. B. Drew, J. F. Desreux, G. Vidick, N. Bouslimani, G. Modolo, A. Wilden, M. Sypula, T. H. Vu and J. P. Simonin, *J. Am. Chem. Soc.*, 2011, **133**, 13093–13102.

32   N. R. Council, *Nuclear Wastes - Technologies for Separations and Transmutations*, National Academies Press, Washington, D.C., 1996.

33   E. Aneheim, C. Ekberg, A. Fermvik, M. R. S. J. Foreman, T. Retegan and G. Skarnemark, *Solvent Extr. Ion Exch.*, 2010, **28**, 437–458.

34   L. R. Morss, N. M. Edelstein, J. Fuger and J. J. Katz, *Choice Rev. Online*, 2007, **44**, 44-4454-44–4454.

35   A. Leoncini, J. Huskens and W. Verboom, *Chem. Soc. Rev.*, 2017, **46**, 7229–7273.

36   E. Philip Horwitz, D. C. Kalina, H. Diamond, G. F. Vandegrift and W. W. Schulz, *Solvent Extr. Ion Exch.*, 1985, **3**, 75–109.

37   A. Afsar, J. S. Babra, P. Distler, L. M. Harwood, I. Hopkins, J. John, J. Westwood and Z. Y. Selfe, *Heterocycles*, 2020, **101**, 209–222.

38   A. Afsar, P. Distler, L. M. Harwood, J. John, J. S. Babra, Z. Y. Selfe, J. Cowell and J.

Westwood, *Heterocycles*, 2019, **99**, 825–833.

39   K. N. Tevepaugh, J. Coonce, S. Tai, L. H. Delmau, J. D. Carrick and D. D. Ensor, *J. Radioanal. Nucl. Chem.*, 2017, **314**, 371–376.

40   A. Afsar, L. M. Harwood, M. J. Hudson, J. Westwood and A. Geist, *Chem. Commun.*, 2015, **51**, 5860–5863.

41   F. W. Lewis, L. M. Harwood, M. J. Hudson, M. G. B. Drew, J. F. Desreux, G. Vidick, N. Bouslimani, G. Modolo, A. Wilden, M. Sypula, T.-H. Vu and J.-P. Simonin, *J. Am. Chem. Soc.*, 2011, **133**, 13093–13102.

42   G. R. Dutton and C. R. Noller, *Org. Synth.*, 1943, **2**, 109.

43   G. Uchiyama, T. Asakura, S. Hotoku and S. Fujine, *Solvent Extr. Ion Exch.*, 1998, **16**, 1191–1213.

44   E. R. Irish and W. H. Reas, *The PUREX Process - A Solvent Extraction Reprocessing Method for Irradiated Uranium*, 1957.

45   R. J. Taylor, C. R. Gregson, M. J. Carrott, C. Mason and M. J. Sarsfield, *Solvent Extr. Ion Exch.*, 2013, **31**, 442–462.

46   J. Westwood, University of Reading, 2018.

47   O. Courson, M. Lebrun, R. Malmbeck, G. Pagliosa, K. Römer, B. Sätmark and J. P. Glatz, *Radiochim. Acta*, 2000, **88**, 857.

48   R. Smoum, A. Rubinstein, M. Srebnik, B. Walker, J. F. Lynas, D. Leung, G. Abbenante, D. P. Fairlie, R. Babin, S. L. Bender, H. U. Demuth, J. C. Powers, J. L. Asgian, O. D. Ekici, K. E. James, P. E. J. Sanderson, F. Al-Obeidi, J. A. Ostrem, M. R. Wiley, M. J. Fisher, J. P. Vacca, K. Tomoo, K. Satoh, Y. Tsuda, K. Wanaka, S. Okamoto, A. Hijikata-Okunomiya, Y. Okada, T. Ishida, S. R. Presnell, G. S. Patil, C. Mura, K. M. Jude, J. M. Conley, J. A. Bertrand, C.-M. Kam, J. C. Powers, L. D. Williams, K. A. Koehler, G. E. Lienhard, R. V. Wolfenden, G. E. Lienhard, R. V. Wolfenden, A. Radzicka, E. Tsilikounas, C. A. Kettner, W. W. Bachovchin, W. W. Bachovchin, W. Y. L. Wong, S. Farr-Jones, A. B. Shenvi, C. A. Kettner, T. Ohba, E. Ikeda, H. Takei, A. Kashima, Y. Inove, S. Sugio, I. Maeda, T. Nose, Y. Shimoshigashi, M. F. Parisi, R. H. Abeles, D. H. Kinder, J. A. Katzenellenbogen, E. Vedejs, R. W. Chapman, S. C. Fields, S. Lin, M. R. Shrimpf, S. Darses, G. Michaud, J.-P. Genêt, H.-J. Frohn, H. Franke, P. Fritzen, V. V. Bardin, S. Darses, J.-P. Genêt, J.-P. Tremblay-Morin, S. Raeppel, F. Gaudette, T. E. Barder, S. L. Buchwald, M. Dixon, D. G. Gorenstein, D. O. Shah, D. O. Shah, D. G. Gorenstein, A. Saika, C. P. Slichter, M. Karplus, T. P. Das, M. Tsavalos, B. C. Nicholson, T. M. Spotswood, H. J. Knight, E. H. Williams, T. M. Spotswood, D. G. Gorenstein and D. O. Shah, *Org. Biomol. Chem.*, 2005, **3**, 941–944.

49   G. Modolo, H. Vijgen, D. Serrano-Purroy, B. Christiansen, R. Malmbeck, C. Sorel and P. Baron, *Sep. Sci. Technol.*, 2007, **42**, 439–452.

50   M. J. Hudson, F. W. Lewis and L. M. Harwood, *Strateg. Tactics Org. Synth.*, 2013, **9**, 177–202.

51   F. W. Lewis, M. J. Hudson and L. M. Harwood, *Synlett*, 2011, 2609–2632.

52   M. J. Hudson, L. M. Harwood, D. M. Laventine and F. W. Lewis, *Inorg. Chem.*, 2013, **52**, 3414–3428.

53   B. Weaver and F. A. Kappelmann, *TALSPEAK: A New Method of Separating Americium and Curium form the Lanthanides by Extraction from an Aqueous Solution of An Aminopolyacetic acid complex with a monoacidic organophosphate or phosphonate*, 1964.

54   K. L. Nash, *Solvent Extr. Ion Exch.*, 2015, **33**, 1–55.

55   A. E. Martell, R. S. Smith and R. J. Motekaitis, *NIST Critically Selected Stability Constants of Metal Complexes*, Maryland, 2004.

56   A. E. V. Gorden, M. A. DeVore and B. A. Maynard, *Inorg. Chem.*, 2013, **52**, 3445–3458.

57   H. H. Dam, D. N. Reinhoudt and W. Verboom, *Chem. Soc. Rev.*, 2007, **36**, 367–377.

58   P. J. Panak and A. Geist, *Chem. Rev.*, 2013, **113**, 1199–1236.

59   A. Geist, J. M. Adnet, S. Bourg, C. Ekberg, H. Galán, P. Guilbaud, M. Miguirditchian, G. Modolo, C. Rhodes and R. Taylor, *Sep. Sci. Technol.*, , DOI:10.1080/01496395.2020.1795680.

60   A. Geist, U. Müllich, D. Magnusson, P. Kaden, G. Modolo, A. Wilden and T. Zevaco, *Solvent Extr. Ion Exch.*, 2012, **30**, 433–444.

61   E. Mossini, E. Macerata, A. Wilden, P. Kaufholz, G. Modolo, N. Iotti, A. Casnati, A. Geist and M. Mariani, *Solvent Extr. Ion Exch.*, 2018, **36**, 373–386.

62   D. M. Whittaker, T. L. Griffiths, M. Helliwell, A. N. Swinburne, L. S. Natrajan, F. W. Lewis, L. M. Harwood, S. A. Parry and C. A. Sharrad, *Inorg. Chem.*, 2013, 52, 3429–3444.

63   K. Bell, C. Carpentier, M. Carrott, A. Geist, C. Gregson, X. Hérès, D. Magnusson, R. Malmbeck, F. McLachlan, G. Modolo, U. Müllich, M. Sypula, R. Taylor and A. Wilden, *Procedia Chem.*, 2012, **7**, 392–397.

64   C. Hill, C. Madic, P. Baron, M. Ozawa and Y. Tanaka, *J. Alloys Compd.*, 1998, **271**–**273**, 159–162.

65   Y. Zhu, *Radiochim. Acta*, 1995, **68**, 95–98.

66   G. Modolo and R. Odoj, *J. Alloys Compd.*, 1998, **271**–**273**, 248–251.

67   F. W. Lewis, M. J. Hudson and L. M. Harwood, *Synlett*, 2011, 2609–2632.

68   F. W. Lewis, L. M. Harwood, M. J. Hudson, M. G. B. Drew, M. Sypula, G. Modolo, D. Whittaker, C. A. Sharrad, V. Videva, V. Hubscher-Bruder and F. Arnaud-Neu, *Dalt. Trans.*, 2012, **41**, 9209–9219.

69   P. J. Panak and A. Geist, *Chem. Rev.*, 2013, 113, 1199–1236.

70   M. J. Hudson, F. W. Lewis and L. M. Harwood, in *Strategies and Tactics in Organic Synthesis*, Academic Press Inc., 2013, vol. 9, pp. 177–202.

71   S. Davey, *Nat. Chem.*, 2011, **3**, 753–753.

72   M. M. Heaton, *J. Am. Chem. Soc.*, 1978, **100**, 2004–2008.

73   F. H. Case, *J. Heterocycl. Chem.*, 1971, 8, 1043–1046.

74   Z. Kolarik, U. Müllich and F. Gassner, *Solvent Extr. Ion Exch.*, 1999, **17**, 1155–1170.

75   C. Madic, B. Boullis, P. Baron, F. Testard, M. J. Hudson, J. O. Liljenzin, B. Christiansen, M. Ferrando, A. Facchini, A. Geist, G. Modolo, A. G. Espartero and J. De Mendoza, *J. Alloys Compd.*, 2007, **444–445**, 23–27.

76   F. W. Lewis, L. M. Harwood, M. J. Hudson, M. G. B. Drew, G. Modolo, M. Sypula, J. F. Desreux, N. Bouslimani and G. Vidick, *Dalt. Trans.*, 2010, **39**, 5172.

77   M. Nilsson, C. Ekberg, M. Foreman, M. Hudson, J. Liljenzin, G. Modolo and G. Skarnemark, *Solvent Extr. Ion Exch.*, 2006, **24**, 823–843.

78   M. J. Hudson, C. E. Boucher, D. Braekers, J. F. Desreux, M. G. B. Drew, M. R. S. J. Foreman, L. M. Harwood, C. Hill, C. Madic, F. Marken and T. G. A. Youngs, *New J. Chem.*, 2006, **30**, 1171–1183.

79   H. Schmidt, A. Wilden, G. Modolo, D. Bosbach, B. Santiago-Schübel, M. Hupert, J. Švehla, B. Grüner and C. Ekberg, *Procedia Chem.*, 2016, **21**, 32–37.

80   A. Afsar, P. Distler, L. M. Harwood, J. John and J. Westwood, *J. Org. Chem.*, 2016, **81**, 10517–10520.

81   P. J. Panak and A. Geist, *Chem. Rev.*, 2013, **113**, 1199–1236.

82   F. W. Lewis, L. M. Harwood, M. J. Hudson, M. G. B. Drew, G. Modolo, M. Sypula, J. F. Desreux, N. Bouslimani and G. Vidick, *Dalt. Trans.*, 2010, **39**, 5172–5182.

83   F. W. Lewis, L. M. Harwood, M. J. Hudson, M. G. B. Drew, V. Hubscher-Bruder, V. Videva, F. Arnaud-Neu, K. Stamberg and S. Vyas, *Inorg. Chem.*, 2013, **52**, 4993–5005.

84   A. C. Edwards, C. Wagner, A. Geist, N. A. Burton, C. A. Sharrad, R. W. Adams, R. G. Pritchard, P. J. Panak, R. C. Whitehead and L. M. Harwood, *Dalt. Trans.*, 2016, **45**, 18102–18112.

85   D. M. Laventine, A. Afsar, M. J. Hudson and L. M. Harwood, *Heterocycles*, 2012, **86**, 1419–1429.

86   A. Daane, *Yttrium - The Encyclopedia of the Chemical Elements*, Reinhold Book Corporation, New York, 1968.

87   N. N. Greenwood and A. Earnshaw, *Chemistry of the Elements - 2nd Edition*, 2nd ed., 1997.

88   A. C. Edwards, P. Mocilac, A. Geist, L. M. Harwood, C. A. Sharrad, N. A. Burton, R. C. Whitehead and M. A. Denecke, *Chem. Commun*, 2017, **53**, 5001.

89   F. W. Lewis, L. M. Harwood, M. J. Hudson, M. G. B. Drew, A. Wilden, M. Sypula, G. Modolo, T.-H. Vu, J.-P. Simonin, G. Vidick, N. Bouslimani and J. F. Desreux, *Procedia Chem.*, 2012, **7**, 231–238.

90   J. P. Manion and M. Burton, *J. Phys. Chem.*, 1952, **56**, 560–569.

91   A. Fermvik, M. Nilsson and C. Ekberg, in *Nuclear Energy and the Environment*, eds. C. M. Wai and B. J. Mincher, American Chemical Society, Washington, DC, 2010, vol. 1046, pp. 215–229.

92   A. Fermvik, M. Nilsson and C. Ekberg, in *ACS Symposium Series*, American Chemical Society, 2010, vol. 1046, pp. 215–229.

93   D. Magnusson, B. Christiansen, R. Malmbeck and J.-P. Glatz, *Radiochim. Acta*, 2009, **97**, 497–502.

94   J. Kondé, P. Distler, J. John, J. Švehla, B. Grüner and Z. Bělčická, *Procedia Chem.*, 2016, **21**, 174–181.

95   E. Aneheim, L. Bauhn, C. Ekberg, M. Foreman and E. Löfström-Engdahl, *Procedia Chem.*, 2012, **7**, 123–129.

96   E. Aneheim, C. Ekberg, M. R. S. Foreman, E. Löfström-Engdahl and N. Mabile, *Sep. Sci. Technol.*, 2012, **47**, 663–669.

97   D. Magnusson, B. Christiansen, M. R. S. Foreman, A. Geist, J. P. Glatz, R. Malmbeck, G. Modolo, D. Serrano-Purroy and C. Sorel, *Solvent Extr. Ion Exch.*, 2009, **27**, 97–106.

98   T. Retegan, C. Ekberg, S. Englund, A. Fermvik, M. R. S. Foreman and G. Skarnemark, *Radiochim. Acta*, 2007, **95**, 637–642.

99   G. P. Horne, S. P. Mezyk, N. Moulton, J. R. Peller and A. Geist, *Dalt. Trans.*, 2019, **48**, 4547–4554.

100   A. Afsar, *Unpubl. results*, **EPSRC**, University of Reading.

101   H. Schmidt, G. Modolo, A. Wilden, C. Ekberg, J. Hallerod, B. Grüner and J. Svehla, in *SACESS Interrnational Workshop*, Warsaw, 2015.

102   M. Zalas, B. Gierczyk, M. Cegłowski and G. Schroeder, *Chem. Pap.*, 2012, **66**, 733–740.

103   M. Rubio, G. Ramírez-Galicia and L. J. López-Nava, *J. Mol. Struct. THEOCHEM*, 2005, **726**, 261–269.

104   L. Kaczmarek, R. Balicki and P. Nantka-Namirski, *Chem. Ber.*, 1992, 125, 1965–1966.

105   R. Balicki and J. Golinski, *Synth. Commun.*, 2000, **30**, 1529–1534.

106   D. Swern, *Chem. Rev.*, 1949, **45**, 1–68.

107   K. Kodama, A. Kobayashi and T. Hirose, *Tetrahedron Lett.*, 2013, **54**, 5514–5517.

108   Z. Y. Selfe and L. M. Harwood, University of Reading, 2017.

109   M. Zalas, B. Gierczyk, M. Klein, K. Siuzdak, T. Pędziński and T. Łuczak, *Polyhedron*, 2014, **67**, 381–387.

110   A. O. Adeloye, *Molecules*, 2011, **16**, 8353–8367.

111   P. V. Vyas, A. K. Bhatt, G. Ramachandraiah and A. V. Bedekar, *Tetrahedron Lett.*, 2003, **44**, 4085–4088.

112   J. G. Stark and H. G. Wallace, *Chemistry Data Book*, Hodder Education, London, 2nd

edn., 1982.

113   D. Wenkert and R. B. Woodward, *J. Org. Chem.*, 1983, **48**, 283–289.

114   S. S. Zhu, R. P. Kingsborough and T. M. Swager, *J. Mater. Chem.*, 1999, **9**, 2123–2131.

115   D. Zhang, E. J. Dufek and E. L. Clennan, *J. Org. Chem.*, 2006, **71**, 315–319.

116   P. Kavanagh and D. Leech, *Tetrahedron Lett.*, 2004, **45**, 121–123.

117   W. K. Fife, *J. Org. Chem.*, 1983, **48**, 1375–1377.

118   X. S. Miao, R. E. March and C. D. Metcalfe, *Int. J. Mass Spectrom.*, 2003, **230**, 123–133.

119   T. B. Mete, A. Singh and R. G. Bhat, *Tetrahedron Lett.*, 2017, **58**, 4709–4712.

120   P. Gros, Y. Fort and P. Caubère, *J. Chem. Soc. Trans. 1*, 1997, 3597–3600.

121   L. Y. Liao, X. R. Kong and X. F. Duan, *J. Org. Chem.*, 2014, **79**, 777–782.

122   W. Han, F. Jin, Q. Zhao, H. Du and L. Yao, *Synlett*, 2016, **27**, 1854–1859.

123   US2009/0239876 A1, 2009, 1–77.

124   C. Kruck, P. Nazari, C. Dee, B. S. Richards, A. Turshatov and M. Seitz, *Inorg. Chem.*, 2019, **58**, 6959–6965.

125   K. RÜHLMANN, *Synthesis (Stuttg).*, 1971, **1971**, 236–253.

126   Available from Sigma-Aldrich, http://www.sigmaaldrich.com/united-kingdom.html, (accessed 12 September 2016).

127   WO2012010651 (A2), 2012, 1–34.

128   R. M. Beesley, C. K. Ingold and J. F. Thorpe, *J. Chem. Soc. Trans.*, 1915, **107**, 1080–1106.

129   Y. Peng, L. Luo, C. S. Yan, J. J. Zhang and Y. W. Wang, *J. Org. Chem.*, 2013, **78**, 10960–10967.

130   Y. Cai, X. Qian and C. Gosmini, *Adv. Synth. Catal.*, 2016, **358**, 2427–2430.

131   A. J. Canner, L. M. Harwood, J. Cowell, J. S. Babra, S. F. Brown and M. D. Ogden, *J. Solution Chem.*, 2020, **49**, 52–67.

132   F. W. Lewis, L. M. Harwood, M. J. Hudson, A. Geist, V. N. Kozhevnikov, P. Distler and J. John, *Chem. Sci.*, 2015, **6**, 4812–4821.

133   M. A. Larsen and J. F. Hartwig, *J. Am. Chem. Soc.*, 2014, **136**, 4287–4299.

134   T. Ishiyama, J. Takagi, K. Ishida, N. Miyaura, N. R. Anastasi and J. F. Hartwig, *J. Am. Chem. Soc.*, 2002, **124**, 390–391.

135   C. Thiebes, G. K. S. Prakash, N. A. Petasis and G. A. Olah, *Synlett*, 1998, **1998**, 141–142.

136   A. Klapars and S. L. Buchwald, *J. Am. Chem. Soc.*, 2002, **124**, 14844–14845.

137   W. L. F. Armarego and C. L. L. Chai, *Purification of Laboratory Chemicals*, Elsevier, Oxford, Seventh Ed., 2013.

138   T. Norby, A. Borje, L. Zhang and B. Akermark, *Acta Chem. Scand.*, 1998, **52**, 77–85.

139   T. Mizuno, M. Takeuchi, I. Hamachi, K. Nakashima and S. Shinkai, *J. Chem. Soc. Perkin Trans. 2*, 1998, 2281–2288.

140   S. S. Zhu, R. P. Kingsborough and T. M. Swager, *Materials Conducting redox polymers: investigations of polythiophene-Ru(bpy) 3 n+ hybrid materials*, .

141   R. A. Jones, B. D. Roney, W. H. F. Sasse and K. O. Wade, *J. Chem. Soc. B Phys. Org.*, 1967, 106–111.

142   US2012247546 (A1), 2012, 1–76.

143   D. O. Kirsanov, N. E. Borisova, M. D. Reshetova, A. V. Ivanov, L. A. Korotkov, I. I. Eliseev, M. Y. Alyapyshev, I. G. Spiridonov, A. V. Legin, Y. G. Vlasov and V. A. Babain, *Russ. Chem. Bull.*, 2012, **61**, 881–890.

144   E. S. Andreiadis, R. Demadrille, D. Imbert, J. Pécaut and M. Mazzanti, *Chem. - A Eur. J.*, 2009, **15**, 9458–9476.

145   J. Stanek, G. Caravatti, H. G. Capraro, P. Furet, H. Mett, P. Schneider and U. Regenass, *J. Med. Chem.*, 1993, **36**, 46–54.

146   M. R. S. Foreman, M. J. Hudson, M. G. B. Drew, C. Hill and C. Madic, *Dalt. Trans.*, 2006, **0**, 1645–1653.

147   D. E. Applequist, P. A. Gebauer, D. E. Gwynn and L. H. O. Connor, *J. Am. Chem. Soc.*, 1972, **94**, 4272–4278.

148   A. Afsar, D. M. Laventine, L. M. Harwood, M. J. Hudson and A. Geist, *Chem. Commun*, 2013, **49**, 8534.

149   A. Afsar, D. M. Laventine, L. M. Harwood, M. J. Hudson and A. Geist, *Chem. Commun.*, 2013, **49**, 8534–8536.

150   B. A. Howell and A. Dumitrascu, in *Journal of Thermal Analysis and Calorimetry*, Springer, 2010, vol. 102, pp. 505–512.

151   B. A. Howell and A. Dumitrascu, in *Journal of Thermal Analysis and Calorimetry*, Springer, 2010, vol. 102, pp. 505–512.

152   A. Afsar, J. Cowell, P. Distler, L. M. Harwood, J. John and J. Westwood, *Synlett*, 2017, **28**, 2795–2799.

153   A. C. Edwards, C. Wagner, A. Geist, N. A. Burton, C. A. Sharrad, R. W. Adams, R. G. Pritchard, P. J. Panak, R. C. Whitehead and L. M. Harwood, *Dalt. Trans.*, 2016, **45**, 18102.

154   F. W. Lewis, L. M. Harwood, M. J. Hudson, M. G. B. B. Drew, J. F. Desreux, G. Vidick, N. Bouslimani, G. Modolo, A. Wilden, M. Sypula, T.-H. H. Vu and J.-P. P. Simonin, *J. Am. Chem. Soc.*, 2011, **133**, 13093–13102.

155   L. M. Harwood, A. Afsar, A. C. Edwards, A. Geist, M. J. Hudson, J. Westwood and R. C. Whitehead, *Heterocycles*, 2017, **95**, 575.

156   M. L. O'Duill, R. Matsuura, Y. Wang, J. L. Turnbull, J. A. Gurak, D. W. Gao, G. Lu, P. Liu

and K. M. Engle, *J. Am. Chem. Soc.*, 2017, **139**, 15576–15579.

157   WO2012160464 (A1), 2012, 1–176.

158   M. R. Kidd and W. H. Watson, *Inorg. Chem.*, 1969, **8**, 1886–1891.